AD-774 804

WIND-TUNNEL TEST OF A SPINNING, LOW-DRAG PROJECTILE WITH CANTED BORE RIDERS AT MACH NUMBERS FROM 1.75 TO 2.5

Klaus O. Opalka

Ballistic Research Laboratories
Aberdeen Proving Ground, Maryland

January 1974

DISTRIBUTED BY:

NTIS

National Technical Information Service
U. S. DEPARTMENT OF COMMERCE
5285 Port Royal Road, Springfield Va. 22151

Unclassified
Security Classification

AD 774804

DOCUMENT CONTROL DATA - R & D

(Security classification of title, body of abstract and indexing annotation must be entered when the overall report is classified)

1. ORIGINATING ACTIVITY *(Corporate author)*

U.S. Army Ballistic Research Laboratories
Aberdeen Proving Ground, Maryland 21005

2a. REPORT SECURITY CLASSIFICATION

Unclassified

2b. GROUP

3. REPORT TITLE

WIND-TUNNEL TEST OF A SPINNING, LOW-DRAG PROJECTILE WITH CANTED BORE RIDERS AT MACH NUMBERS FROM 1.75 TO 2.5

4. DESCRIPTIVE NOTES *(Type of report and inclusive dates)*

5. AUTHOR(S) *(First name, middle initial, last name)*

Klaus O. Opalka

6. REPORT DATE	7a. TOTAL NO. OF PAGES	7b. NO. OF REFS
JANUARY 1974	81	6

8a. CONTRACT OR GRANT NO.	9a. ORIGINATOR'S REPORT NUMBER(S)
b. PROJECT NO. RDT&E Project No. 1T362301A201	BRL Memorandum Report No. 2349
c.	9b. OTHER REPORT NO(S) *(Any other numbers that may be assigned this report)*
d.	

10. DISTRIBUTION STATEMENT

Approved for public release; distribution unlimited.

11. SUPPLEMENTARY NOTES	12. SPONSORING MILITARY ACTIVITY
	U.S. Army Materiel Command Alexandria, Virginia 22304

13. ABSTRACT

Test data are reported for a spin-stabilized, low-drag projectile with and without bore riders mounted at various angles of cant with respect to the shell axis. Wind-tunnel tests were performed with and without spin at four Mach numbers evenly spaced from 1.75 to 2.5; some of the resulting aerodynamic coefficients are plotted versus spin rate, angle of attack or Mach number.

Reproduced by
NATIONAL TECHNICAL
INFORMATION SERVICE
U S Department of Commerce
Springfield VA 22151

DD FORM 1 NOV 68 1473 REPLACES DD FORM 1473, 1 JAN 64, WHICH IS OBSOLETE FOR ARMY USE.

UNCLASSIFIED
Security Classification

14. KEY WORDS	LINK A		LINK B		LINK C	
	ROLE	WT	ROLE	WT	ROLE	WT
Canted Bore Riders						
Low-Drag Projectile						
Wind Tunnel Test						
Supersonic Flow Test						
Magnus Moment and Force						

B A L L I S T I C R E S E A R C H L A B O R A T O R I E S

MEMORANDUM REPORT NO. 2349

JANUARY 1974

WIND-TUNNEL TEST OF A SPINNING, LOW-DRAG PROJECTILE WITH CANTED BORE RIDERS AT MACH NUMBERS FROM 1.75 TO 2.5

Klaus O. Opalka

Exterior Ballistics Laboratory

Approved for public release; distribution unlimited.

RDT&E Project No. 1T362301A201

A B E R D E E N P R O V I N G G R O U N D, M A R Y L A N D

BALLISTIC RESEARCH LABORATORIES

MEMORANDUM REPORT NO. 2349

KOOpalka/lca
Aberdeen Proving Ground, Md.
January 1974

WIND-TUNNEL TEST OF A SPINNING, LOW-DRAG PROJECTILE WITH CANTED BORE RIDERS AT MACH NUMBERS FROM 1.75 TO 2.5

ABSTRACT

Test data are reported for a spin-stabilized, low-drag projectile without and with bore riders mounted at various angles of cant with respect to the shell axis. Wind-tunnel tests were performed with and without spin at four Mach numbers evenly spaced from 1.75 to 2.5; some of the resulting aerodynamic coefficients are plotted versus spin rate, angle of attack or Mach number.

TABLE OF CONTENTS

LIST OF ILLUSTRATIONS

LIST OF ILLUSTRATIONS (CONTINUED)

LIST OF ILLUSTRATIONS (CONTINUED)

LIST OF SYMBOLS

C_A	axial-force coefficient, $F_A/(qS)$
C_{Af}	forebody-axial-force coefficient, $C_A - C_{Ab}$
C_{Ab}	base-axial-force coefficient, $(p - p_b)\ S_b/(qS)$
C_m	pitching-moment coefficient, $m/(qSD)$, reference at the nose of the model
C_N	normal-force coefficient, $F_N/(qS)$
C_{N_α}	slope of the normal-force curve, $\partial C_N/\partial\alpha$, for $-1.5 < \alpha < +1.5$
C_n	yawing-moment coefficient, $n/(qSD)$, reference at the nose of the model
C_Y	side-force coefficient, $F_Y/(qS)$
D	reference diameter, 5.715 cm
d_b	diameter of the model base
F_A	axial force
F_N	normal force
F_Y	side force
M	Mach number
m	pitching moment
N_{cp}	location of the normal-force center of pressure from the nose of the model
n	yawing moment
P	spin rate
p	free-stream static pressure
p_b	base pressure

LIST OF SYMBOLS (CONTINUED)

PD/V	non-dimensional spin rate
q	free-stream dynamic pressure
Re	Reynolds number, based on free-stream conditions
Re_{ℓ}	Reynolds number, based on free-stream conditions and total model length
S	reference area, $\pi D^2/4$
S_b	area of the model base, $\pi d_b^2/4$
V	free-stream velocity
α	angle of attack
δ	angle of cant of the bore riders

I. INTRODUCTION

The range of an artillery system is the distance over which the system is able to deliver a given explosive payload. It is of greatest interest to the military to make this distance as far as possible. Given an initial velocity and weight, it is the aerodynamic shape and the flight attitude of the projectile which determine its drag, and thereby its range of flight. Range and drag are related such that the lower the drag the further the projectile will fly. To reduce the drag, a projectile needs an optimum shape and a stable attitude at small angles of attack.

The Picatinny Arsenal, Dover, New Jersey, serving as principal investigator, and the Space Research Corporation (SRC), North Troy, Vermont, have proposed a projectile consisting of a long ogive combined with a boattail to fulfill the above mentioned requirements of shape and attitude. The in-bore support is provided by four aerodynamically shaped riders mounted on the ogive and a discarding sabot located at the maximum diameter of the projectile.

Previously, the feasibility of such a design had been demonstrated in a parametric wind-tunnel study (unpublished) and a limited free-flight test[1*] of a pilot project that was carried out at the Exterior Ballistics Laboratory (BRL). The present wind-tunnel investigation at BRL is a further contribution to Picatinny Arsenal's research effort in extending the range of an artillery system. The test permits a study of specially shaped and canted bore riders and their effect on the aerodynamic characteristics of the basic projectile.

II. EXPERIMENTAL INVESTIGATION

A wind tunnel test of five configurations, the differences of which are all in the bore riders, was performed in the Supersonic Wind Tunnel No. 1 of the U.S. Army Ballistic Research Laboratories for the principal investigator, Picatinny Arsenal, in March 1973. Figure 1 illustrates the installation of the test model in the wind tunnel.

A. Equipment

The Supersonic Wind Tunnel No. 1[2] has a flexible, two-dimensional nozzle that is calibrated for fifteen Mach numbers between 1.5 and 5.0 with an accuracy of 0.01 absolute value. The air density can be varied to cover a Reynolds number range from 0.04×10^6 to 0.3×10^6 per

References are listed on page 22.

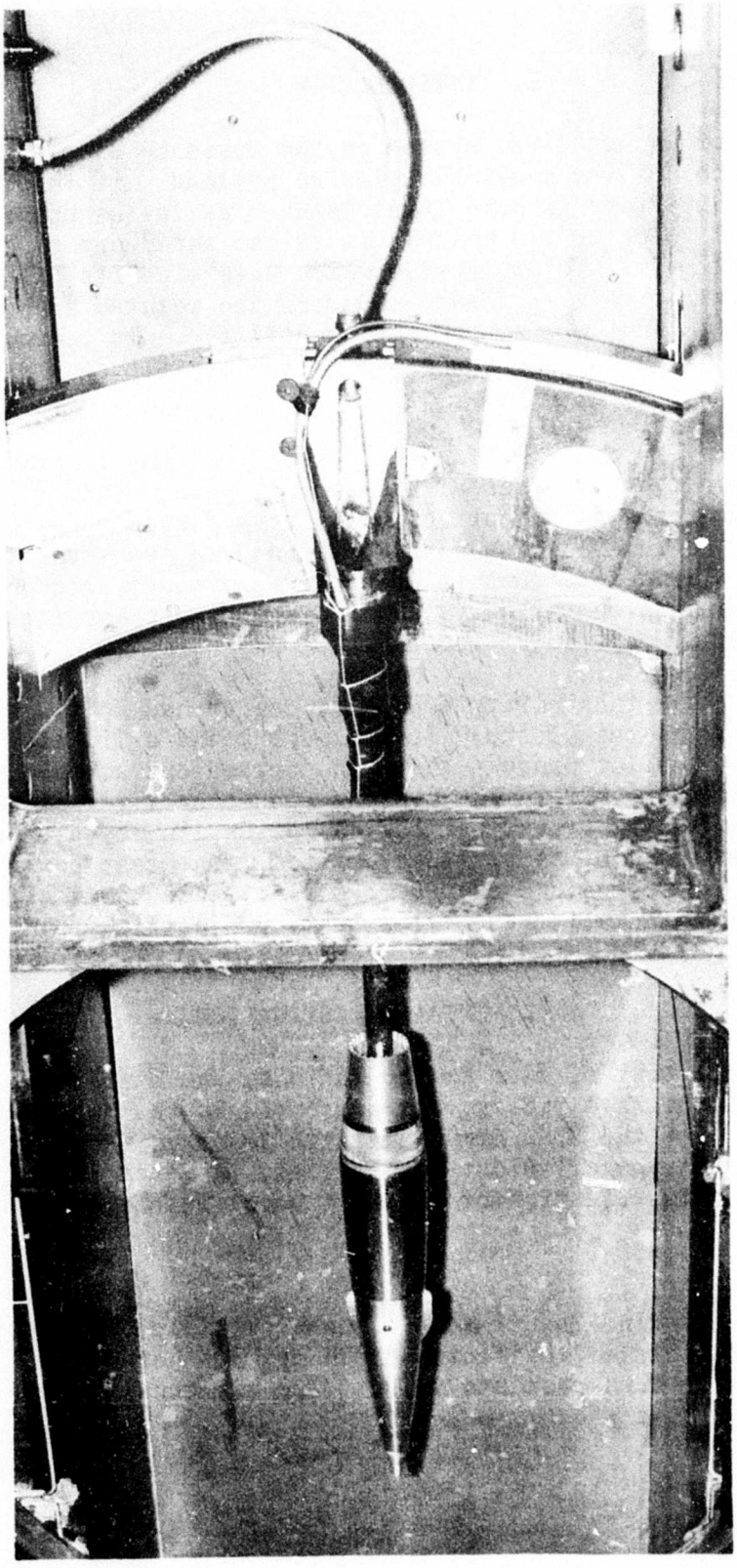

Figure 1. Installation of the Model in Wind Tunnel No. 1

centimeter. The supply pressure can be varied from 25 to 500 cm Hg in continuous operation. The test section measures 38 cm high and 33 cm wide, and allows testing of models of 5 cm diameter and 25 cm length at the most critical Mach number of 1.50. The angle of attack of the model can be changed from -10 to +15 degrees.

A six-component, strain-gage balance was used to measure the aerodynamic forces and moments. The balance has the following capacities (with reference to the center between gages).

900 N	normal force	3400 N·cm	pitching moment
450 N	side force	1400 N·cm	yawing moment
350 N	axial force	700 N·cm	rolling moment

The design of the projectile is shown in Figure 2. The model consists of an ogive of 4.6 calibers length, essentially no cylindrical section, and a boattail length of 1.5 calibers. Four bore-riding nubs are mounted on the ogive. These nubs are aerodynamically shaped to reduce the drag. The five configurations which were tested in the wind tunnel program have changes only in the bore riders: no riders, and cants of the lengthwise rider axis to the shell axis of 0°, 7°, 11° and 15°.

Table I. Model-Configuration Nomenclature

Code	Description
80.00	Basic model: 4.6 caliber ogive, 1.5 caliber boattail, no bore riders
83.00	Basic model with bore riders at 0° cant to the shell axis
83.07	Basic model with bore riders at 7° cant to the shell axis
83.11	Basic model with bore riders at 11° cant to the shell axis
83.15	Basic model with bore riders at 15° cant to the shell axis

The model is equipped with an air turbine which provides the spin either clockwise or counter-clockwise depending on the installation of appropriate nozzle and blades.

B. Procedure

The model configurations were tested under the following conditions.

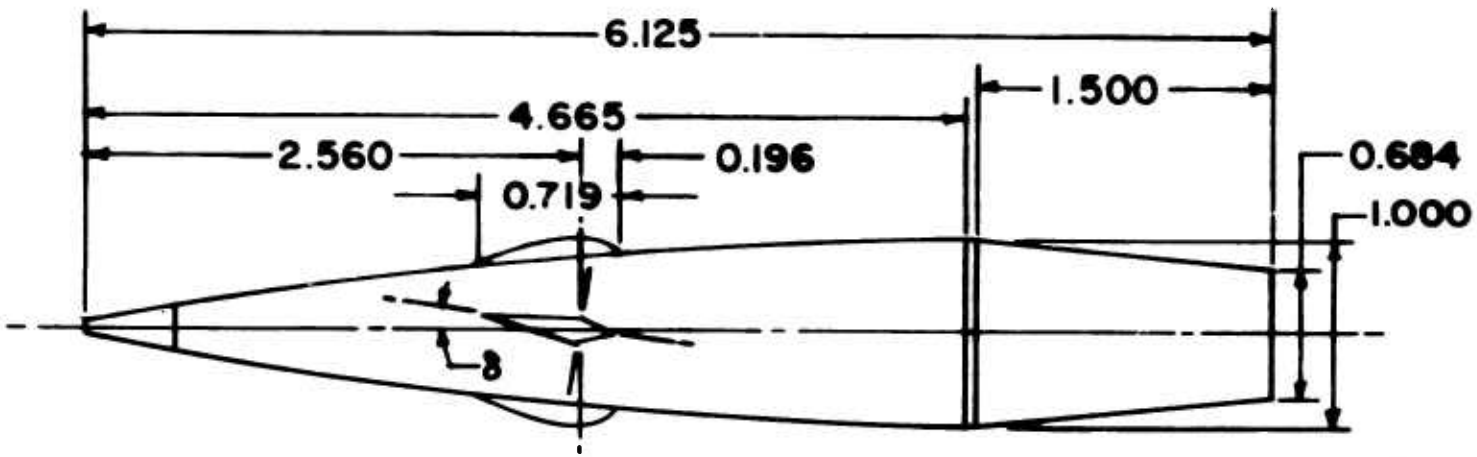

ALL DIMENSIONS IN CALIBERS

REFERENCE DIAMETER: 1 CALIBER = 5.715 cm

RADIUS OF OGIVE: 25.266 CALIBERS

ANGLE OF NUBS [δ]: 0°, 7°, 11°, 15°

Figure 2. Model Geometry

Table II. Test Conditions

Mach Number	1.75	2.00	2.25	2.50
Total Pressure - cm Hg	114	126	142	161
Re/cm x 10^{-6}	0.20	0.20	0.20	0.20

A boundary-layer trip (No. 80 abrasive powder, sparsely populated, 8mm wide) was glued onto the model 12.5 mm from the nose in all of these runs. Base pressures were measured through a pair of tubes of 1.59 mm I.D. mounted on the top and bottom of the supporting strut.

1. Magnus Force Test. Configurations 83.07, 83.11 and 83.15 were subjected to a spin test to measure the Magnus force and the Magnus moment. Data were obtained for all runs over a spin range of at least 10,000 rpm above or below the auto-spin rate (which the canting of the bore riders produces) and at all even angles of attack from +14 to -6 degrees. The data were taken either while the model was coasting down or up, depending on whether the model had been spun-up to its maximum or slowed down to its minimum spin rate, respectively. The limits of these spin rates were dictated by the available pressure of the air supply and the efficiency of the turbine.

The raw data were reduced to coefficient form on the BRL computer (BRLESC) using our standard program for Magnus tests. A linear regression was performed on the side-force and yawing-moment data of each run. A translational and rotational correction was applied to the side-force and yawing-moment data such that the regression of the data at zero angle of attack was reduced to zero. Additional corrections may be indicated depending on the further analysis of these data.

2. Static Force Test. Configurations 80.00, 83.00 and 83.07 underwent a static force test (no spin). The angle of attack was varied from +14 to -6 degrees. A sample reading was taken by the data acquisition system automatically every two seconds corresponding approximately to a change of one quarter of a degree in the angle of attack of the model.

The raw data were reduced to coefficient form on the BRL computer (BRLESC) using our standard program for this purpose. The angles of attack were corrected for strut deflections due to aerodynamic loads and for the flow inclination in the wind tunnel. The derivatives of the normal force and of the pitching moment near zero angle of attack were obtained from a linear regression of the eleven test points between +1.5 and -1.5 degrees. The yaw plane data from these static tests were not corrected for strut deflections and flow inclinations.

III. RESULTS

The data are presented in non-dimensionalized form. The side-force coefficient, C_Y, and the yawing-moment coefficient, C_n, from the Magnus tests are plotted versus spin rate, PD/V, in Figures A1 and A2, respectively, for the bore-rider configurations with cant of the nubs of 7, 11 and 15 degrees. The uncorrected yaw data from the static tests (C_Y and C_n) are plotted versus angle of attack, α, in Figures A3 and A4, respectively, for the model configurations without bore riders and with bore riders at 0° and 7° cant. The curves of the side force and of the yawing moment due to spin do not pass through the origin of the plot (Figures A1 and A2) because the canted bore riders produce a side force at zero spin (Figures A3 and A4). However, for each configuration, Mach number, and angle of attack, there exists a spin rate at which the side force and the yawing moment are zero. For this situation, the Magnus coefficients are no longer independent of the spin rate and cannot be represented as a constant (i.e. the slope of the data curve) at a given angle of attack and Mach number. Although not specifically shown in this report, it should be noted that the center of pressure of the side forces generated by the nubs at zero spin and angle of attack lies well behind the nub position and in the vicinity of the Magnus-force center of pressure. These effects have been observed previously for helical serrations on bullets and are reported in reference 3.

The normal-force coefficient, C_N, the pitching-moment coefficient, C_m, the base-axial-force coefficient, C_{Ab}, and the forebody-axial-force coefficient, C_{Af}, are plotted versus angle of attack in Figures A5, A6 and A7. The slope of the normal-force curve, $C_{N\alpha}$, the normal-force center of pressure, N_{cp}, the forebody-axial-force coefficient, C_{Af}, and the base-axial-force coefficient, C_{Ab}, were determined for angles of attack near zero lift and are tabulated in Table III.

Table III. Summary Data

Configuration	Mach No.	$C_{N\alpha}$	N_{cp}	C_{Af}	C_{Ab}
80.00	1.75	0.0333	1.60	0.162	0.023
	2.00	0.0356	1.84	0.151	0.035
	2.25	0.0371	2.00	0.134	0.035
	2.50	0.0388	2.15	0.127	0.033
83.00	1.75	0.0411	1.80	0.180	0.034
	2.00	0.0437	2.01	0.170	0.039
	2.25	0.0461	2.18	0.153	0.038
	2.50	0.0477	2.37	0.144	0.037

Table III. Summary Data (Continued)

Configuration	Mach No.	$C_{N\alpha}$	N_{cp}	C_{Af}	C_{Ab}
83.07	1.75	0.0419	1.81	0.183	0.039
	2.00	0.0448	2.03	0.172	0.044
	2.25	0.0472	2.18	0.156	0.043
	2.50	0.0490	2.31	0.147	0.041
83.11	1.75	0.0426	1.82	0.184	0.040
	2.00	0.0454	1.87	0.174	0.045
	2.25	0.0473	2.18	0.159	0.042
	2.50	0.0492	2.31	0.149	0.041
83.15	1.75	0.0421	1.84	0.190	0.038
	2.00	0.0447	2.04	0.179	0.043
	2.25	0.0464	2.17	0.162	0.041
	2.50	0.0493	2.31	0.155	0.039

As could be expected, both the normal force and the forebody axial force of the projectile are increased by the bore riders. The increase in the forebody axial force amounts to 17 to 22% of the basic model (without bore riders) within the Mach number range of the test (M = 1.75 to 2.50).

In Figure 3, the zero-lift, axial-force coefficients of various artillery shells are compared with the results of the present study.

The 155mm projectile M101[4] is a conventionally designed and frequently used artillery shell. The geometry of this shell is composed of a 2.69-caliber ogive nose, a 1.39-caliber cylindrical section with rotating band and a 0.45-caliber, 8-degree boattail. The zero-lift, axial-force coefficients of the M101 shell range from 0.311 (at M = 1.75) to 0.251 (at M = 2.50). They were measured in BRL's large and small free flight ranges at Reynolds numbers of $Re_\ell = 15.8 \times 10^6$ for a full-scale model and $Re_\ell = 1.3 \times 10^6$ for a 1/12-scale model. The data for both models show good agreement at supersonic velocities.

The 175mm projectile M437[5] is a low-drag shell of conventional design. The shape of this shell consists of a 2.91-caliber ogive nose, a 1.6-caliber cylindrical body with rotating band and a one-caliber, 8-degree boattail. Its zero-lift, axial-force coefficients of 0.262 to 0.211 over the Mach number range of the test (M = 1.75 to 2.50) present a significant improvement in drag over that of the M101 projectile. In a more recent study[6], the zero-lift, axial-force coefficients of a family of low-drag shell with similar shapes--105mm XM380, T388, and 155mm XM387--were compared. These coefficients lie between those of the M101 and the M437 projectiles.

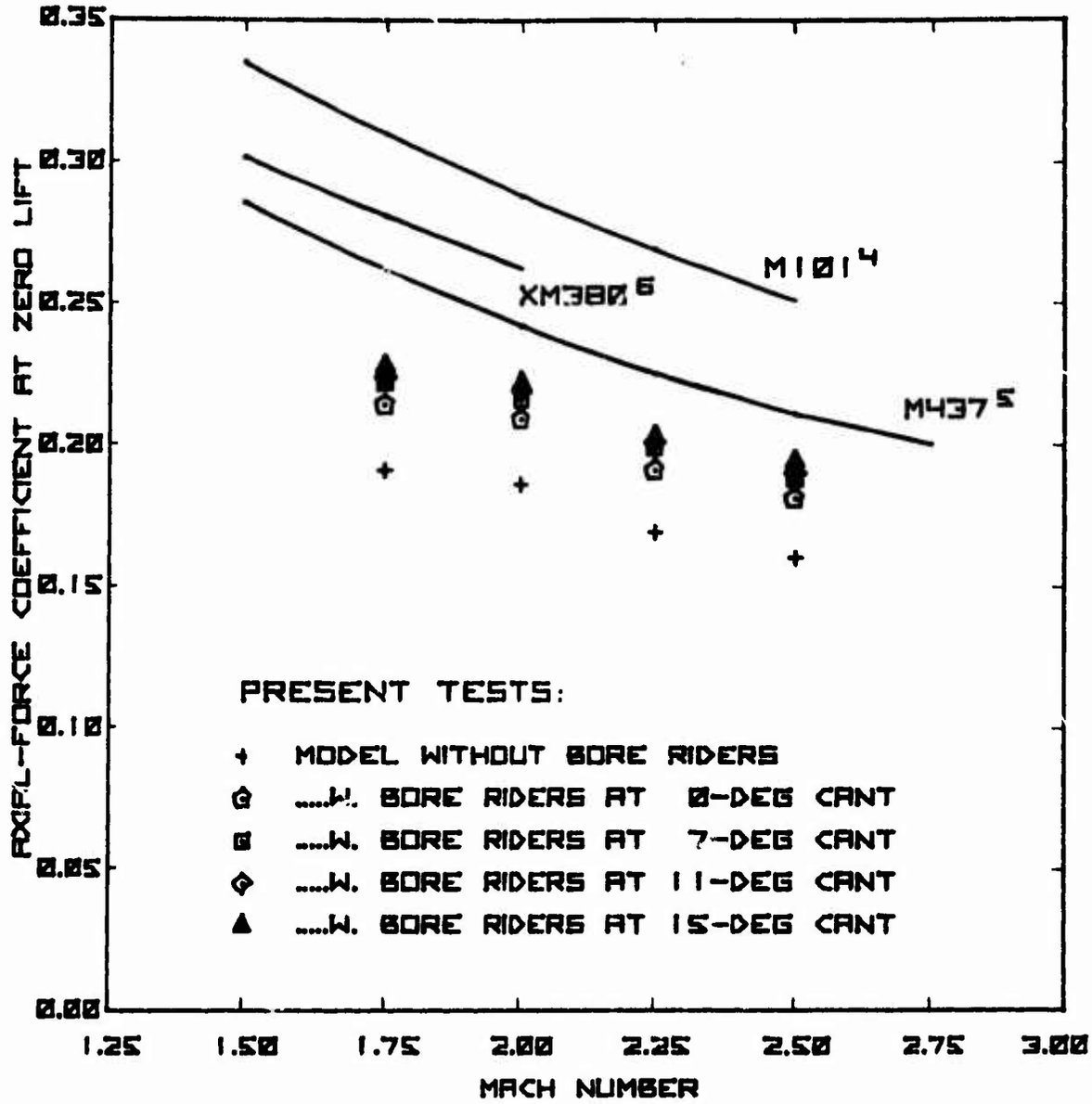

Figure 3. Comparison of the Zero-Lift, Axial-Force Coefficients of Various Artillery Shells With the Results of This Study

The highest zero-lift, axial-force coefficients ($C_{Af} + C_{Ab}$) which were measured in the present investigation range from 0.228 (at M = 1.75) to 0.194 (at M = 2.50) at a Reynolds number, $Re_{\ell} = 7 \times 10^6$, held constant over the range of the wind tunnel test. These values pertain to the model configuration with bore riders of 15-degree cant spinning at the experimental auto-spin rate, which is produced by the cant of the bore riders. This auto-spin rate lies within 16% of the matched-spin rate, PD/V = 2 tan δ; and within this range, the drag coefficients are nearly constant. Nevertheless, the drag coefficient is still lower for the configuration with zero-cant of the bore riders and no spin. This test condition simulates the actual flight condition of the spinning shell with matched cant of the bore riders.

In all cases of the present investigation, however, the drag is less than that of the conventional and low-drag projectiles used in the comparison, and thus it appears that the advantage of the long-ogive, low-drag shape is not nullified by the necessary bore riders.

REFERENCES

1. Eugene D. Boyer, "A Limited Aerodynamic Test of a 175-mm Extended Range Subcaliber Projectile," BRL Memorandum Report No. 2160, U.S. Army Ballistic Research Laboratories, Aberdeen Proving Ground, Maryland, March 1972. AD 893228L.

2. J. C. McMullen, "Wind Tunnel Testing Facilities at the Ballistic Research Laboratories," BRL Memorandum Report No. 1292, U.S. Army Ballistic Research Laboratories, Aberdeen Proving Ground, Maryland, July 1960. AD 244180.

3. M. A. Sylvester and W. F. Braun, "The Influence of Helical Serrations and Bullet Engraving on the Aerodynamic and Stability Properties of a Body of Revolution With Spin," BRL Report No. 1514, U.S. Army Ballistic Research Laboratories, Aberdeen Proving Ground, Maryland, November 1970. AD 719235.

4. B. G. Karpov, L. E. Schmidt, K. S. Krial and L. C. MacAllister, "The Aerodynamic Properties of the 155mm Shell M101 From Free Flight Range Tests of Full Scale and 1/12 Scale Models," BRL Memorandum Report No. 1582, U.S. Army Ballistic Research Laboratories, Aberdeen Proving Ground, Maryland, June 1964. AD 454925.

5. E. R. Dickinson and D. H. McCoy, "The Zero-Yaw Drag Coefficient for the Projectile 175mm, HE, M437," BRL Memorandum Report No. 1568, U.S. Army Ballistic Research Laboratories, Aberdeen Proving Ground, Maryland, March 1964. AD 443811.

6. K. S. Krial and L. C. MacAllister, "Aerodynamic Properties of a Family of Shell of Similar Shape--105mm XM380E5, XM380E6, T388 and 155mm T387," BRL Memorandum Report No. 2023, U.S. Army Ballistic Research Laboratories, Aberdeen Proving Ground, Maryland, February 1970. AD 866610.

APPENDIX

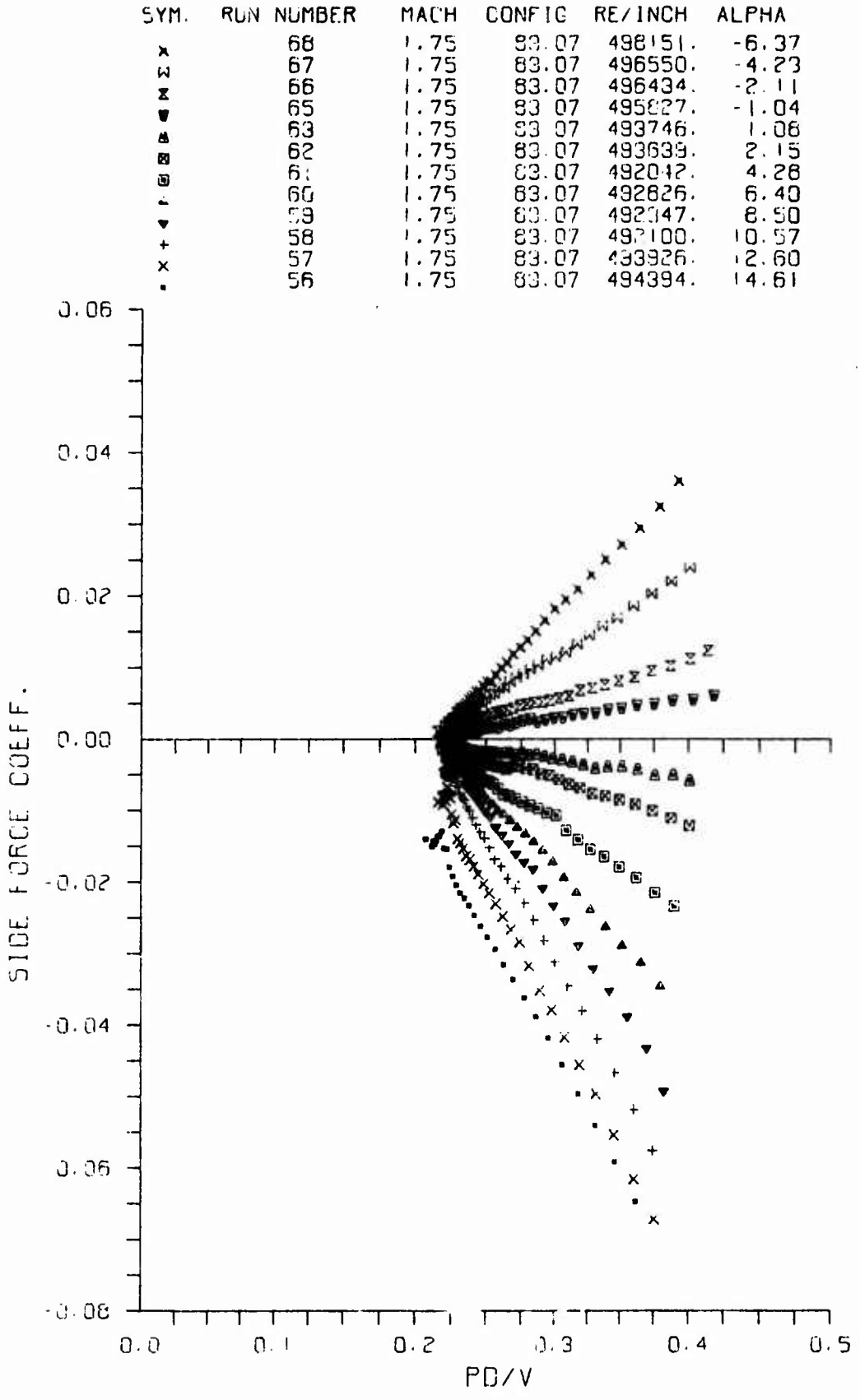

a-1. Model Configuration with 7° Bore-Rider Cant (83.07)--
Mach Number 1.75

Figure A1. Side-Force Coefficient versus Spin Rate

Preceding page blank

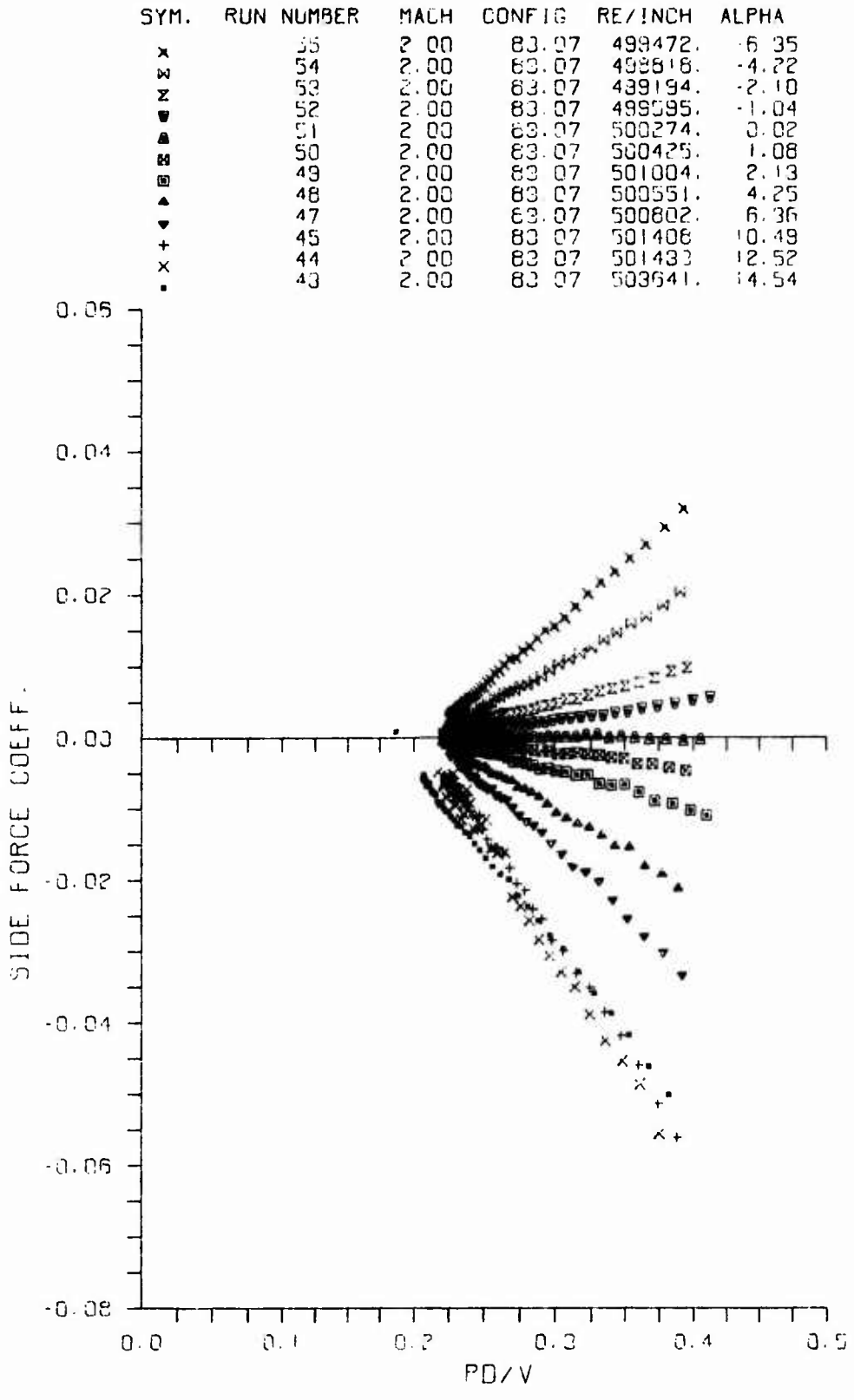

a-2. Model Configuration with 7° Bore-Rider Cant (83.07)-- Mach Number 2.00

Figure A1. Continued

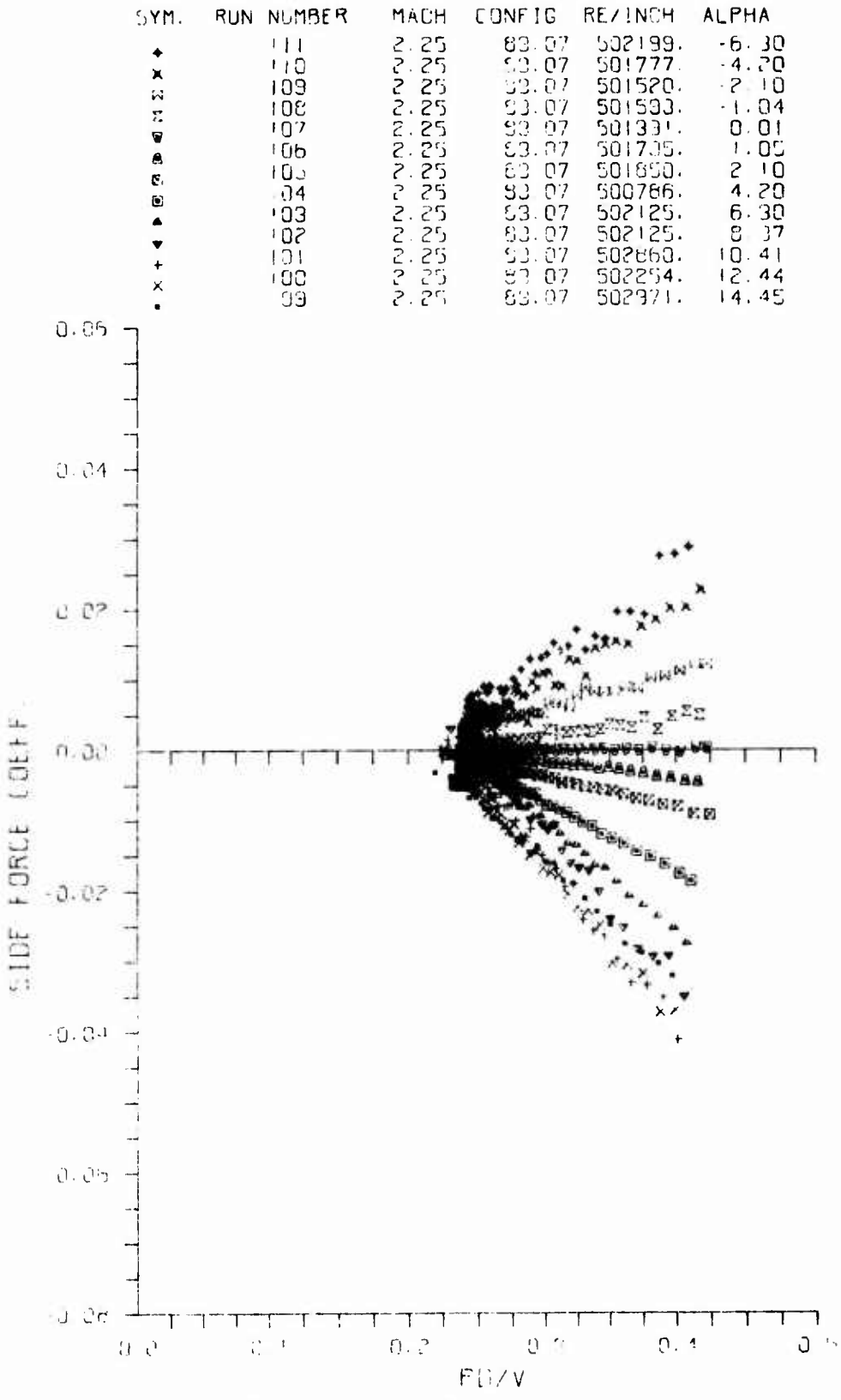

a-3. Model Configuration with 7° Bore-Rider Cant (83.07)-- Mach Number 2.25

Figure A1. Continued

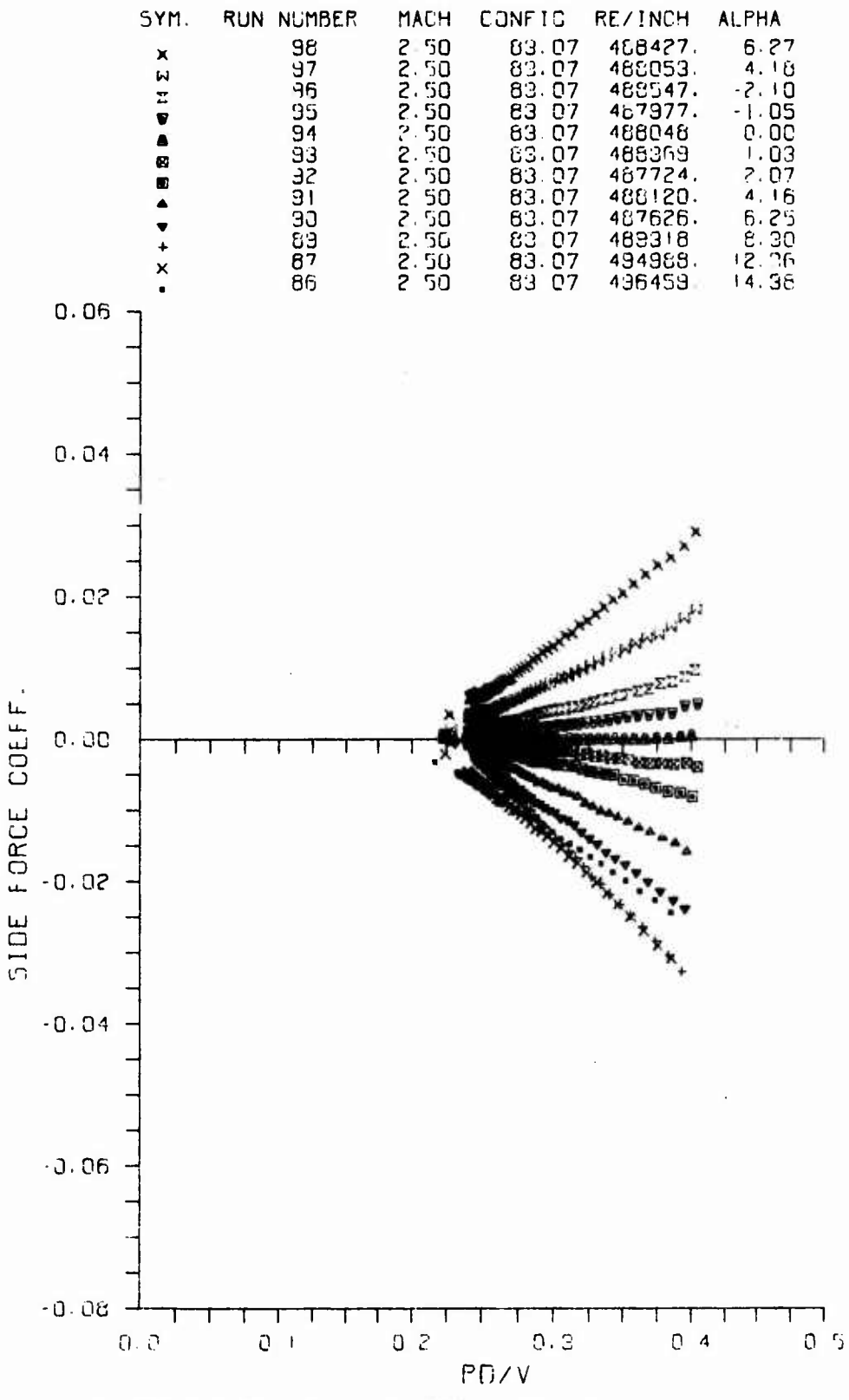

a-4. Model Configuration with 7° Bore-Rider Cant (83.07)-- Mach Number 2.50 (over-spin)

Figure A1. Continued

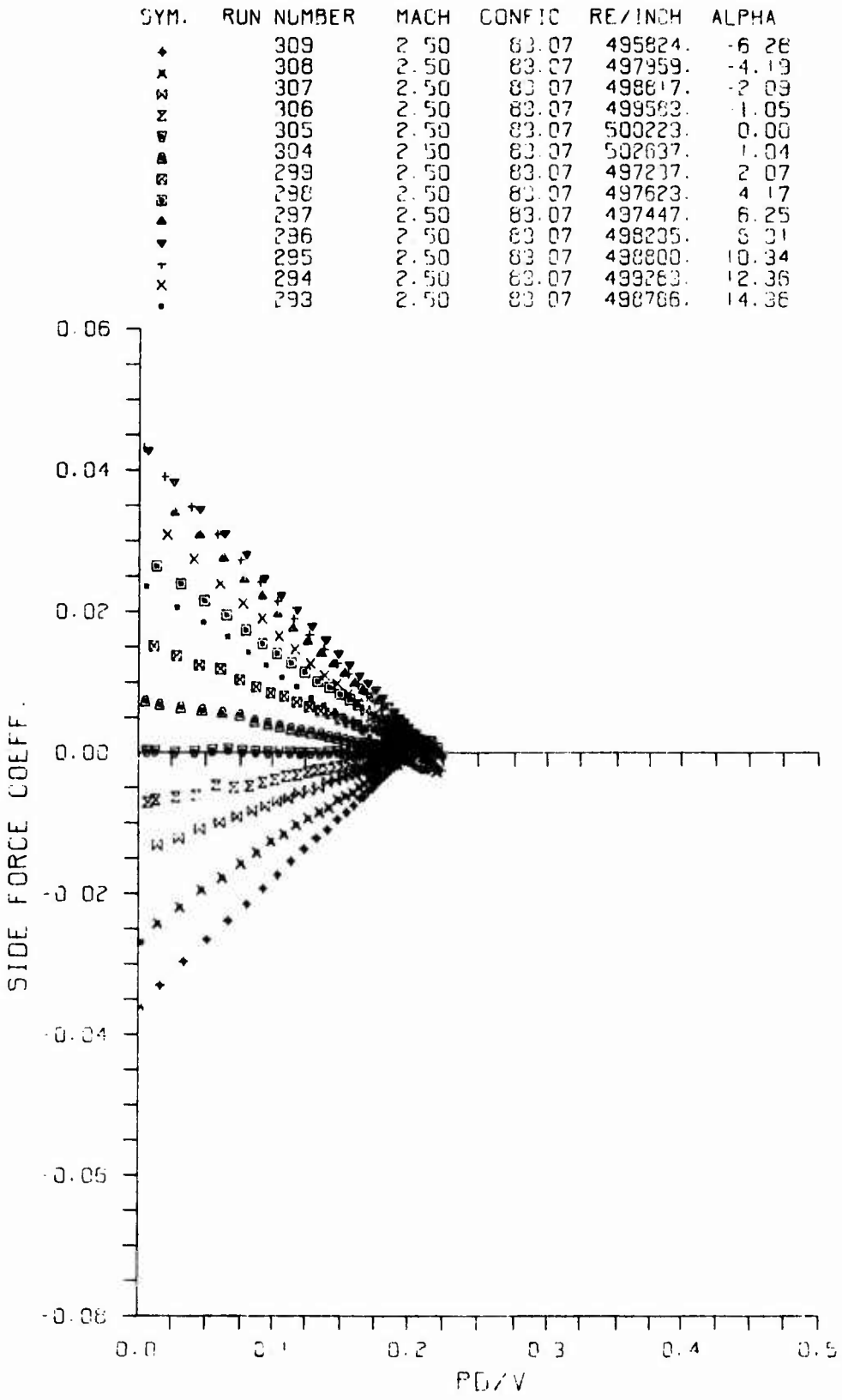

a-5. Mode' Configuration with 7° Bore-Rider Cant (83.07)-- h Number 2.50 (under-spin)

Figure A1. Continued

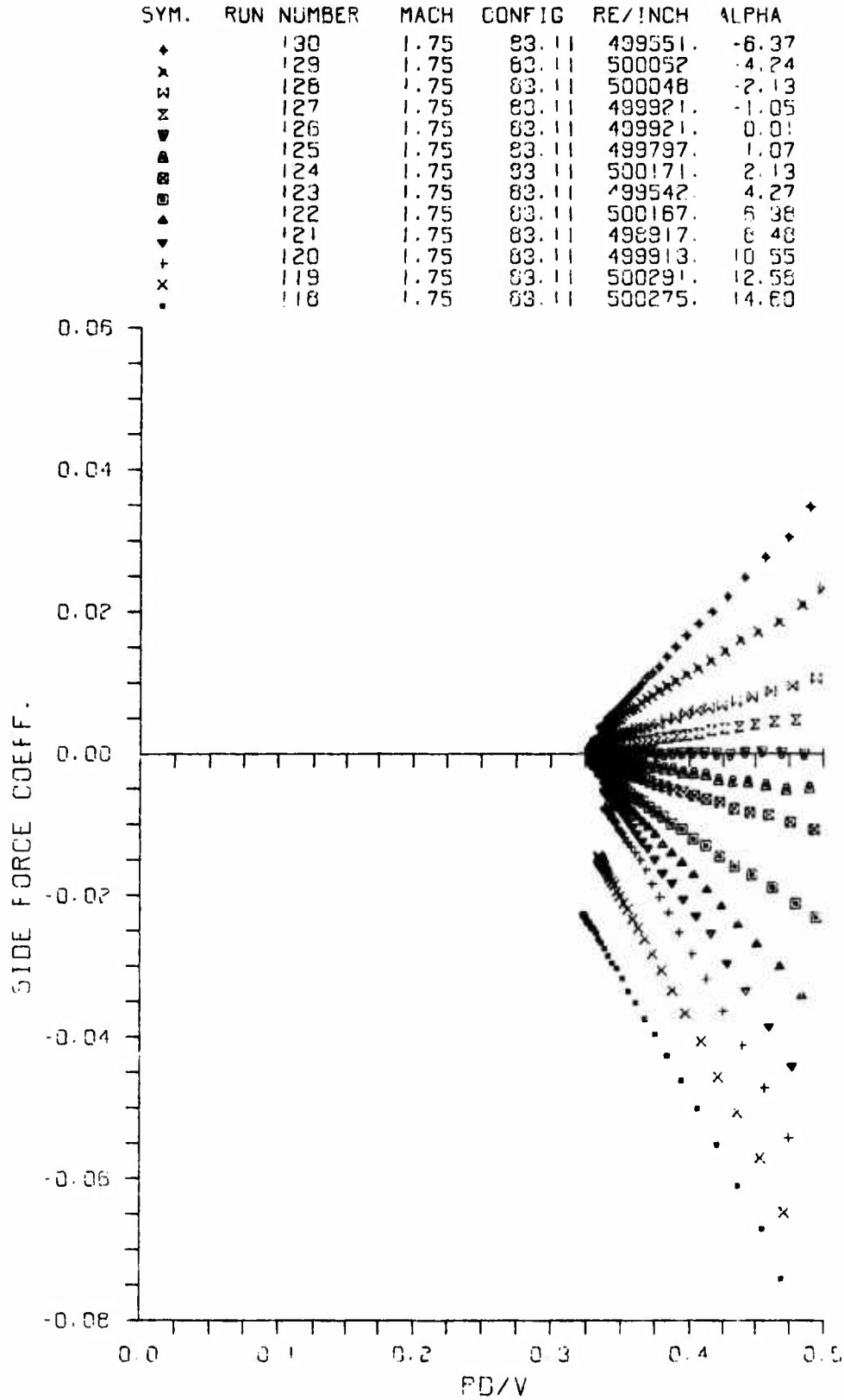

b-1. Model Configuration with 11° Bore-Rider Cant (83.11)-- Mach Number 1.75 (over-spin)

Figure A1. Continued

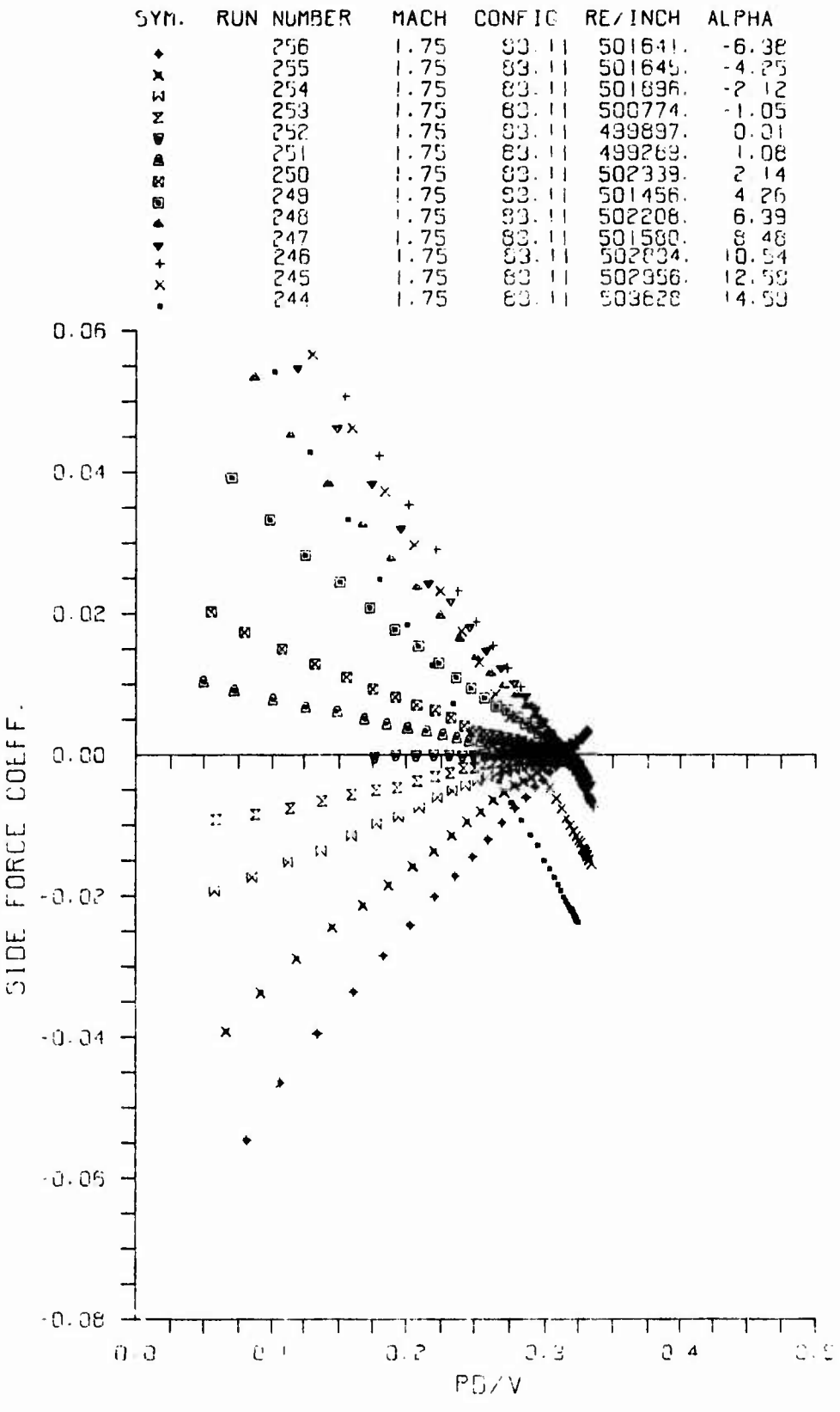

b-2. Model Configuration with 11° Bore-Rider Cant (83.11)-- Mach Number 1.75 (under-spin)

Figure A1. Continued

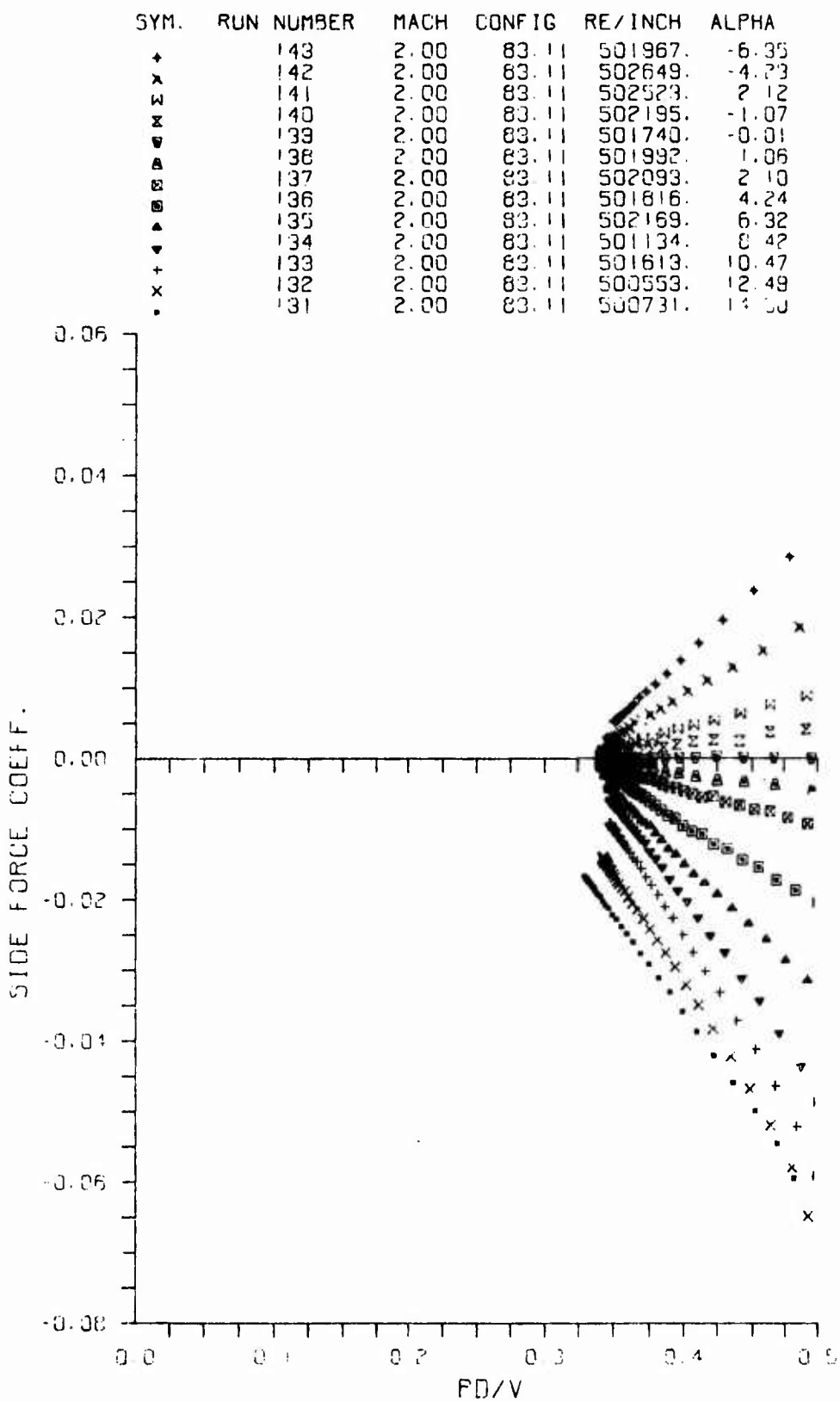

b-3. Model Configuration with 11° Bore-Rider Cant (83.11)-- Mach Number 2.00 (over-spin)

Figure A1. Continued

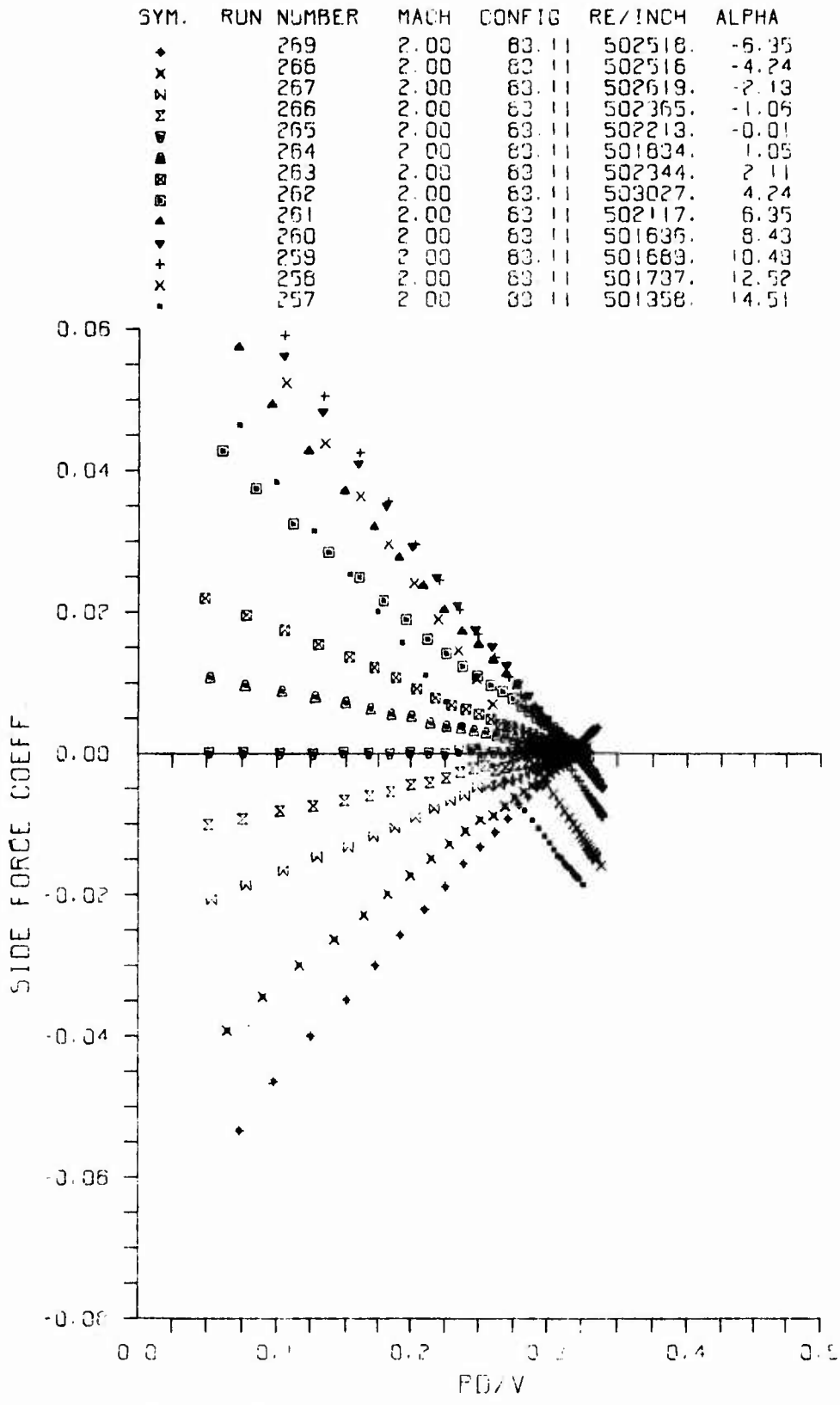

b-4. Model Configuration with 11° Bore-Rider Cant (83.11)-- Mach Number 2.00 (under-spin)

Figure A1. Continued

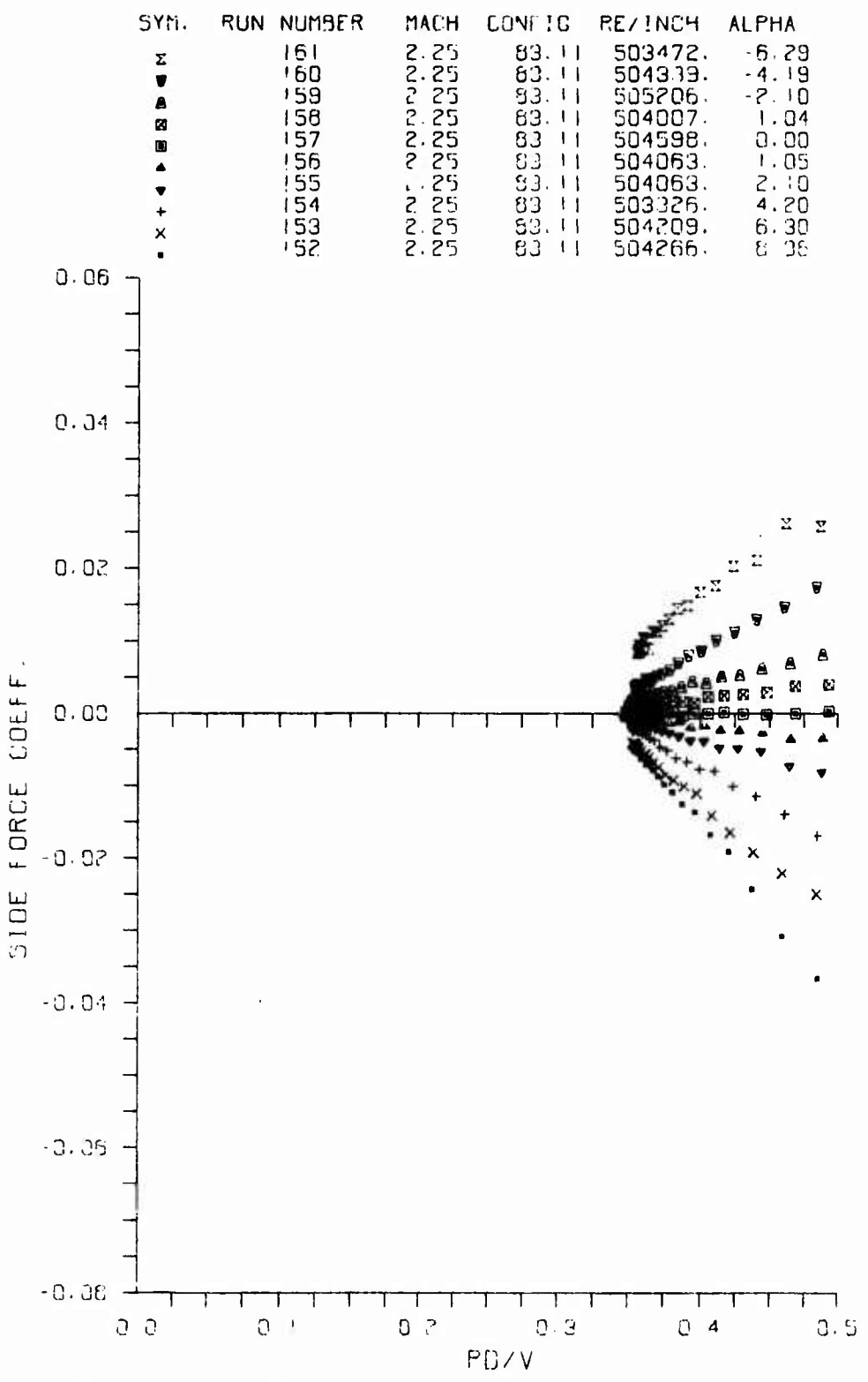

b-5. Model Configuration with 11° Bore-Rider Cant (83.11)-- Mach Number 2.25 (over-spin)

Figure A1. Continued

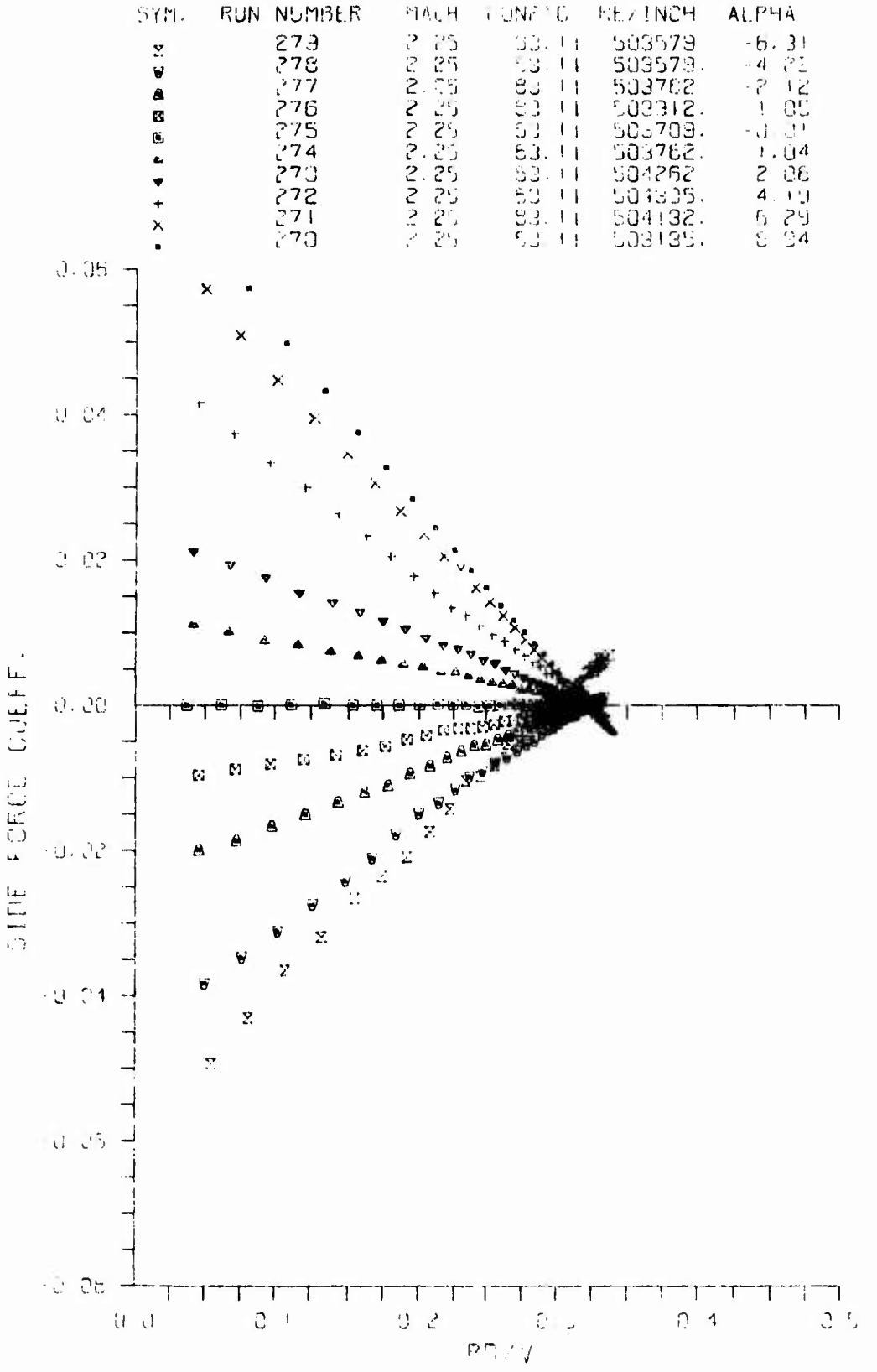

b-6. Model Configuration with 11° Bore-Rider Cant (83.11)-- Mach Number 2.25 (under-spin)

Figure A1. Continued

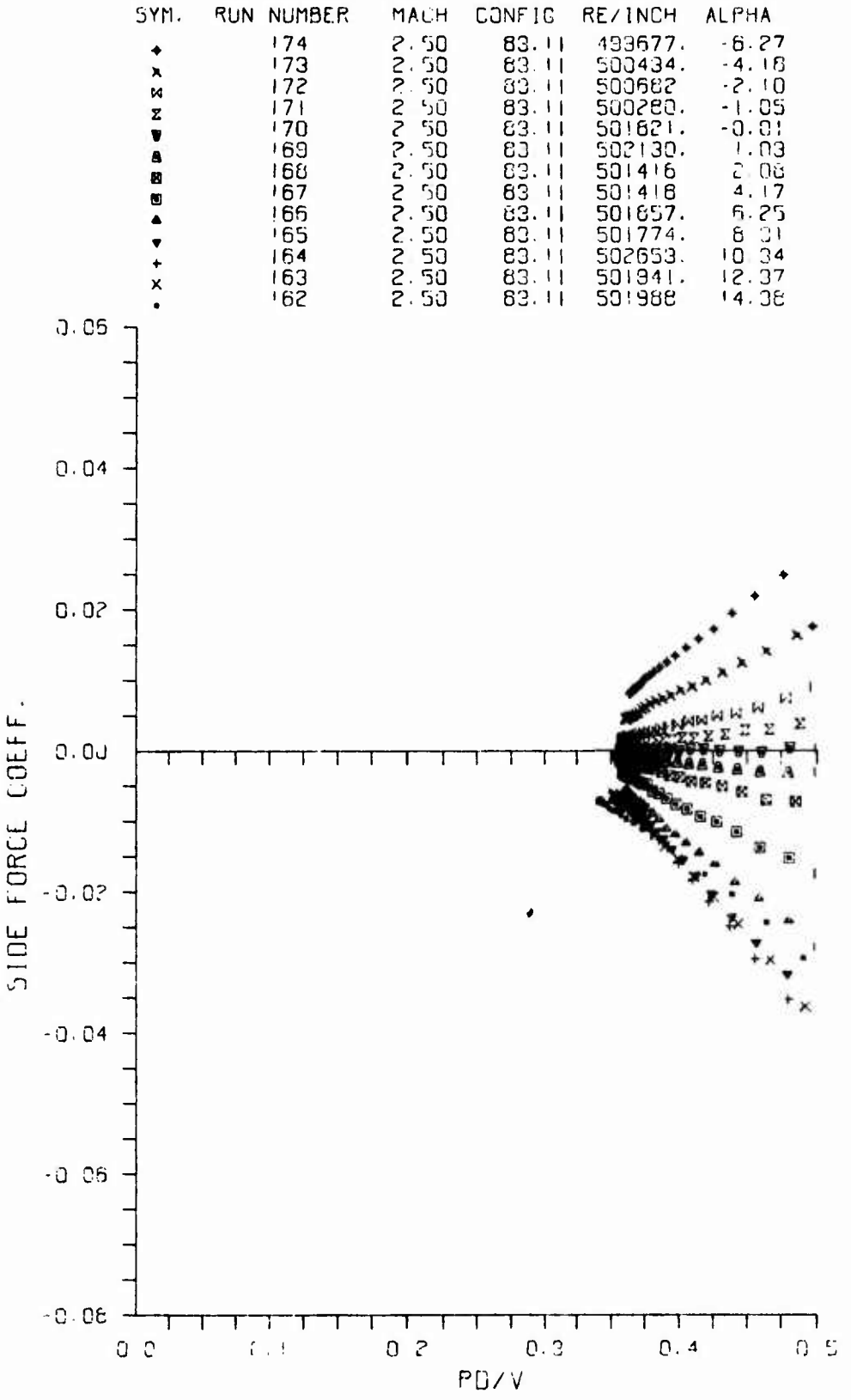

b-7. Model Configuration with 11° Bore-Rider Cant (83.11) Mach Number 2.50 (over-spin)

Figure A1. Continued

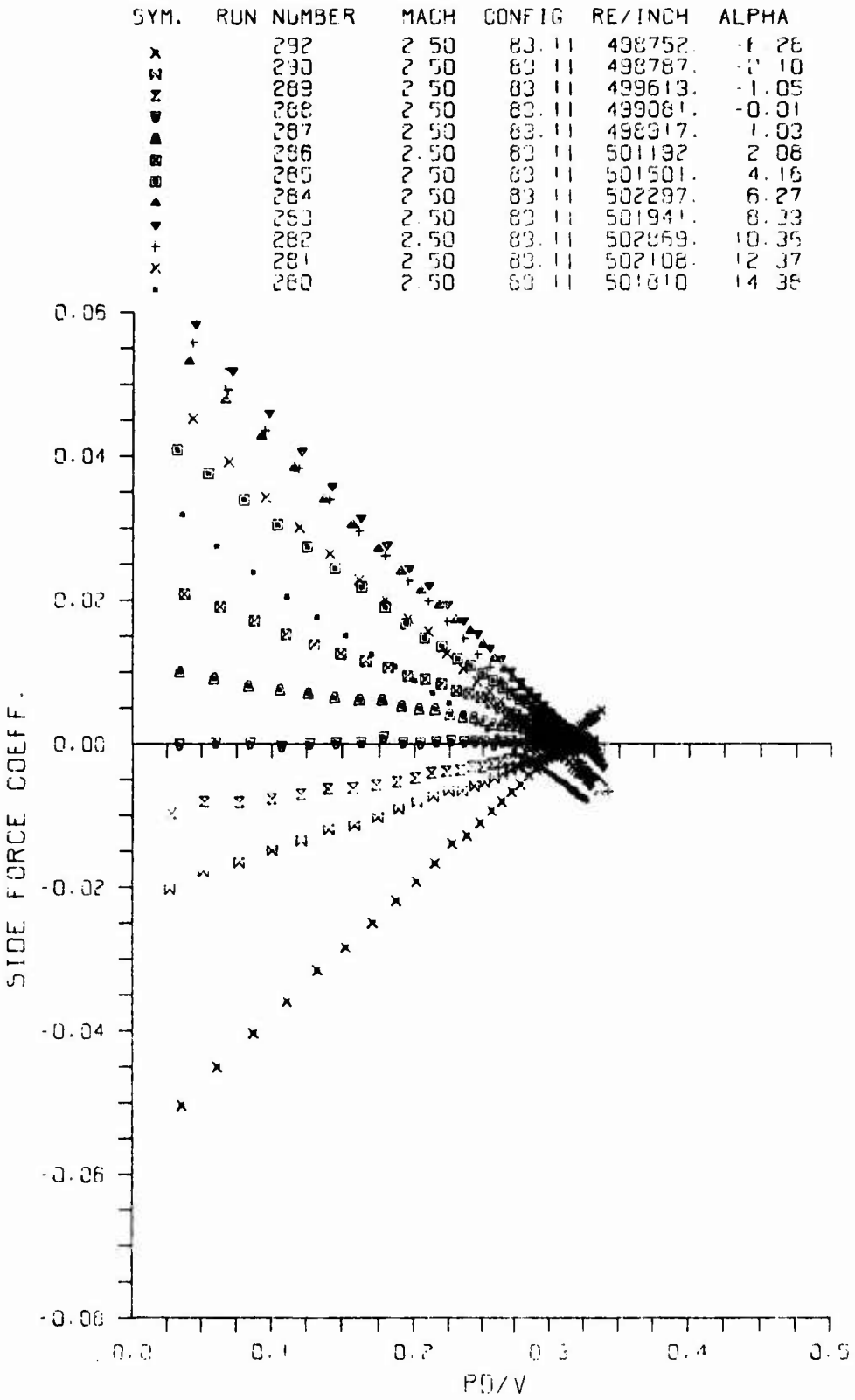

b-8. Model Configuration with 11° Bore-Rider Cant (83.11)-- Mach Number 2.50 (under-spin)

Figure A1. Continued

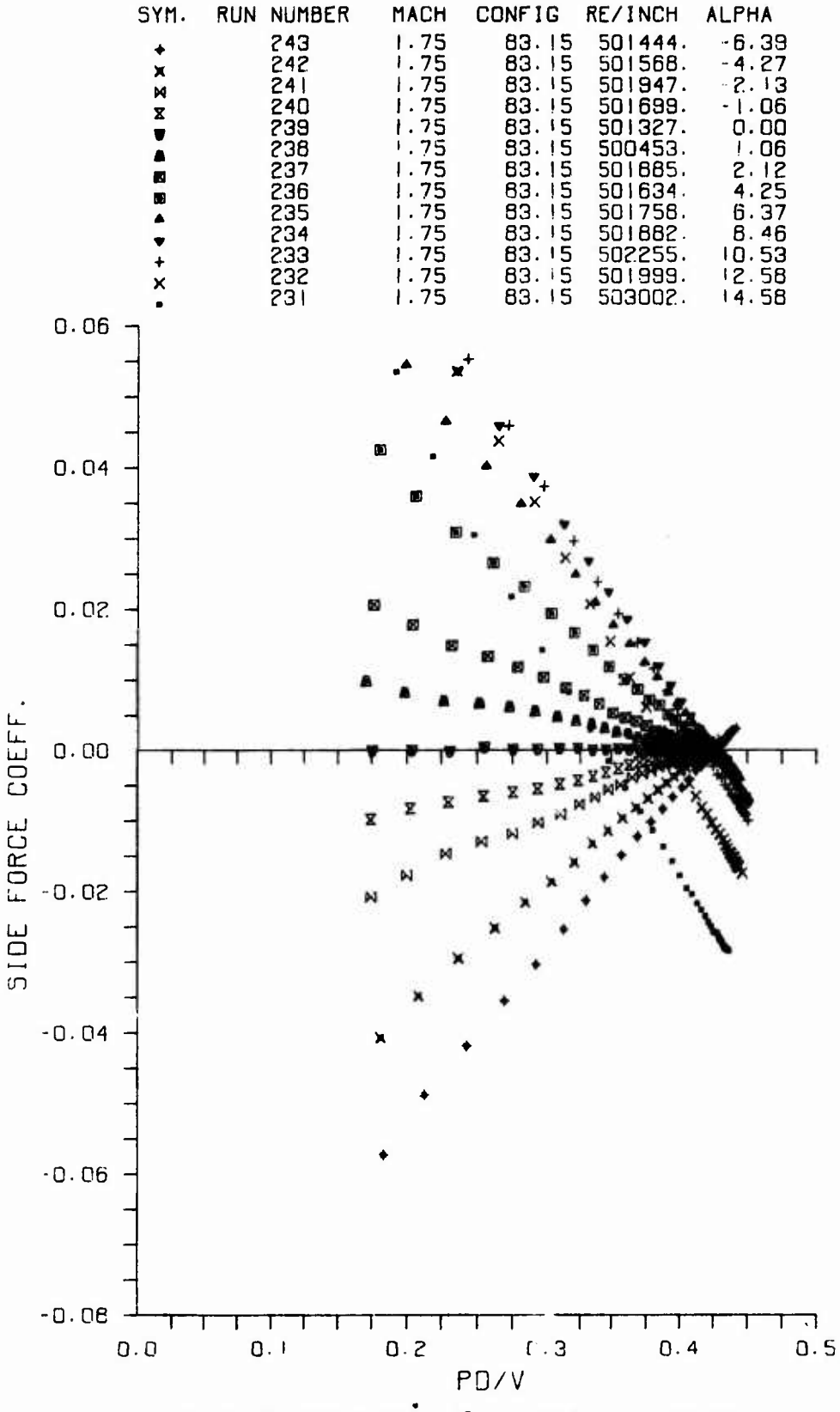

c-1. Model Configuration with 15° Bore-Rider Cant (83.15)--
Mach Number 1.75

Figure A1. Continued

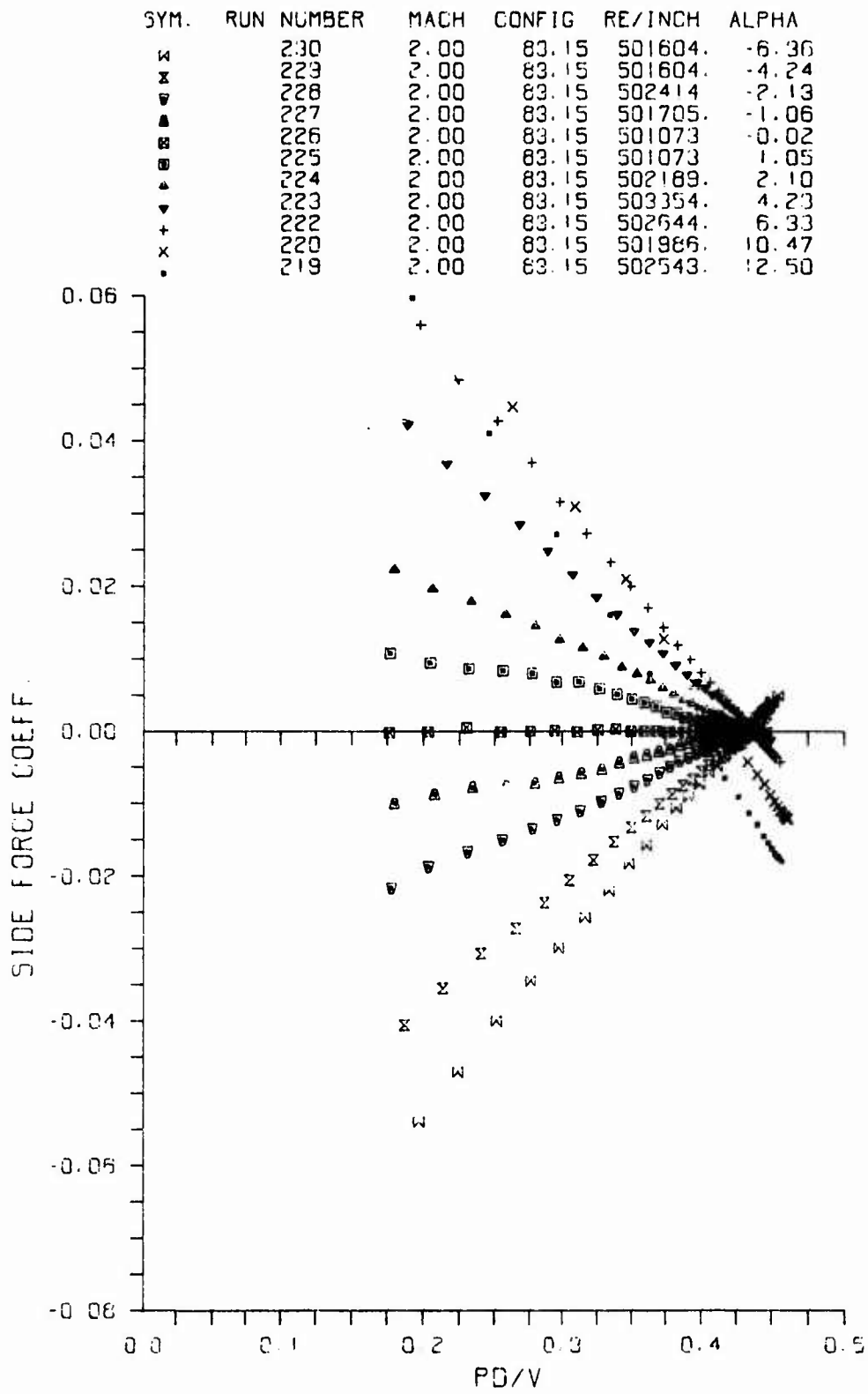

c-2. Model Configuration with 15° Bore-Rider Cant (83.15)-- Mach Number 2.00

Figure A1. Continued

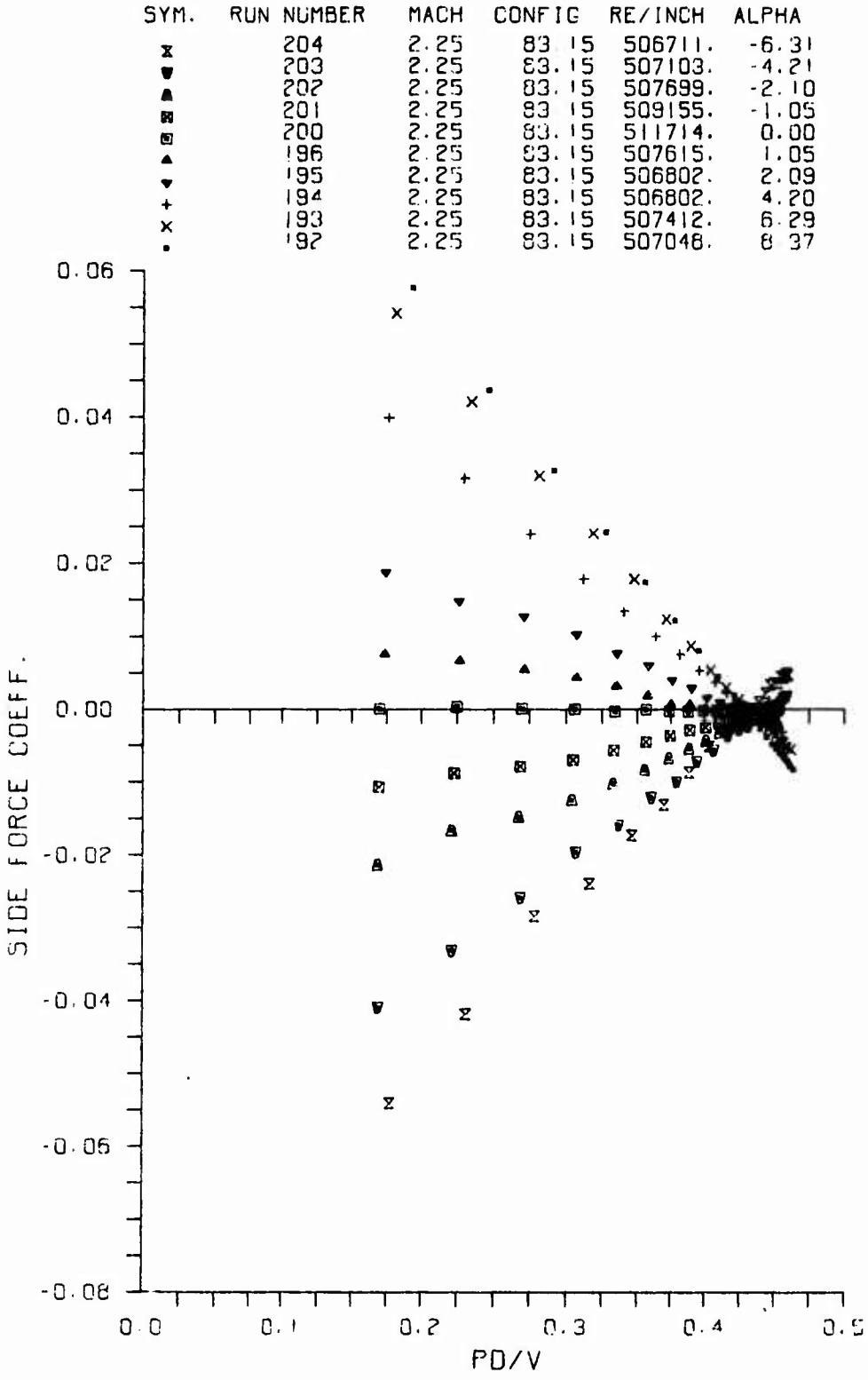

c-3. Model Configuration with 15° Bore-Rider Cant (83.15)-- Mach Number 2.25

Figure A1. Continued

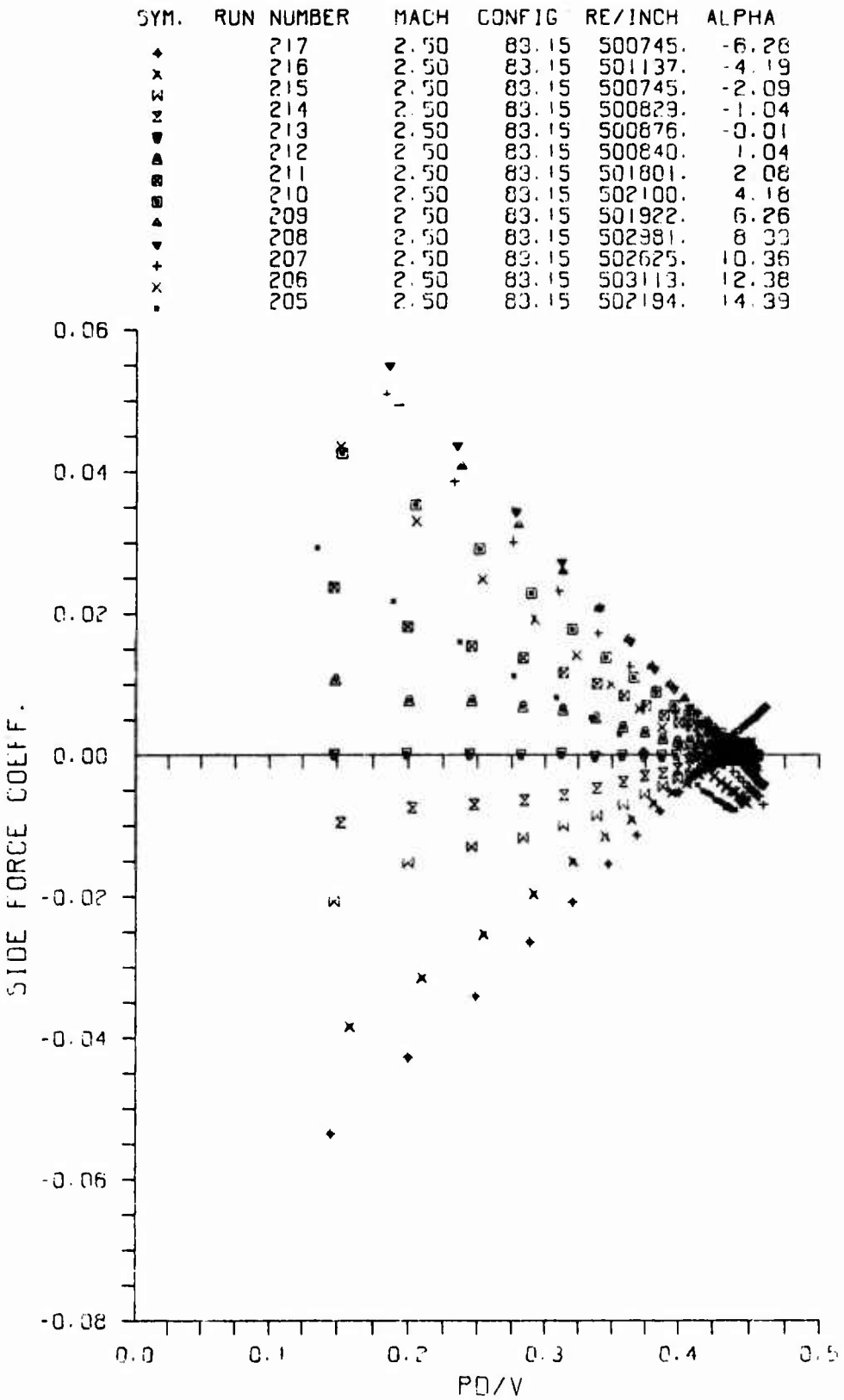

c-4. Model Configuration with 15° Bore-Rider Cant (83.15)-- Mach Number 2.50

Figure A1. Concluded

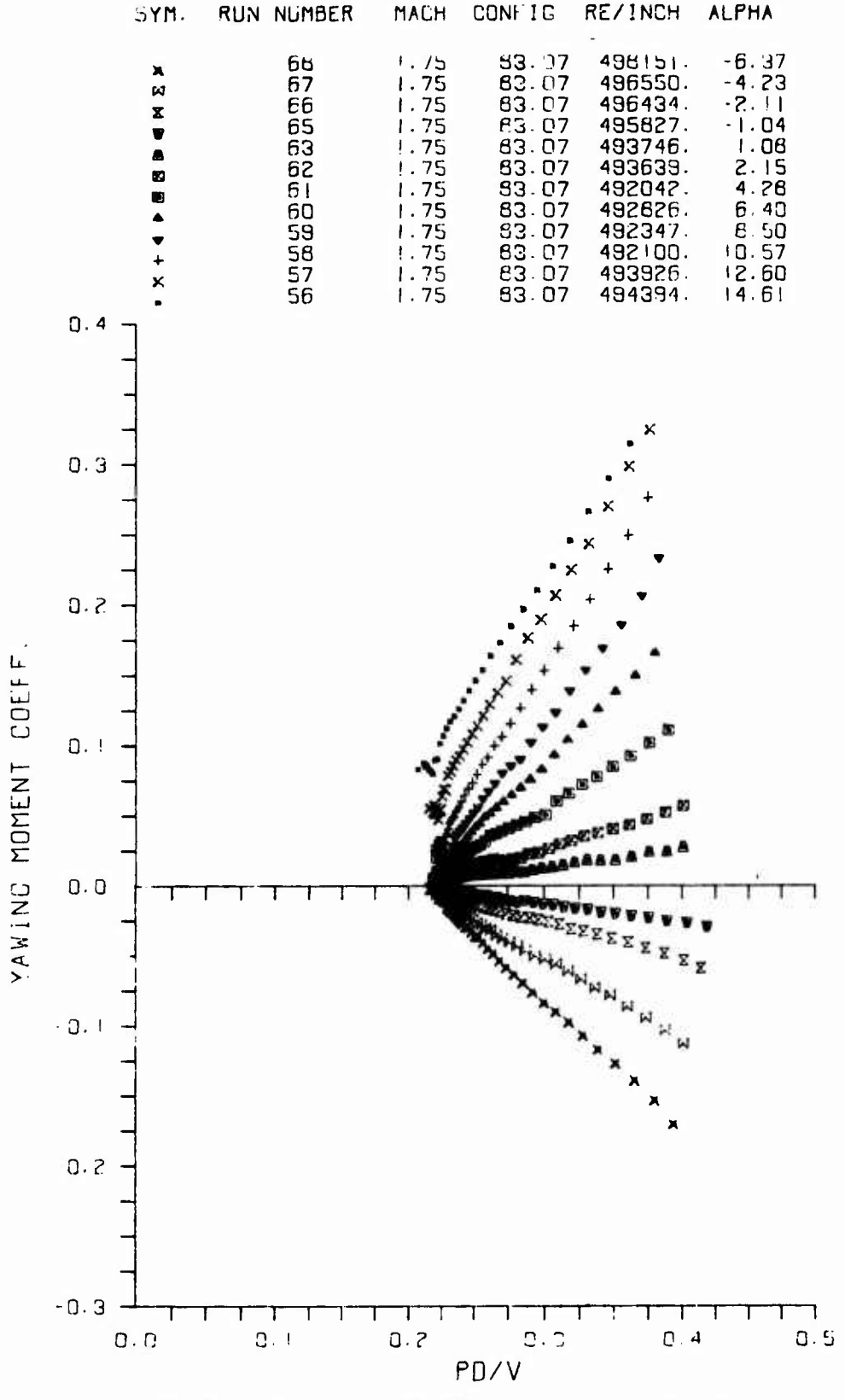

a-1. Model Configuration with 7° Bore-Rider Cant (83.07)-- Mach Number 1.75

Figure A2. Yawing-Moment Coefficient versus Spin Rate

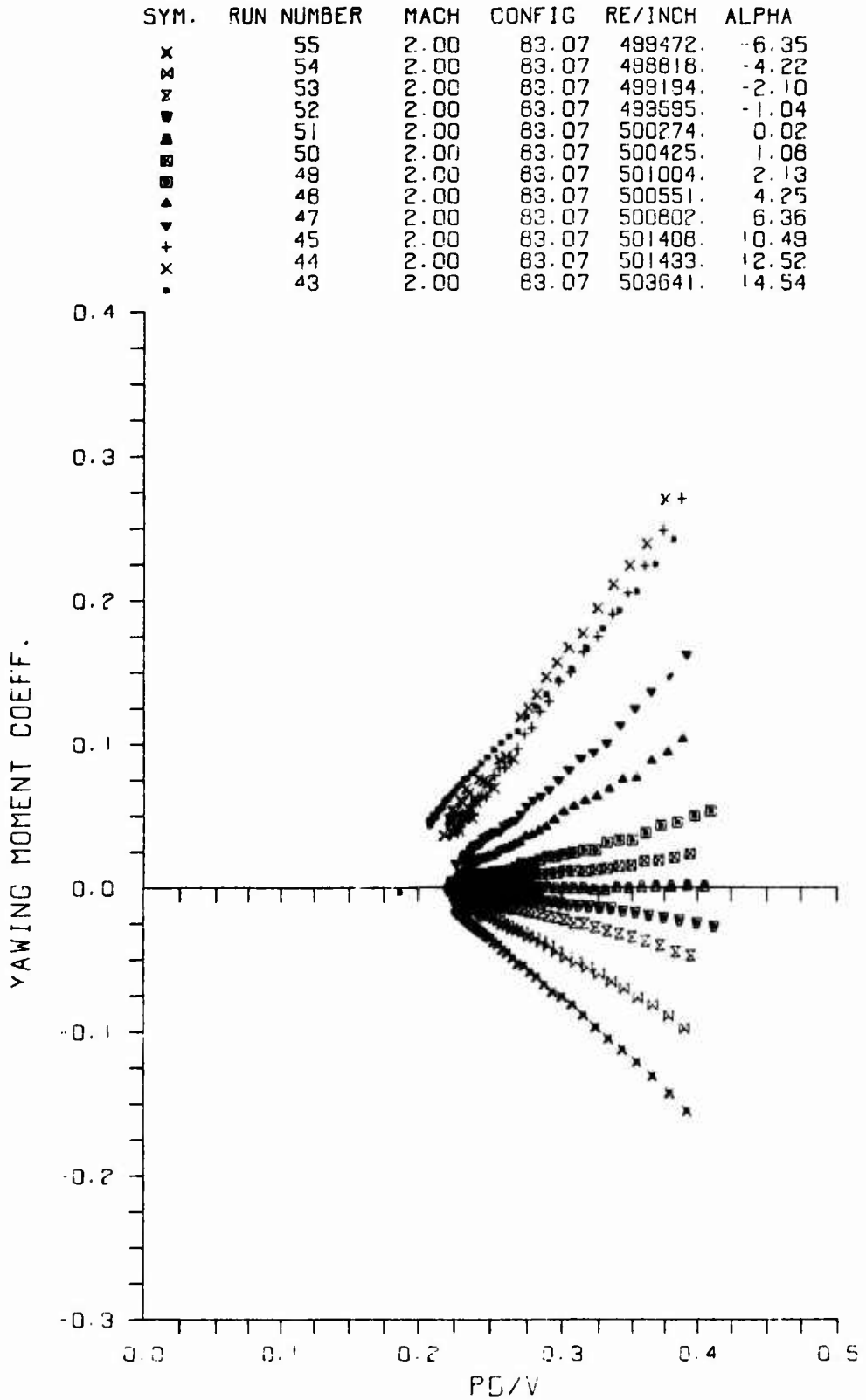

a-2. Model Configuration with 7° Bore-Rider Cant (83.07)-- Mach Number 2.00

Figure A2. Continued

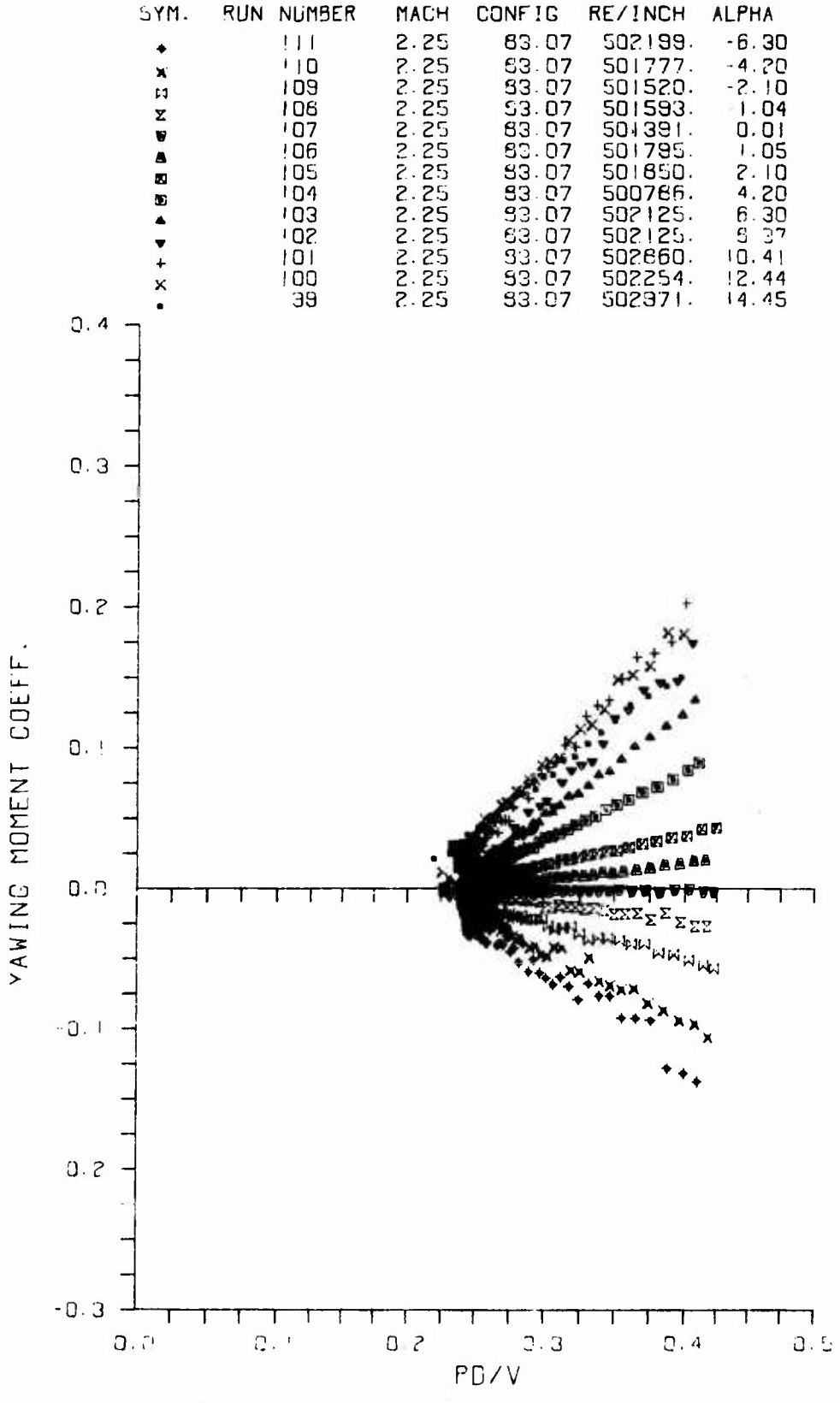

a-3. Model Configuration with 7° Bore-Rider Cant (83.07)-- Mach Number 2.25

Figure A2. Continued

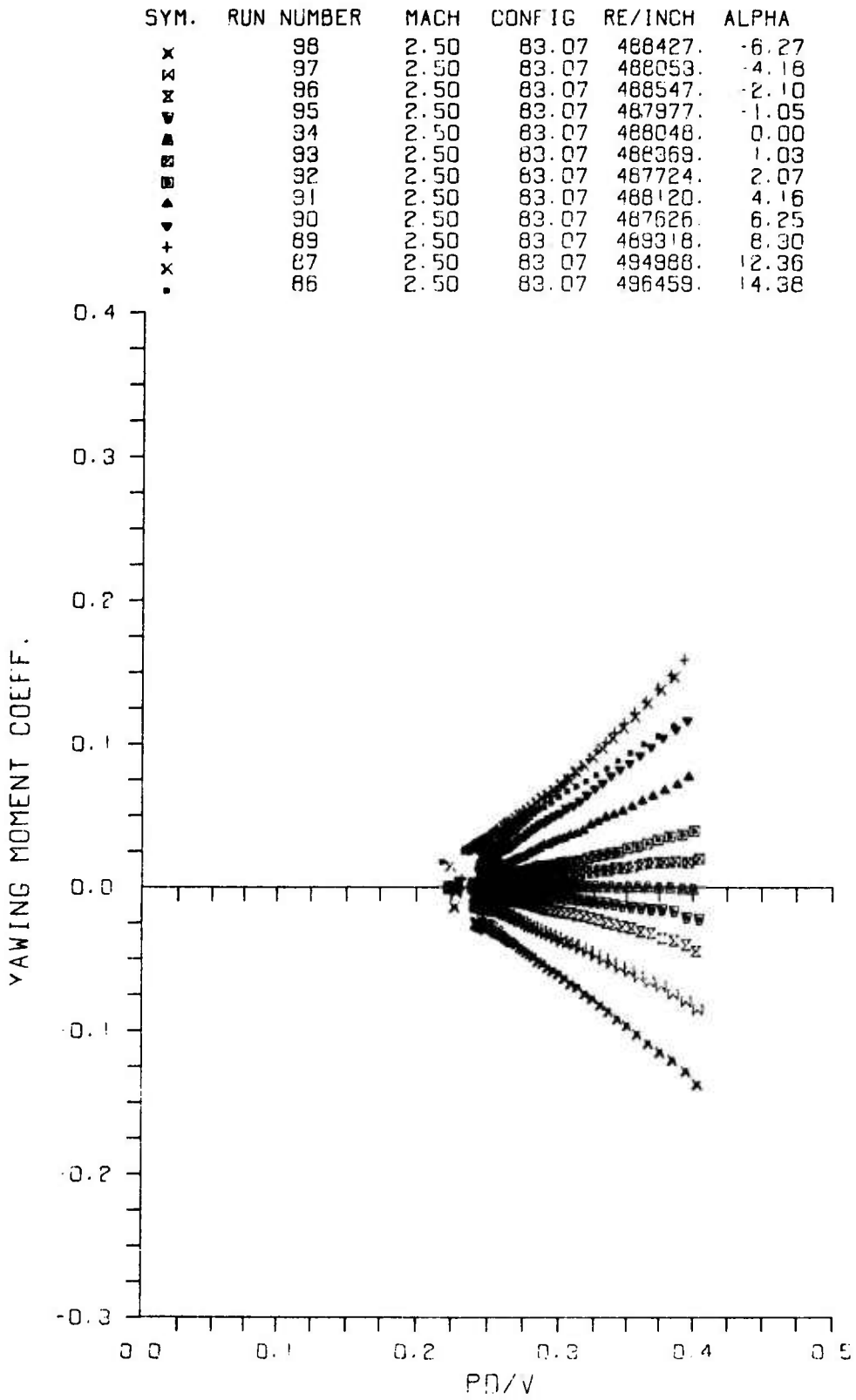

a-4. Model Configuration with 7° Bore-Rider Cant (83.07)-- Mach Number 2.50 (over-spin)

Figure A2. Continued

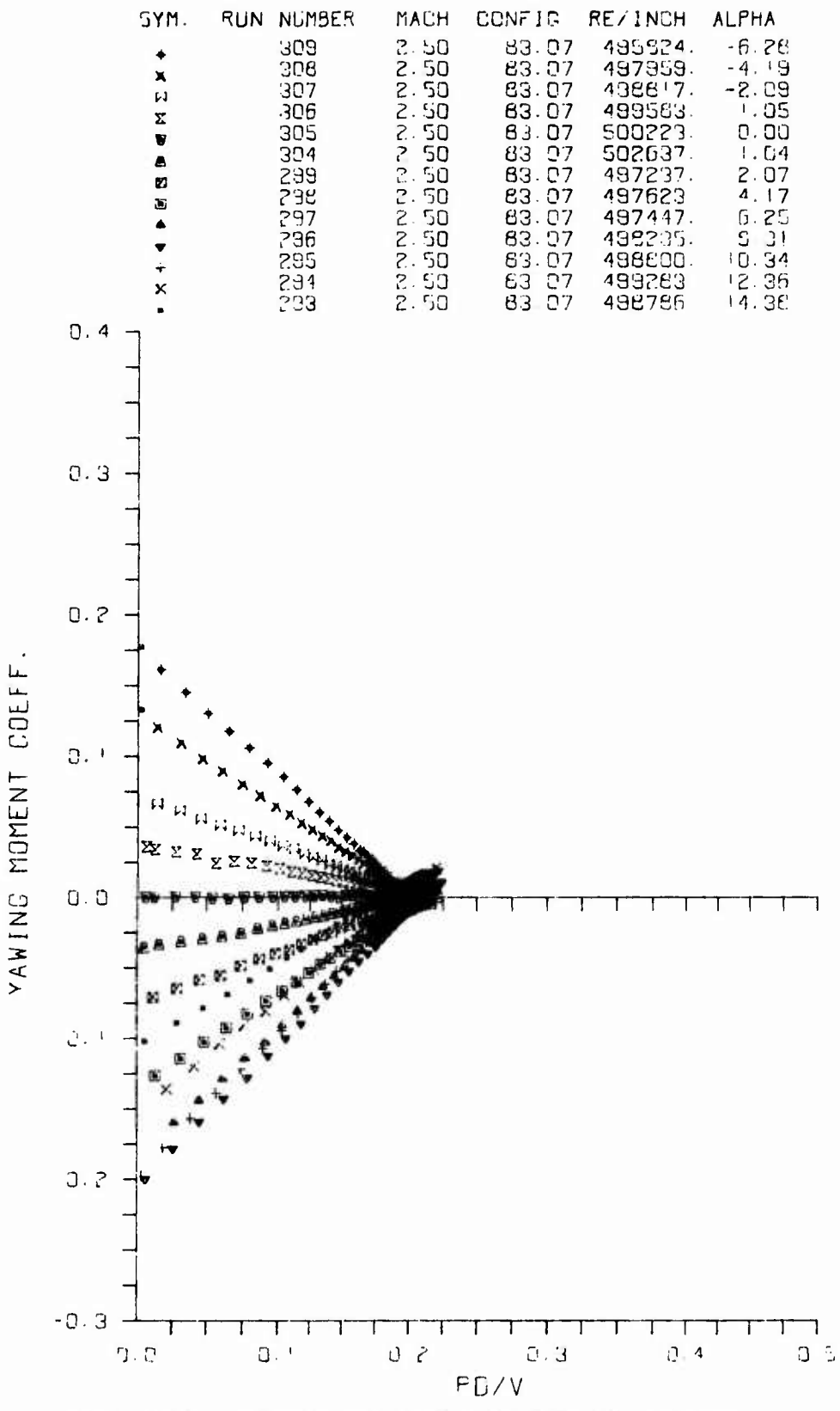

a-5. Model Configuration with 7° Bore-Rider Cant (83.07)-- Mach Number 2.50 (under-spin)

Figure A2. Continued

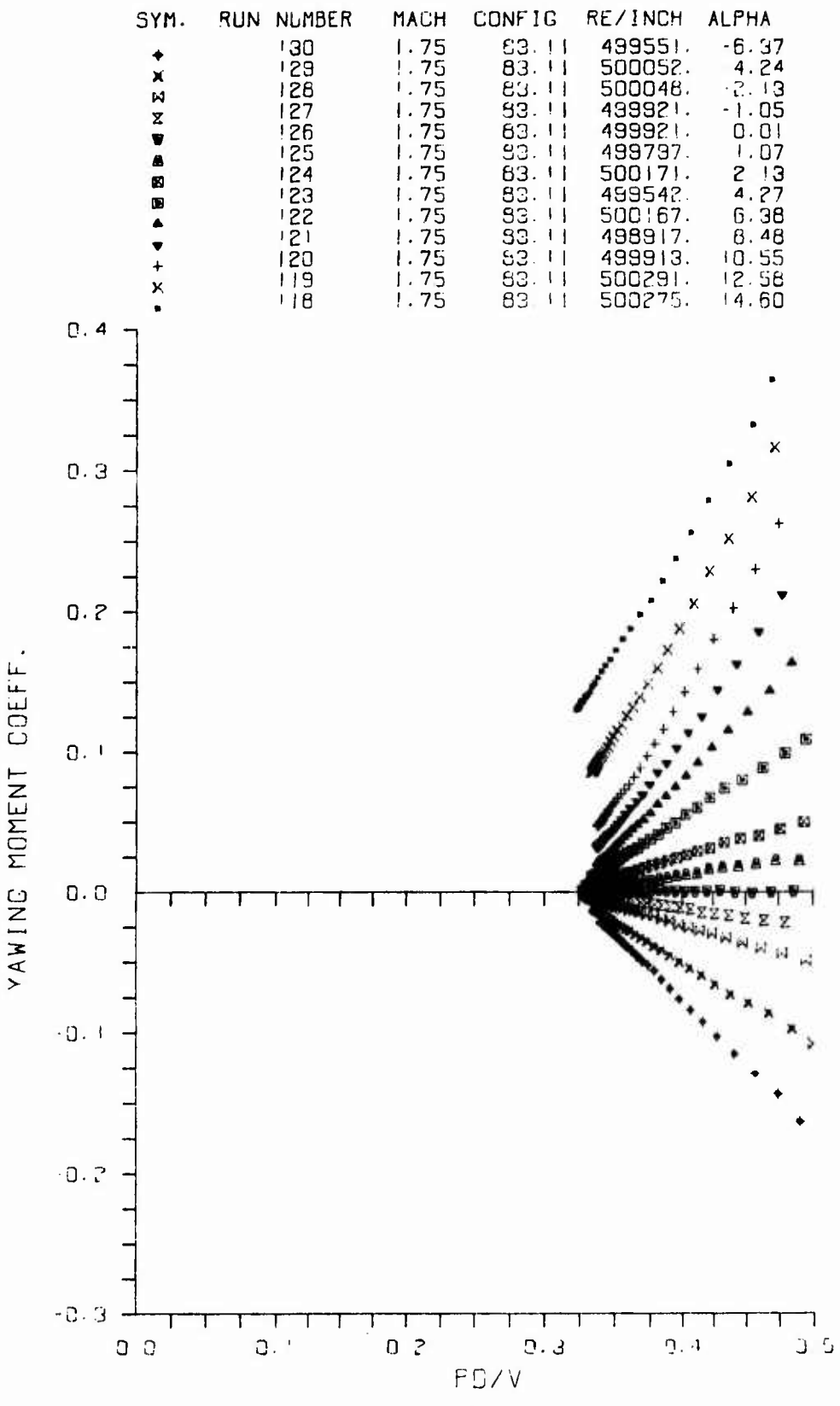

b-1. Model Configuration with 11° Bore-Rider Cant (83.11)-- Mach Number 1.75 (over-spin)

Figure A2. Continued

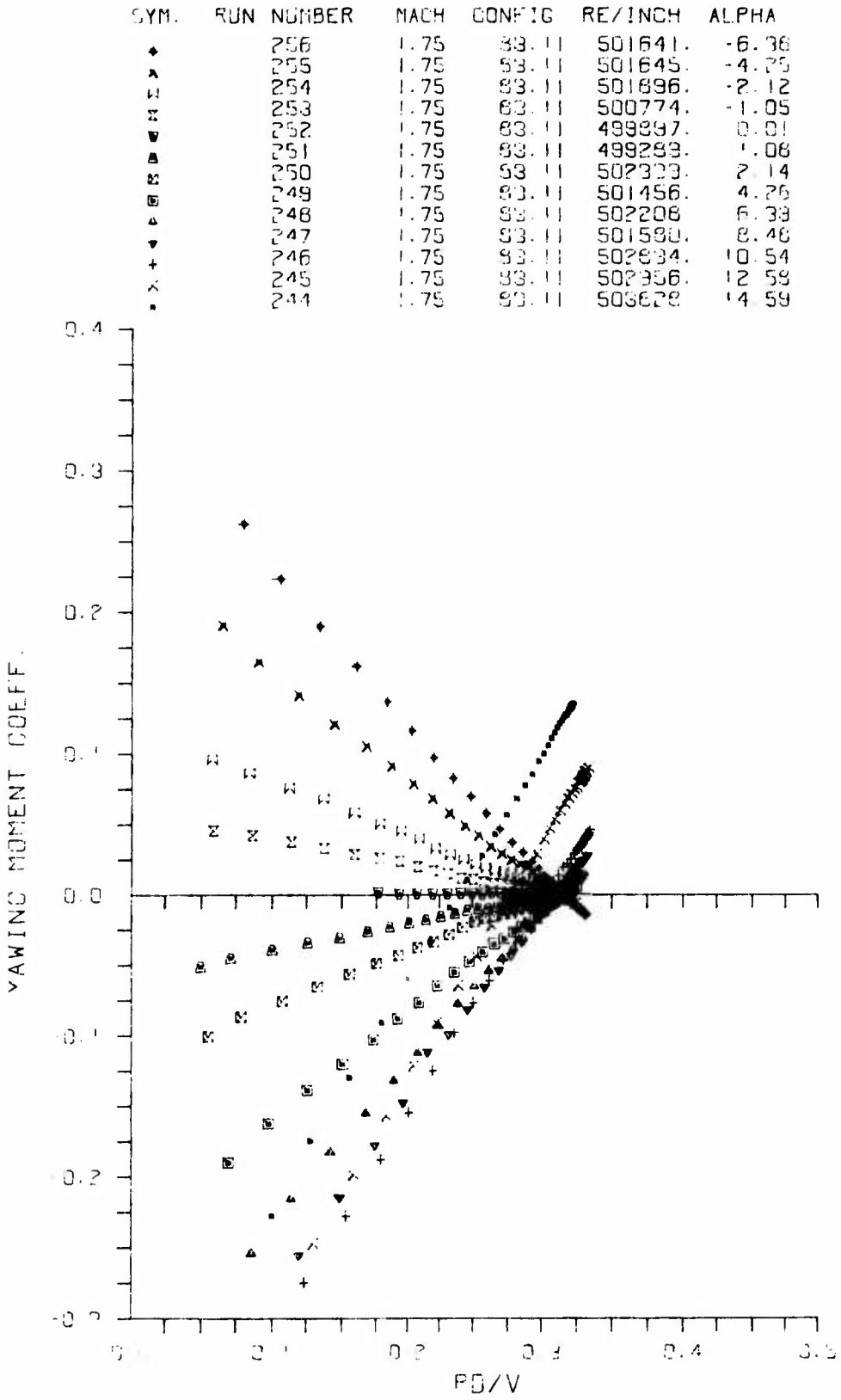

b-2. Model Configuration with 11° Bore-Rider Cant (83.11)-- Mach Number 1.75 (under-spin)

Figure A2. Continued

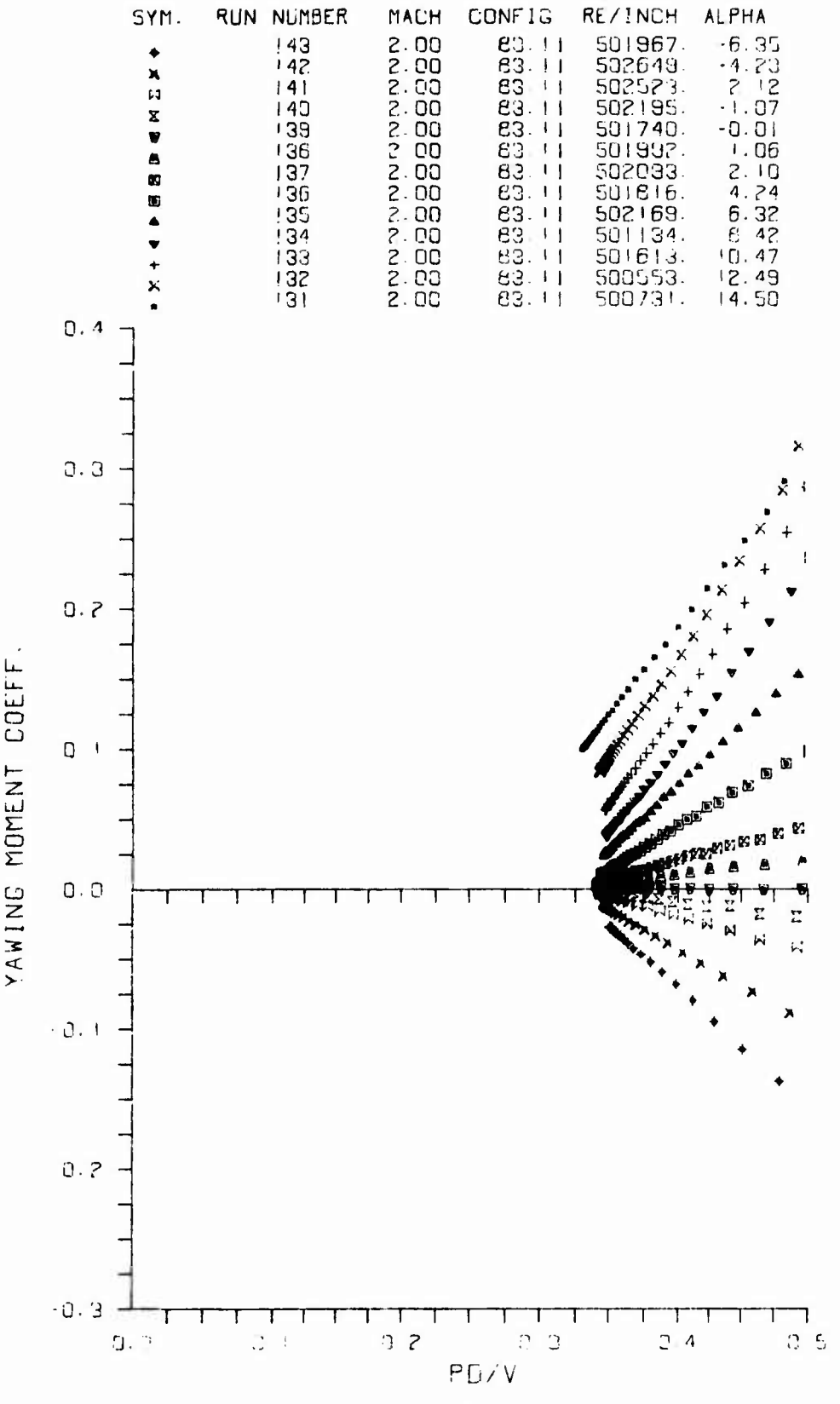

b-3. Model Configuration with 11° Bore-Rider Cant (83.11)-- Mach Number 2.00 (over-spin)

Figure A2. Continued

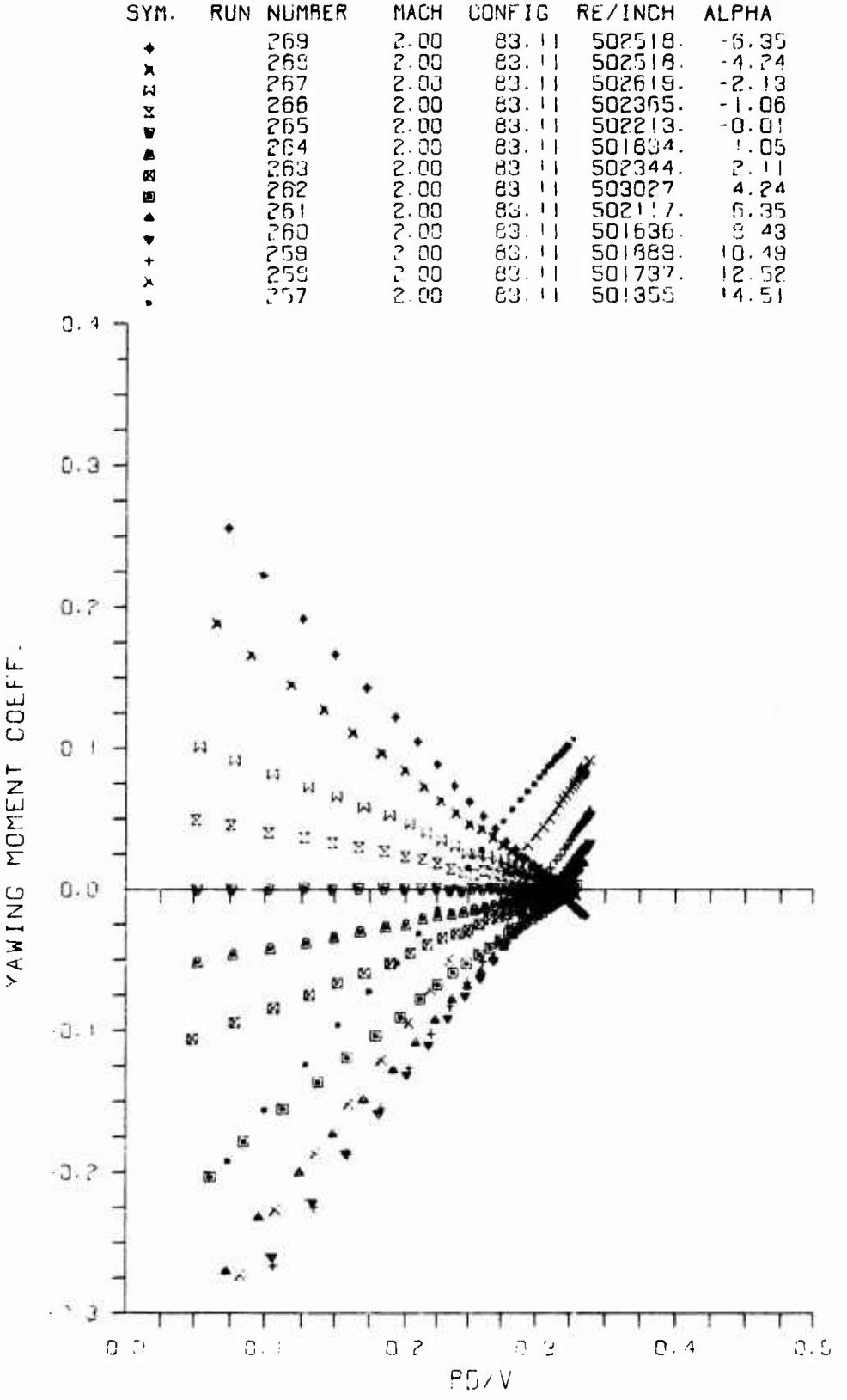

b-4. Model Configuration with 11° Bore-Rider Cant (83.11)-- Mach Number 2.00 (under-spin)

Figure A2. Continued

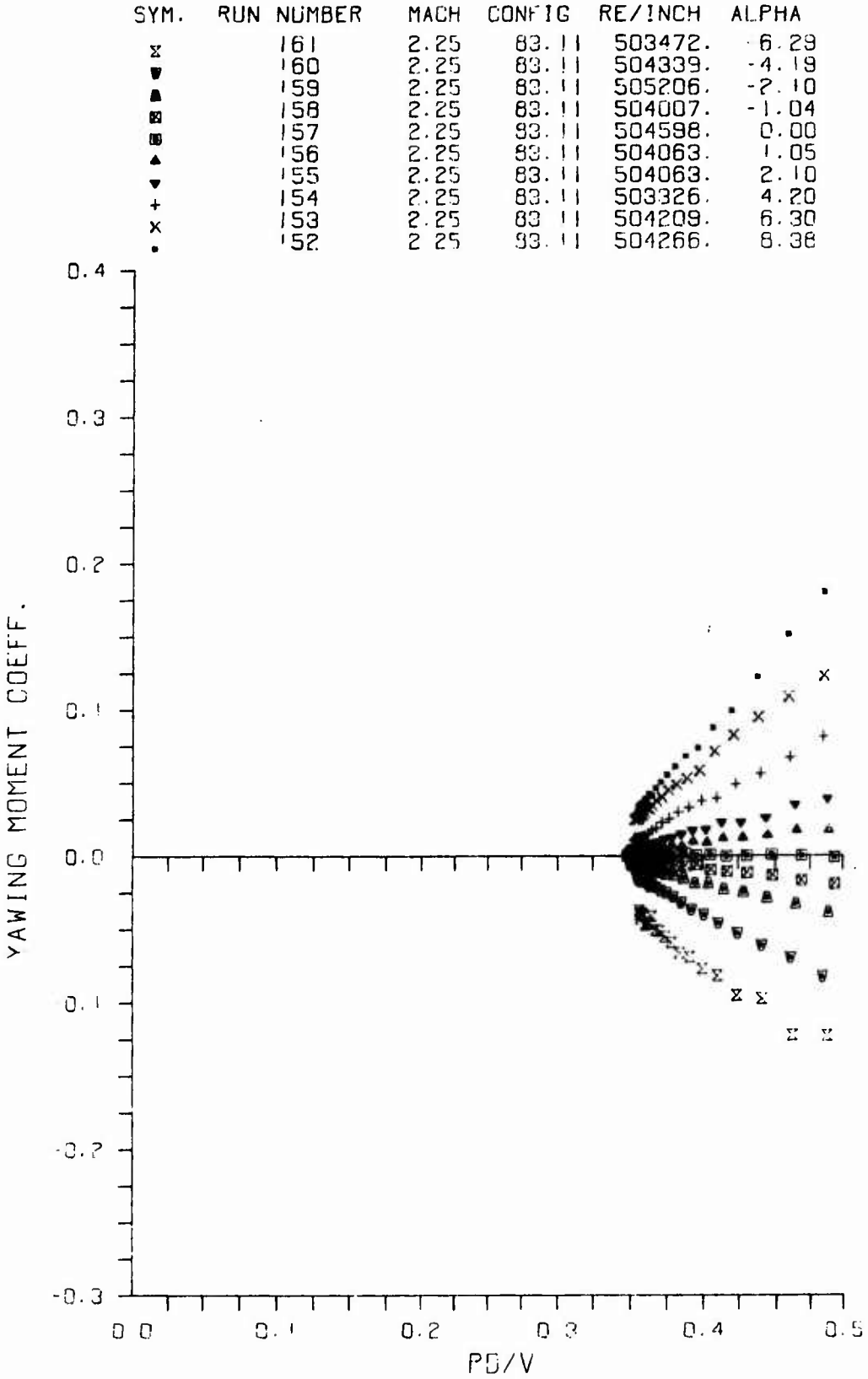

b-5. Model Configuration with 11° Bore-Rider Cant (83.11)-- Mach Number 2.25 (over-spin)

Figure A2. Continued

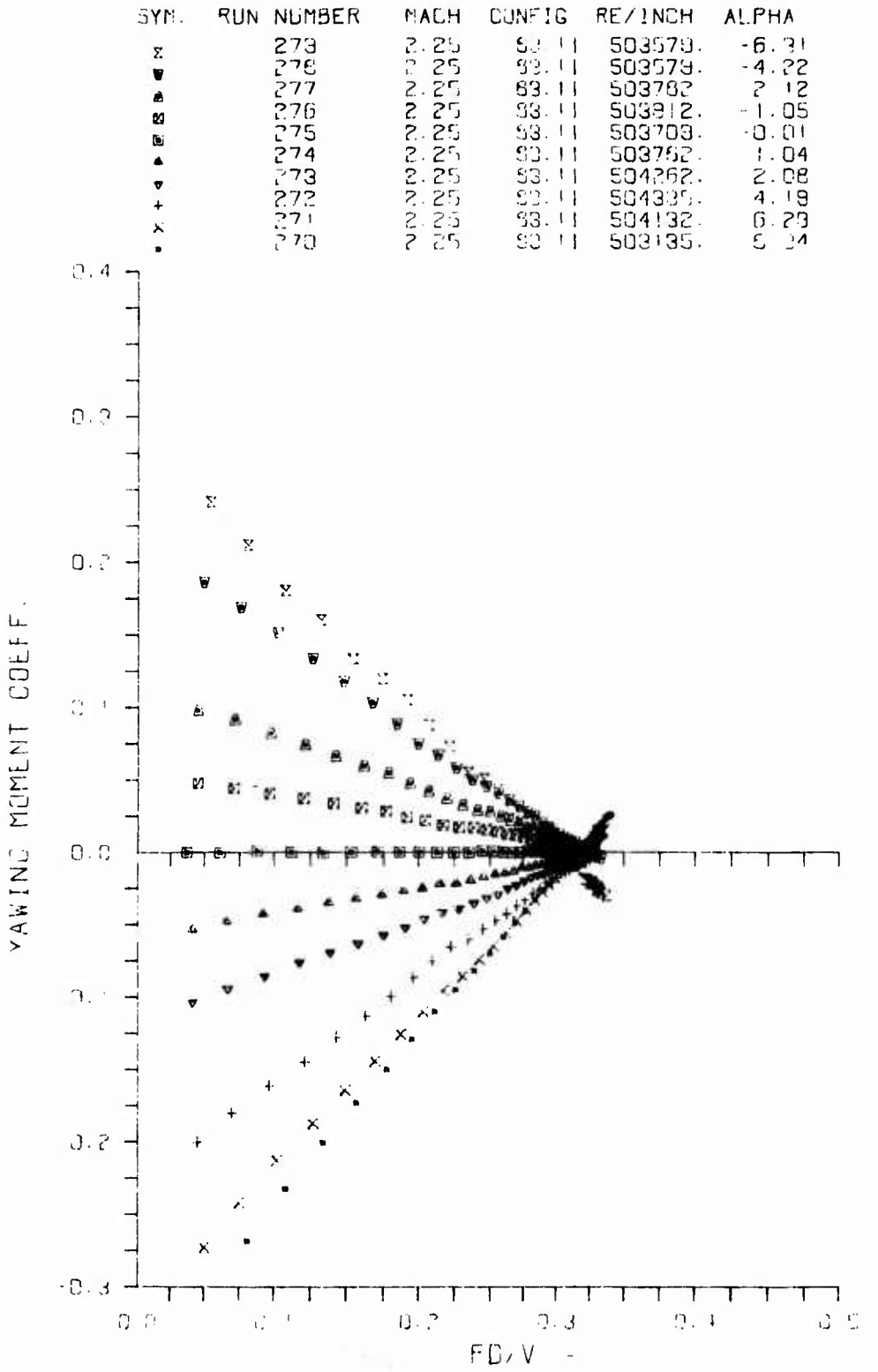

b-6. Model Configuration with 11° Bore-Rider Cant (83.11)-- Mach Number 2.25 (under-spin)

Figure A2. Continued

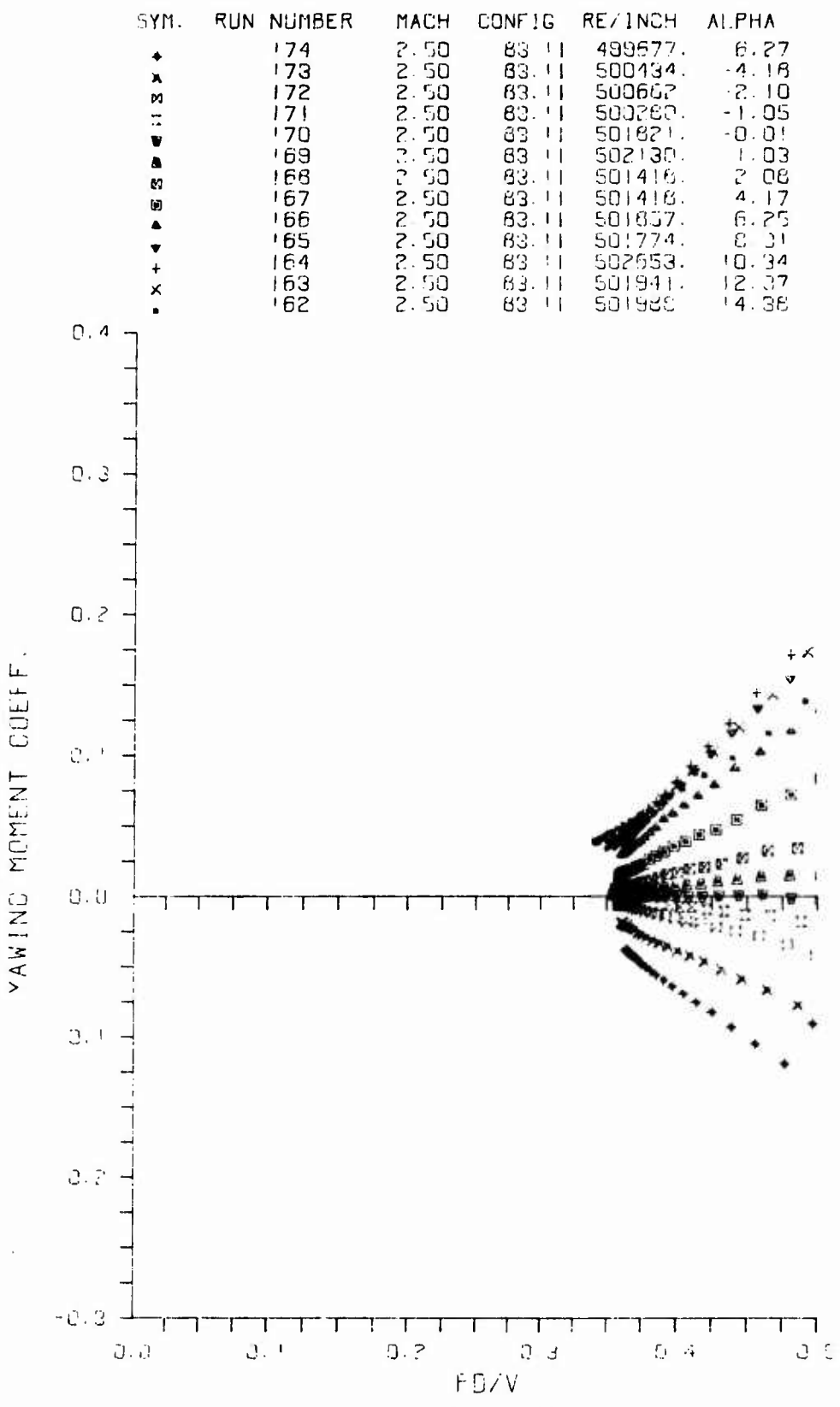

b-7. Model Configuration with 11° Bore-Rider Cant (83.11)-- Mach Number 2.50 (over-spin)

Figure A2. Continued

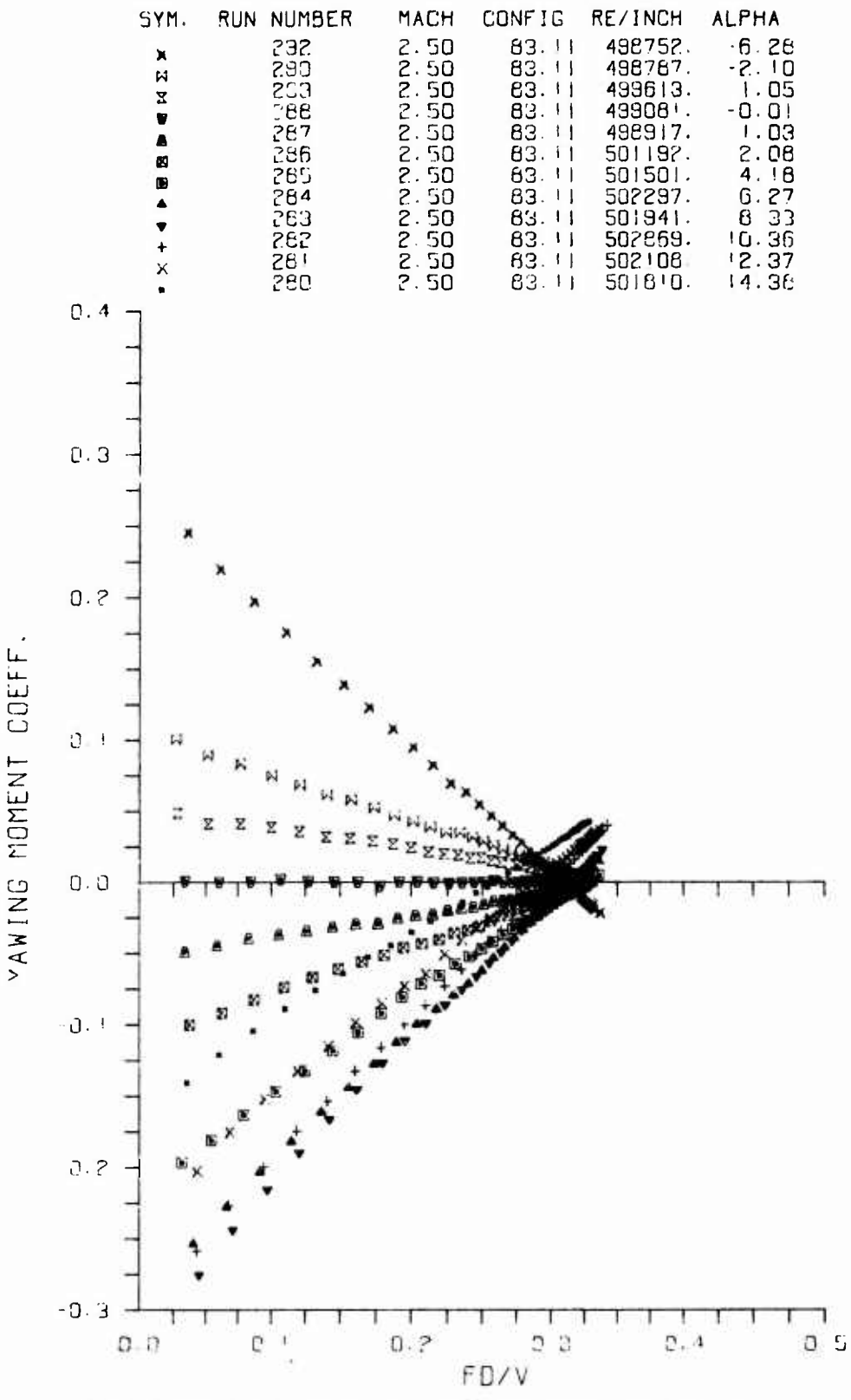

b-8. Model Configuration with 11° Bore-Rider Cant (83.11)-- Mach Number 2.50 (under-spin)

Figure A2. Continued

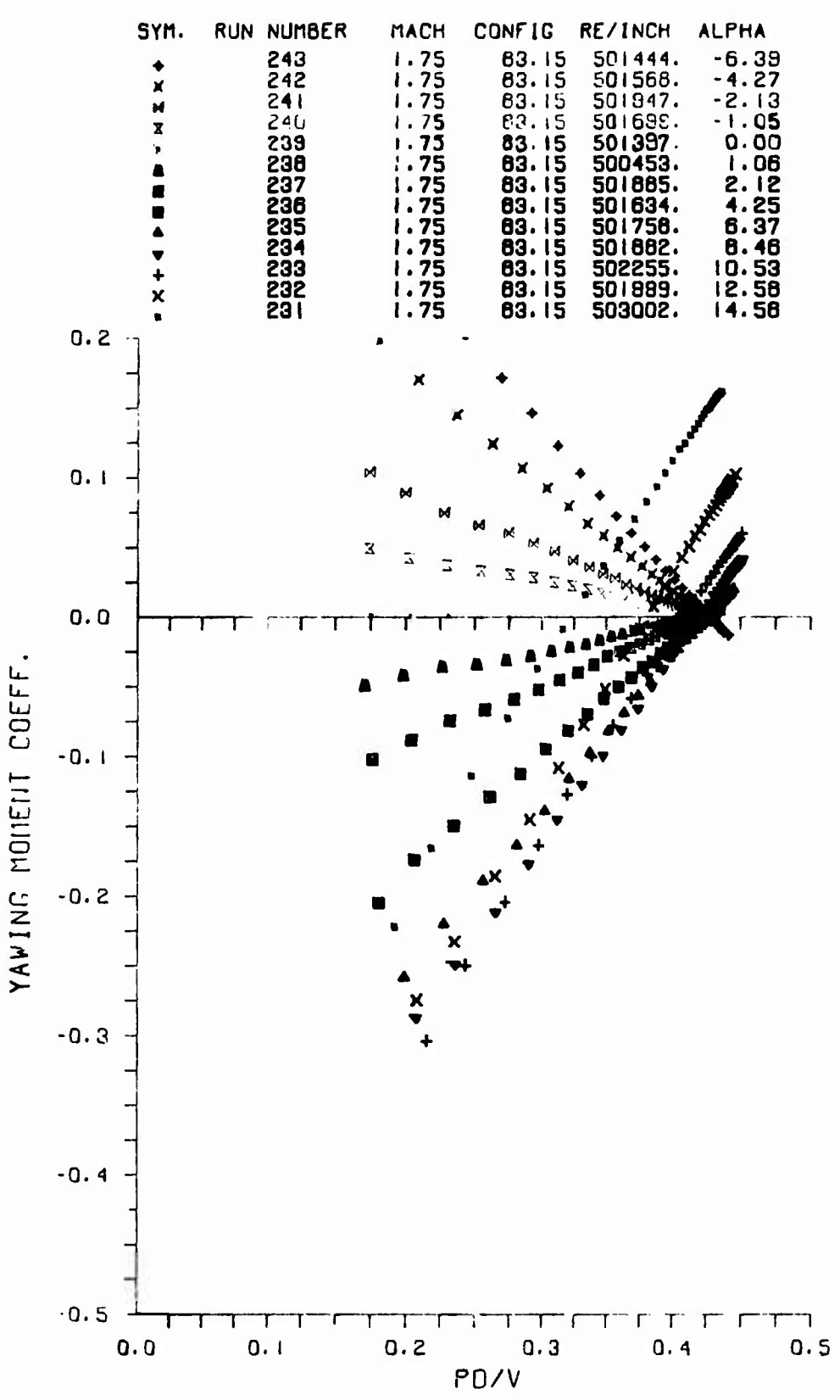

c-1. Model Configuration with 15° Bore-Rider Cant (83.15)-- Mach Number 1.75

Figure A2. Continued

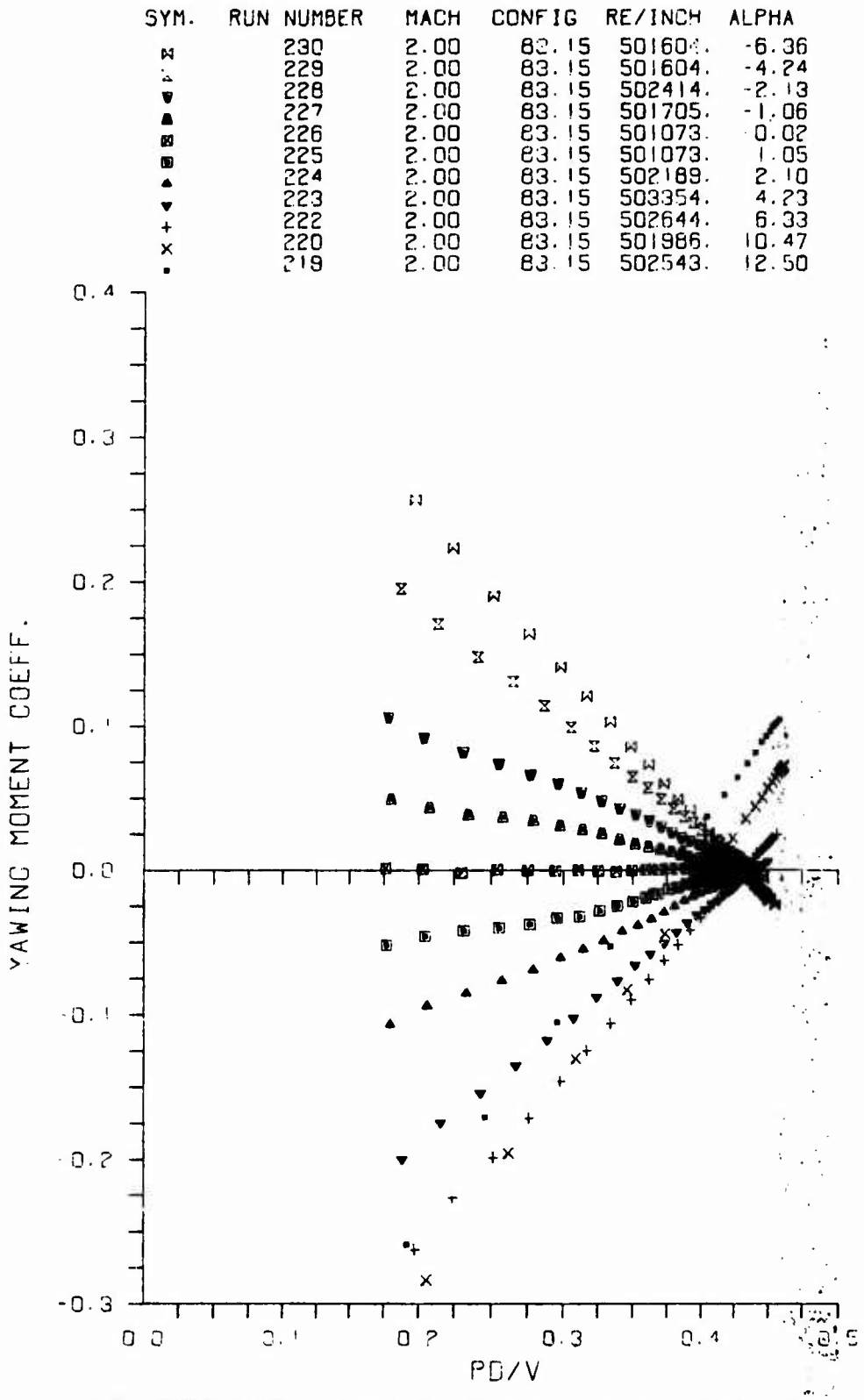

c-2. Model Configuration with 15° Bore-Rider Cant (83.15)-- Mach Number 2.00

Figure A2. Continued

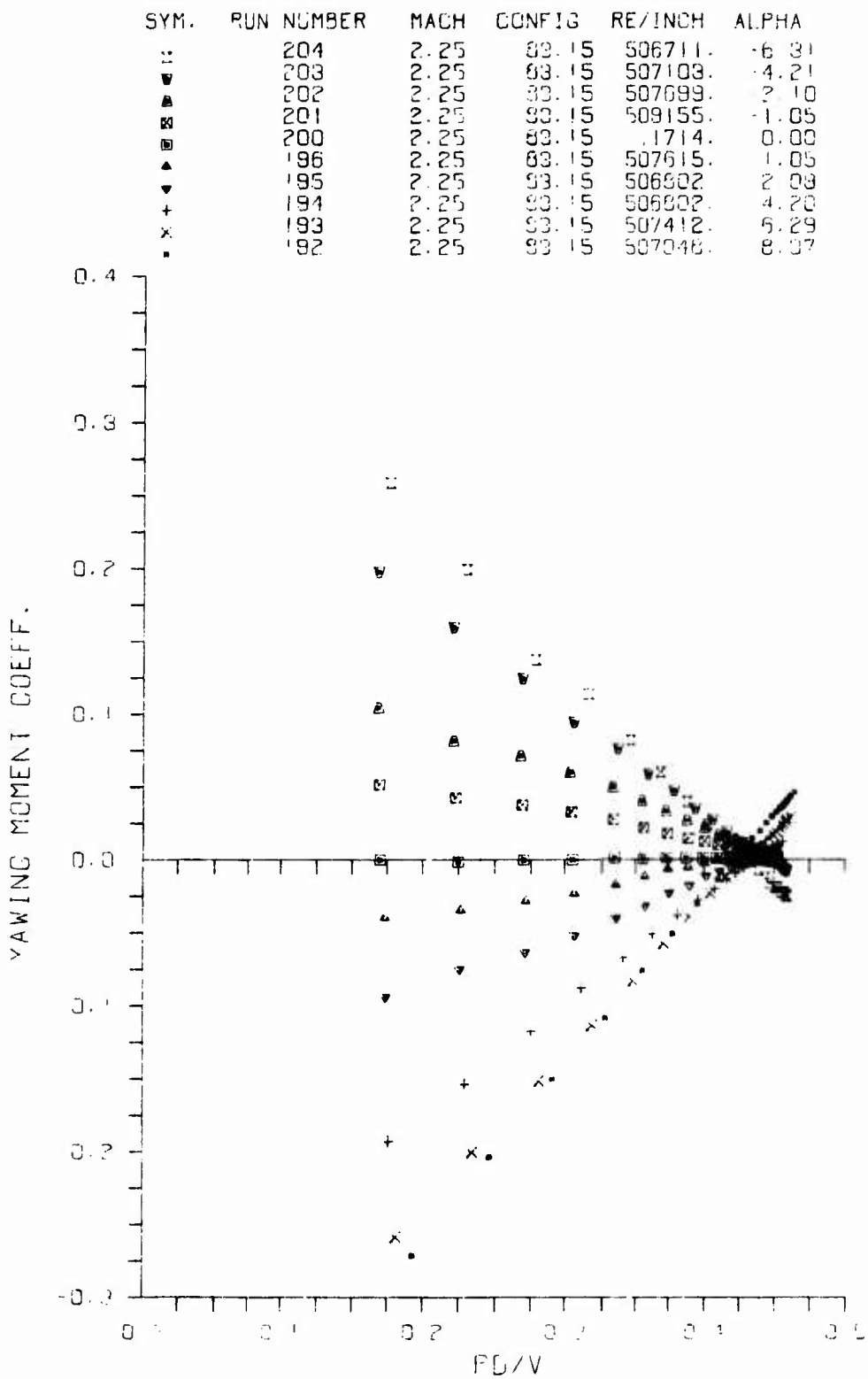

c-3. Model Configuration with 15° Bore-Rider Cant (83.15)-- Mach Number 2.25

Figure A2. Continued

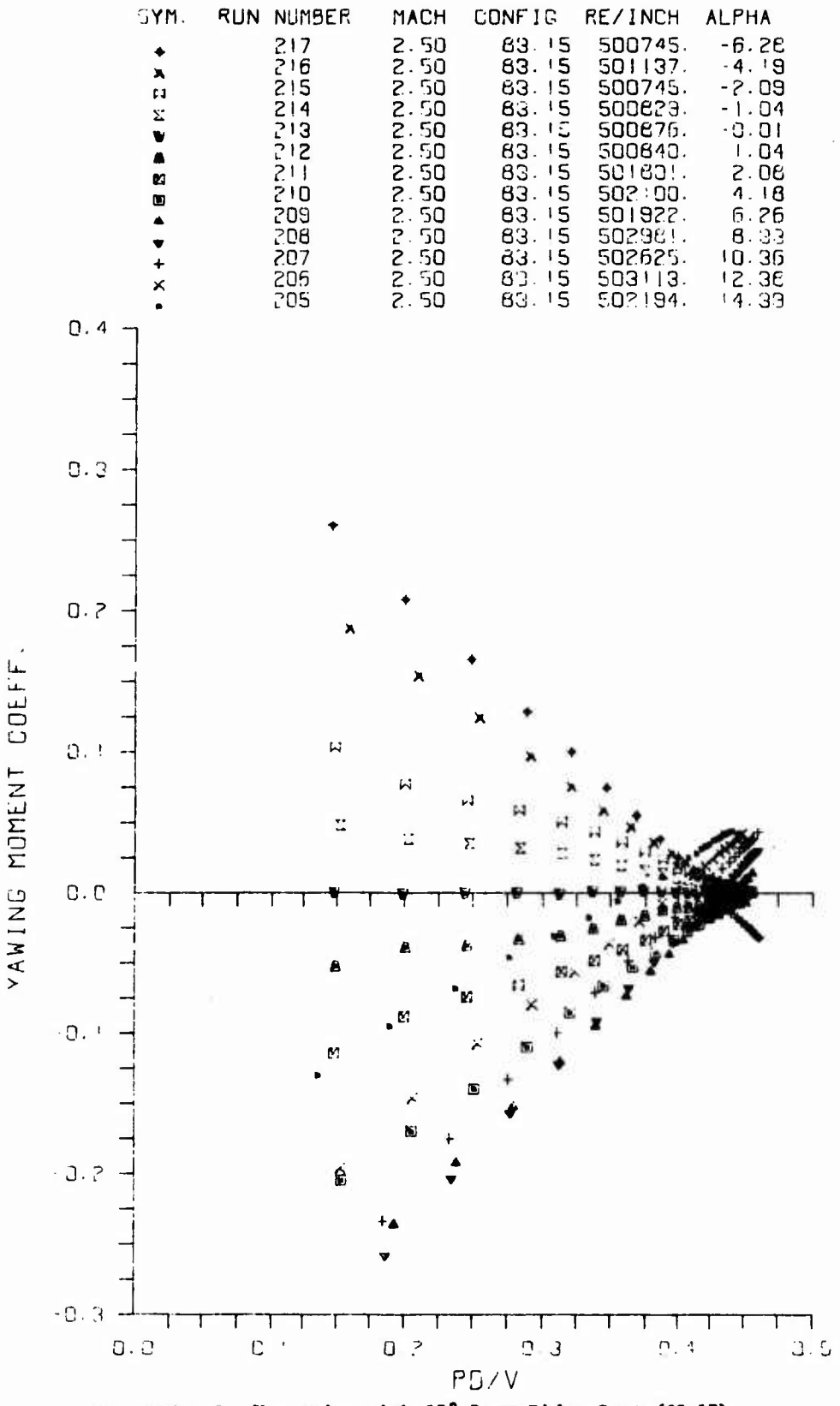

c-4. Model Configuration with 15° Bore-Rider Cant (83.15)-- Mach Number 2.50

Figure A2. Concluded

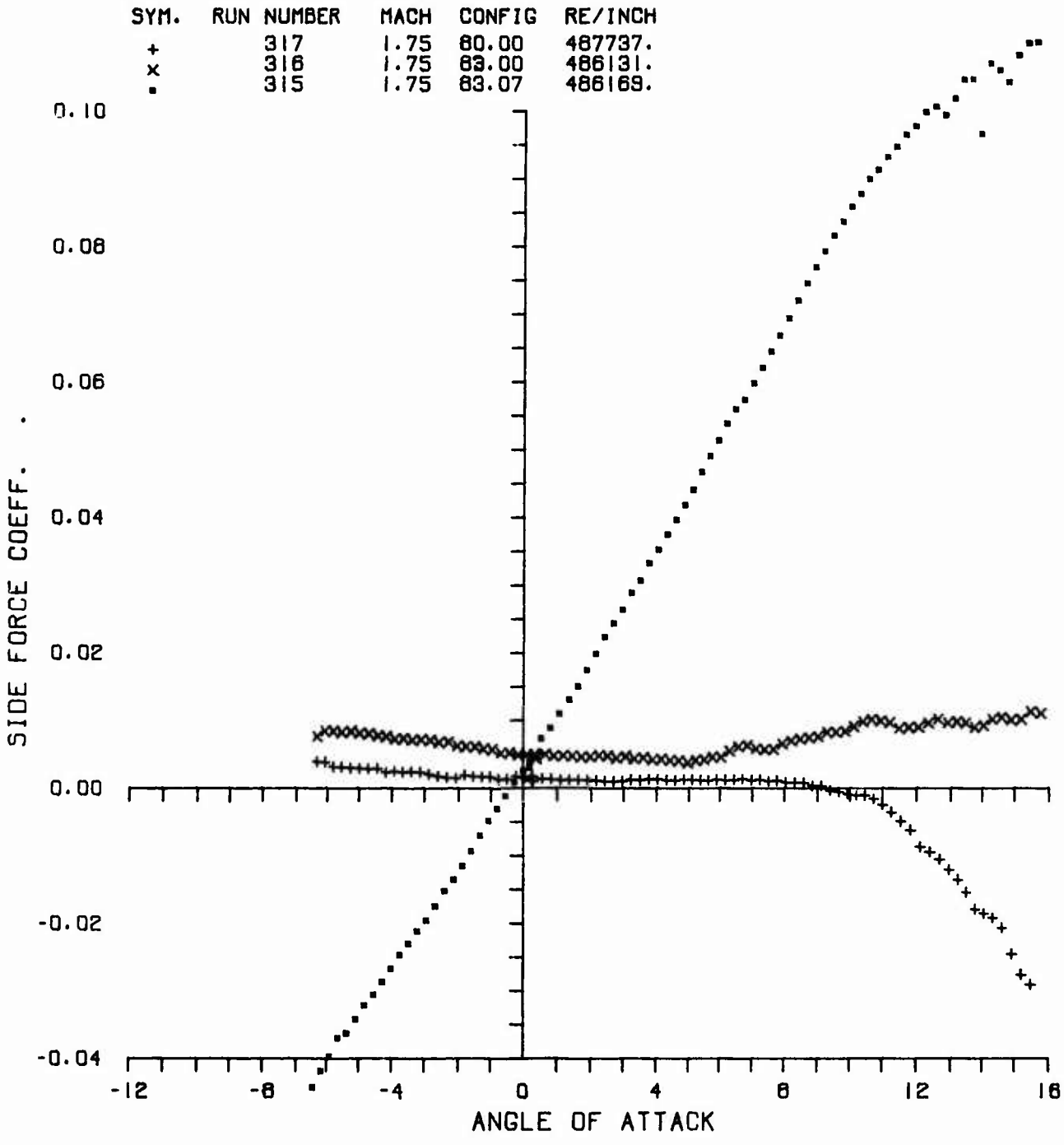

a. Mach Number 1.75

Figure A3. Side-Force Coefficient at Zero Spin versus Angle of Attack

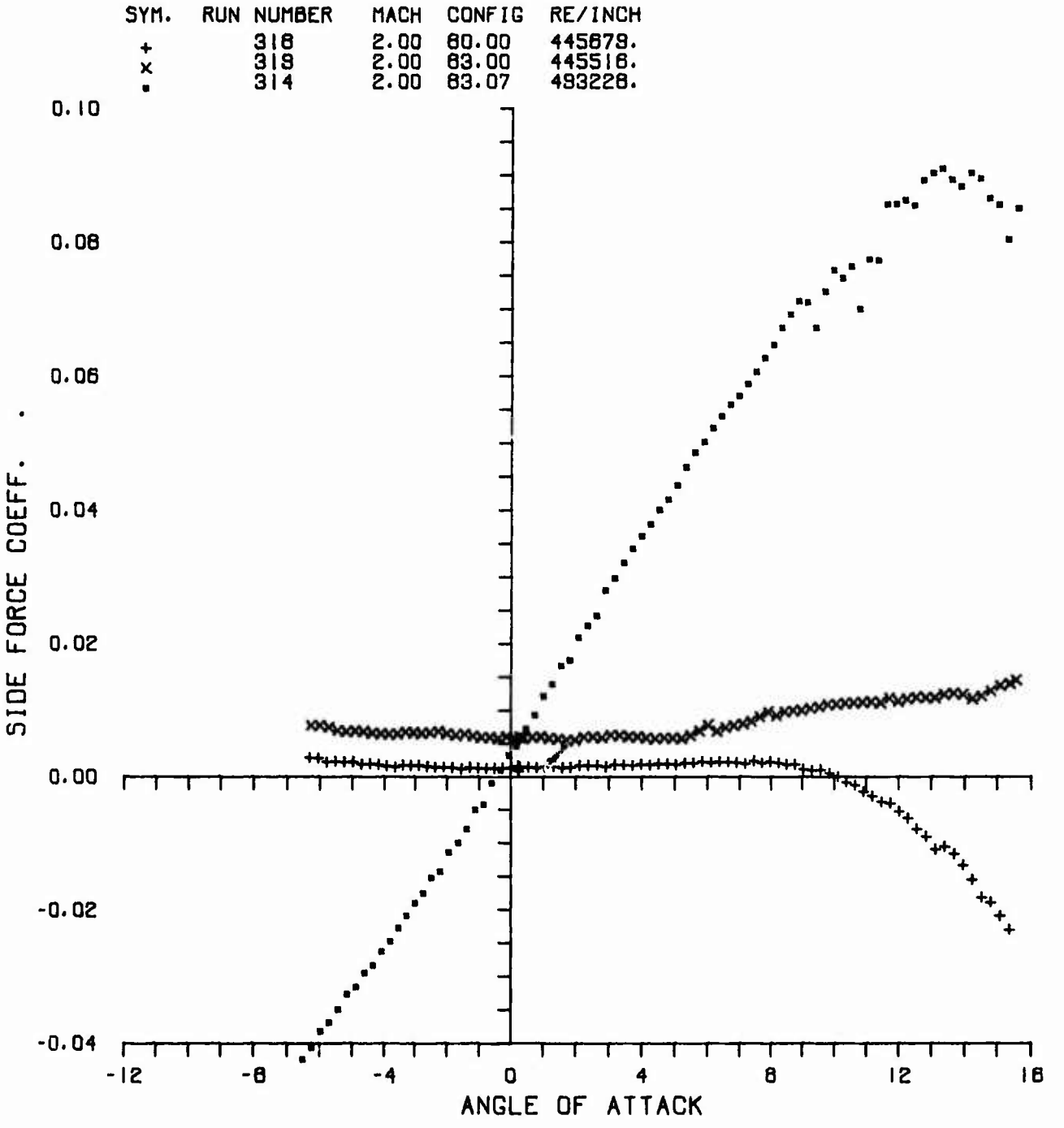

b. Mach Number 2.00

Figure A3. Continued

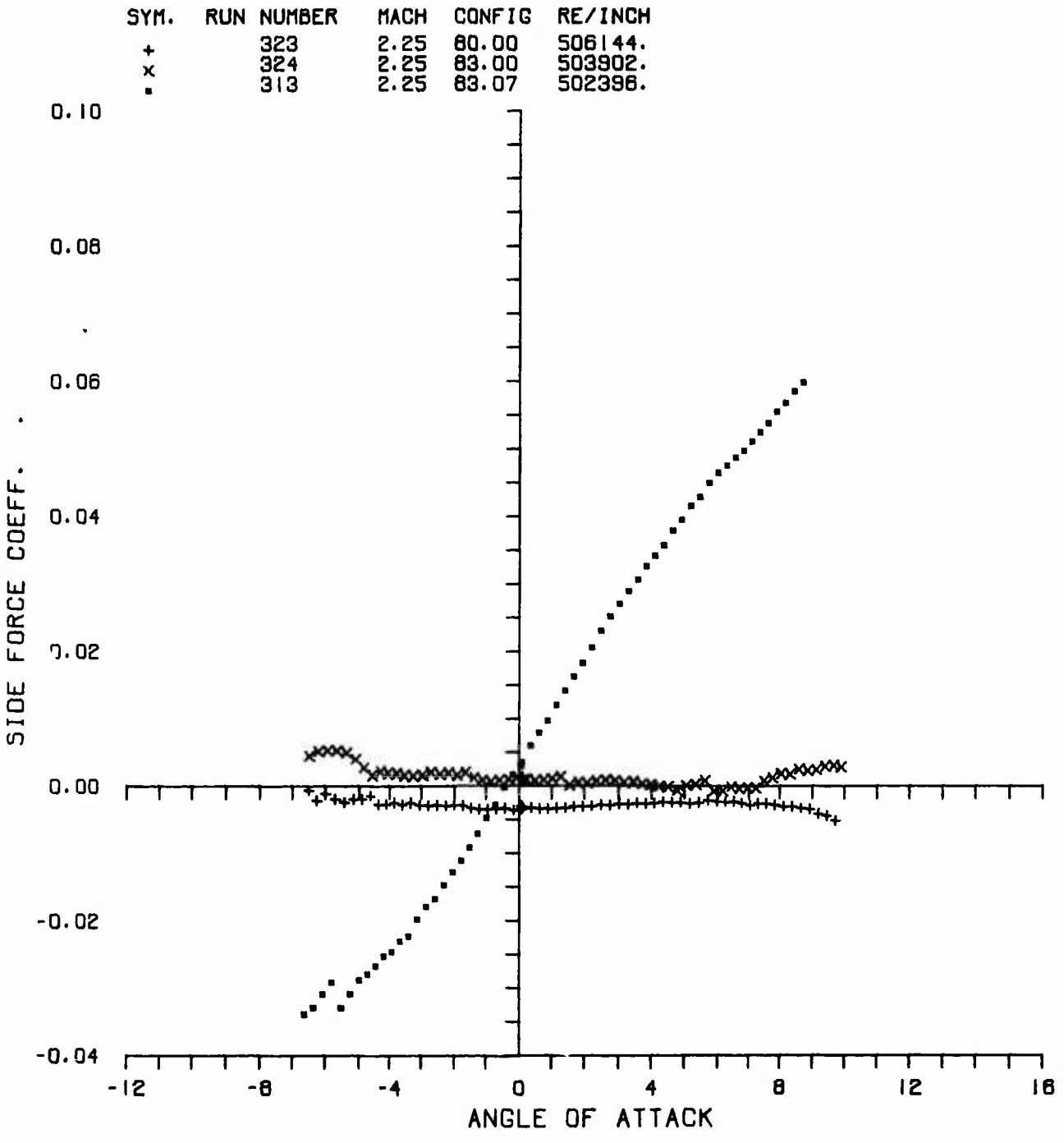

c. Mach Number 2.25

Figure A3. Continued

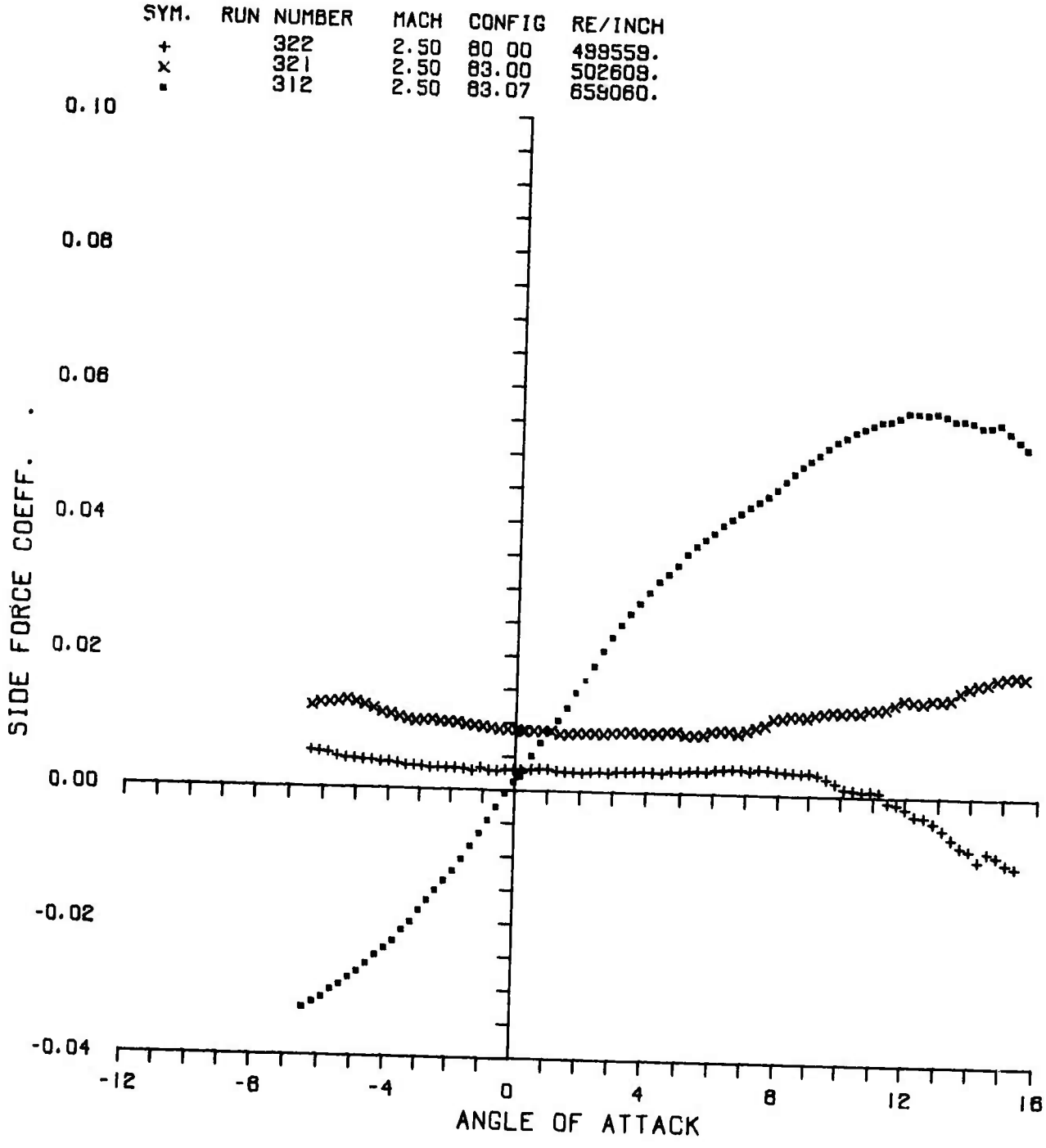

d. Mach Number 2.50

Figure A3. Concluded

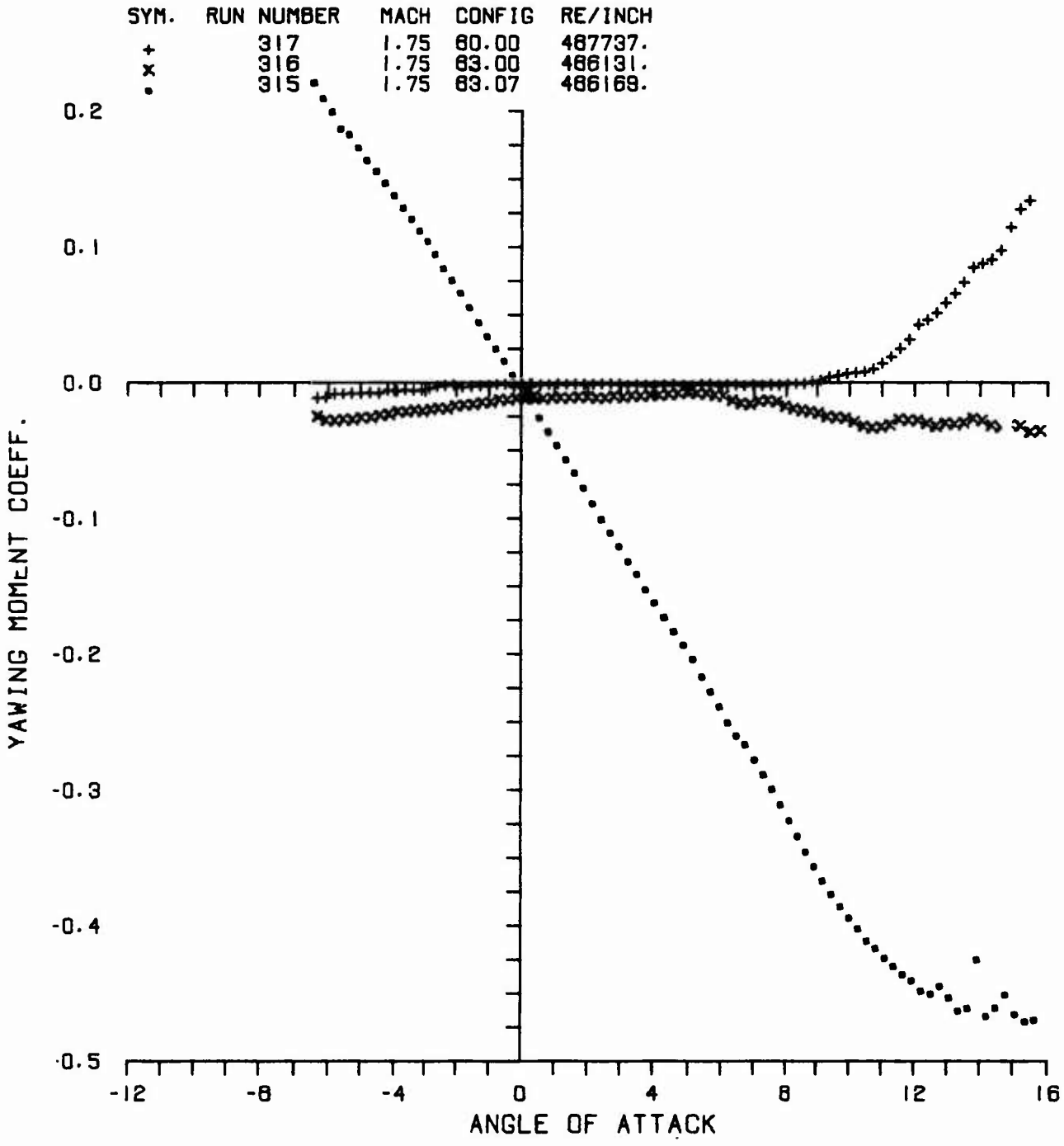

a. Mach Number 1.75

Figure A4. Yawing-Moment Coefficient at Zero Spin versus Angle of Attack

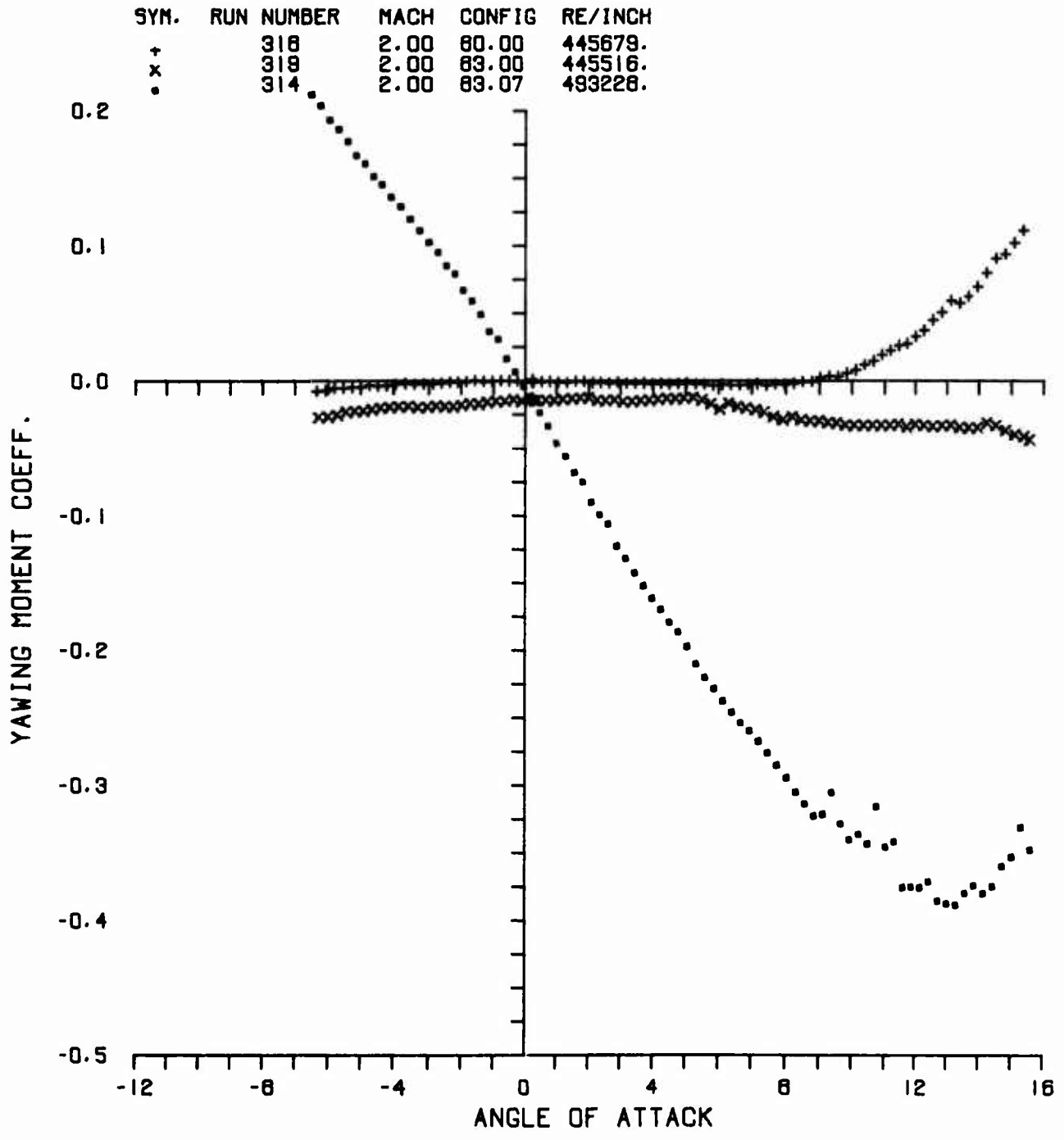

b. Mach Number 2.00

Figure A4. Continued

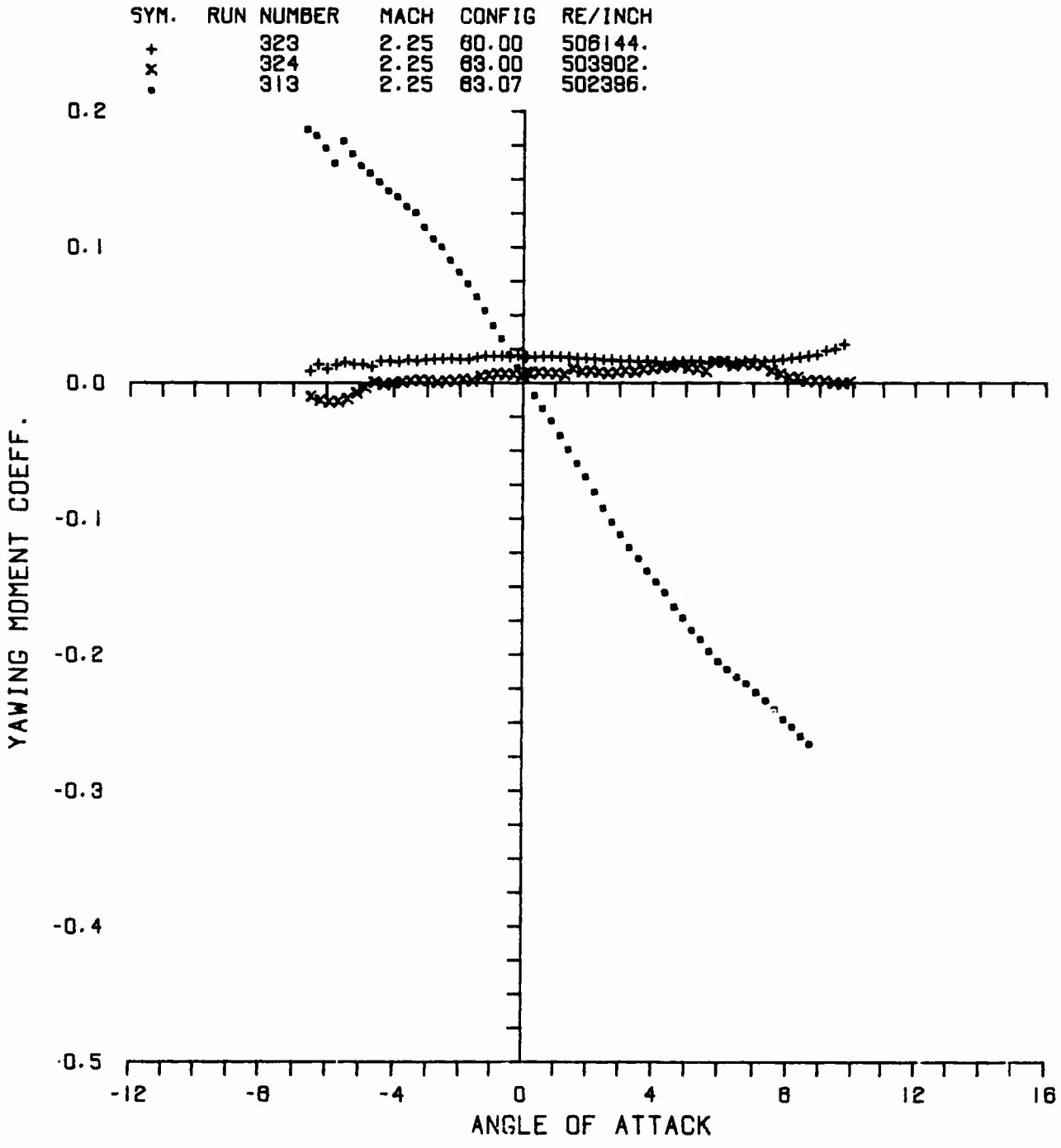

c. Mach Number 2.25

Figure A4. Continued

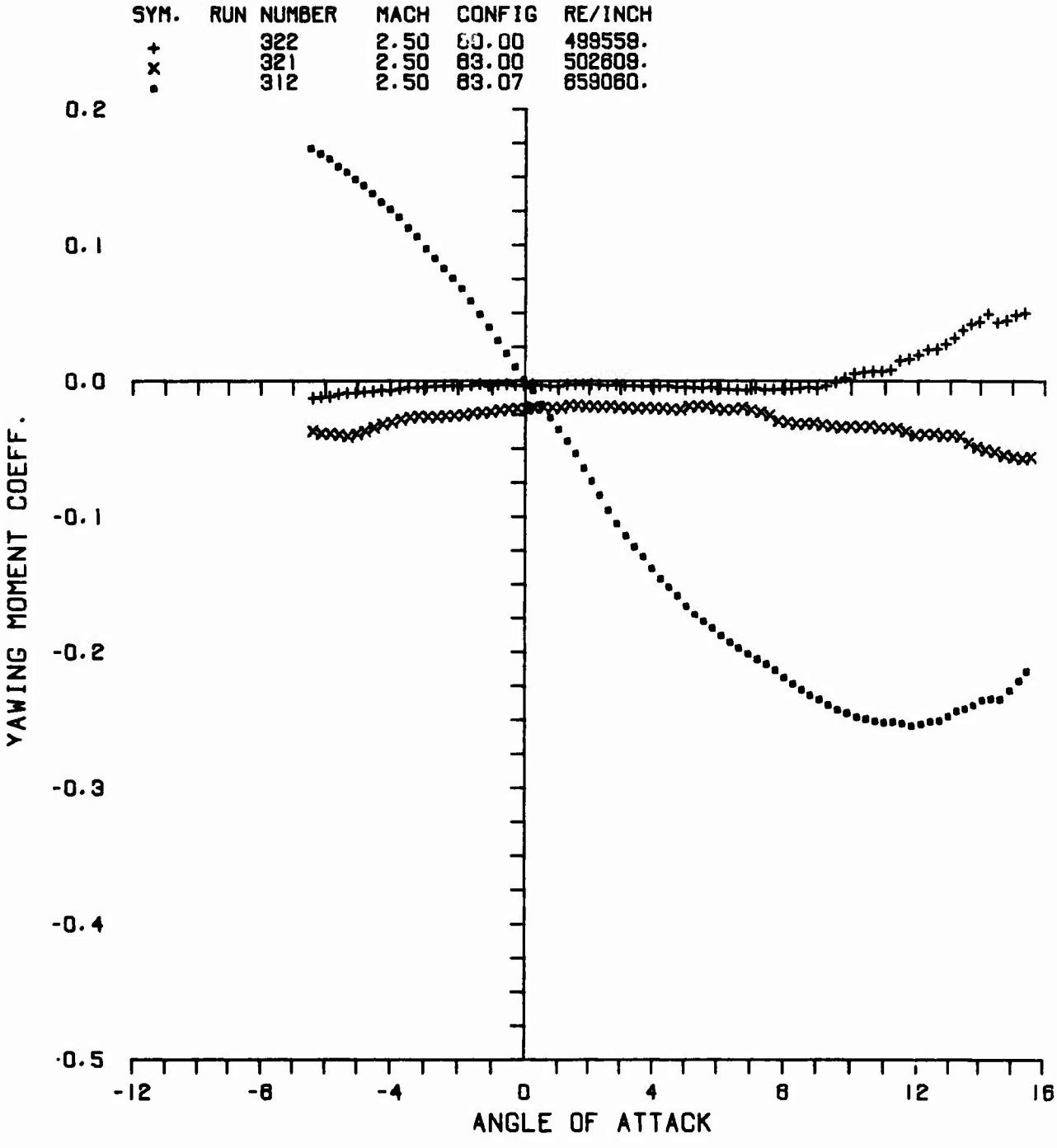

d. Mach Number 2.50

Figure A4. Concluded

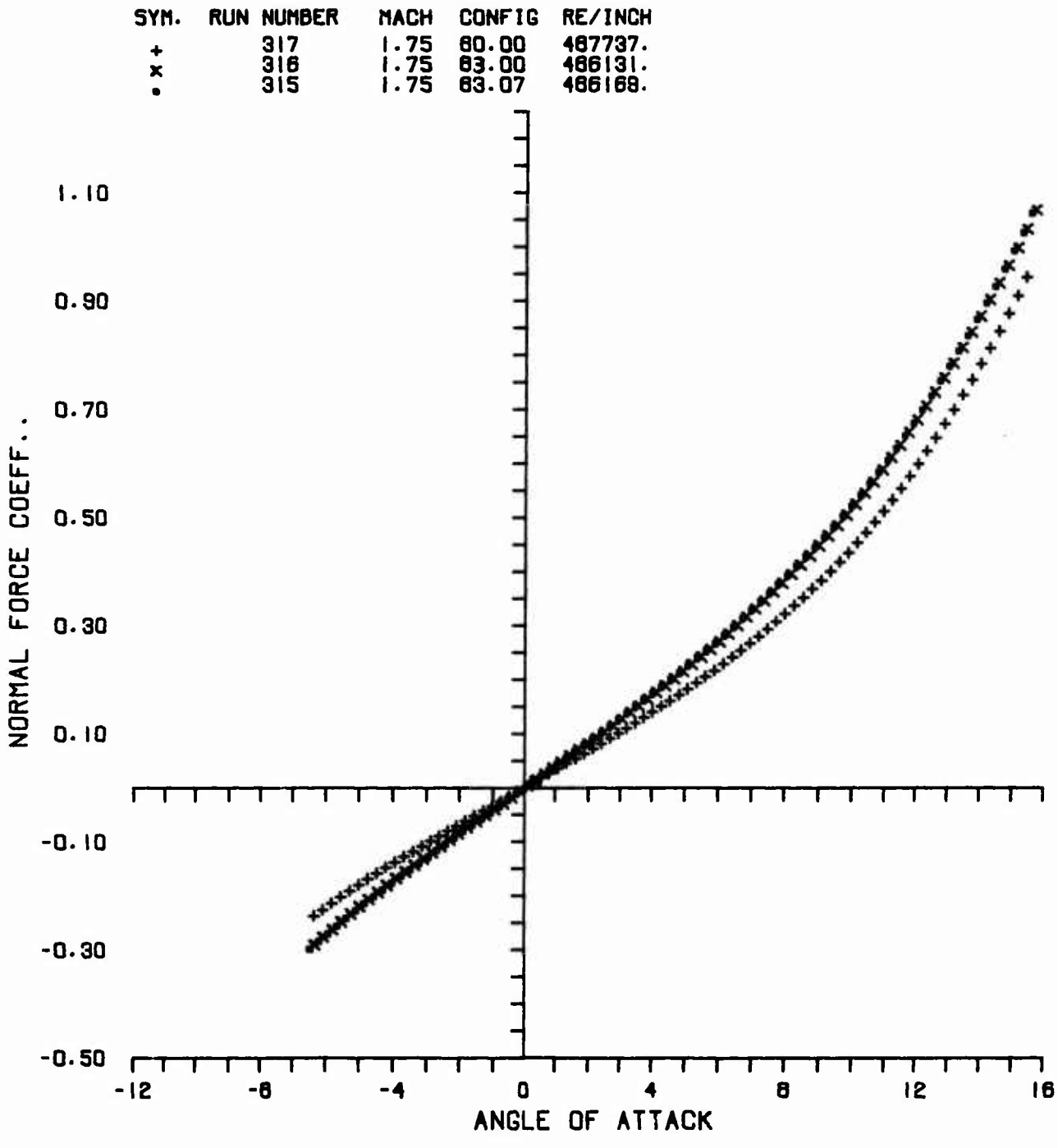

a. Mach Number 1.75

Figure A5. Normal-Force Coefficient versus Angle of Attack

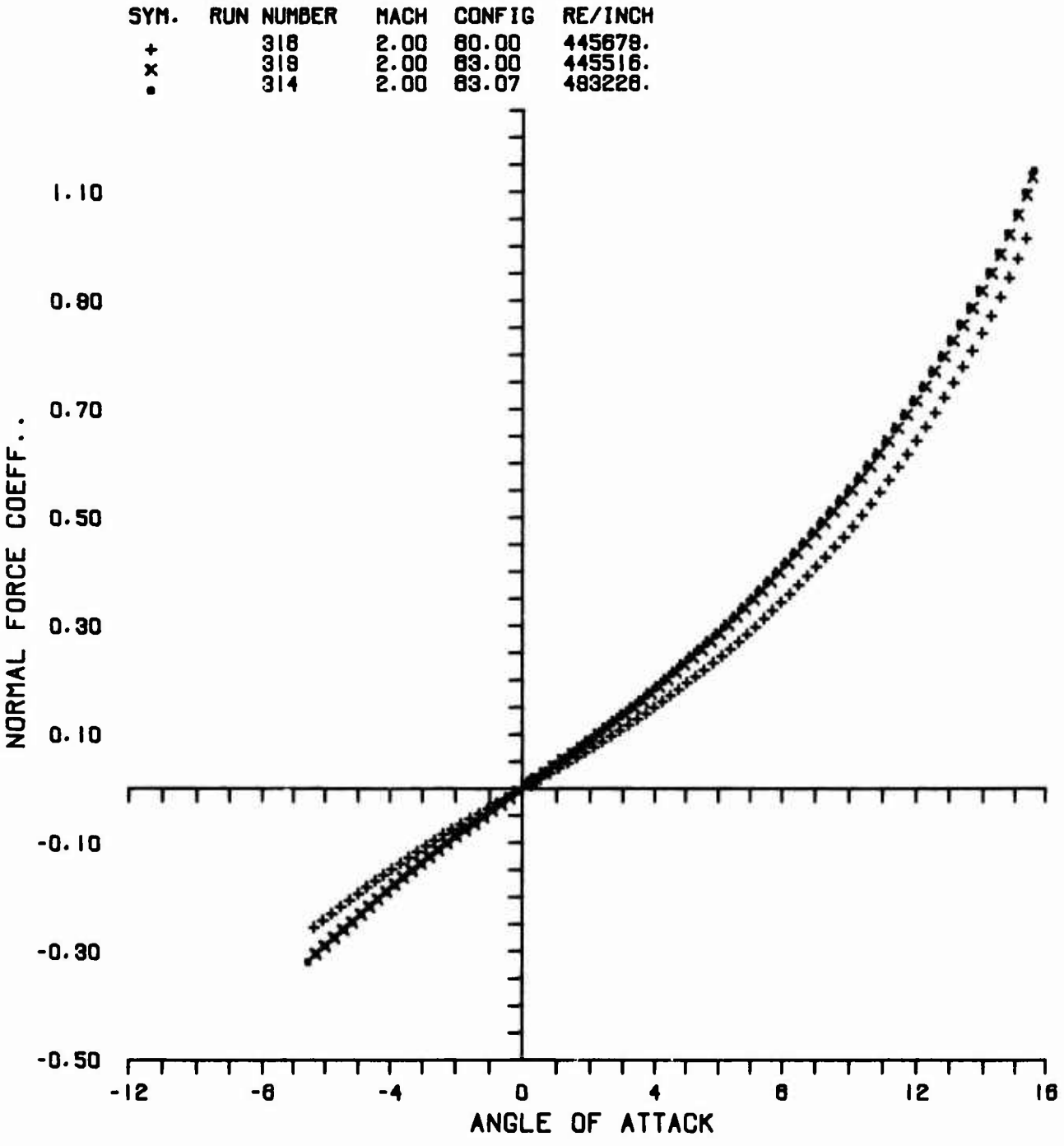

b. Mach Number 2.00

Figure A5. Continued

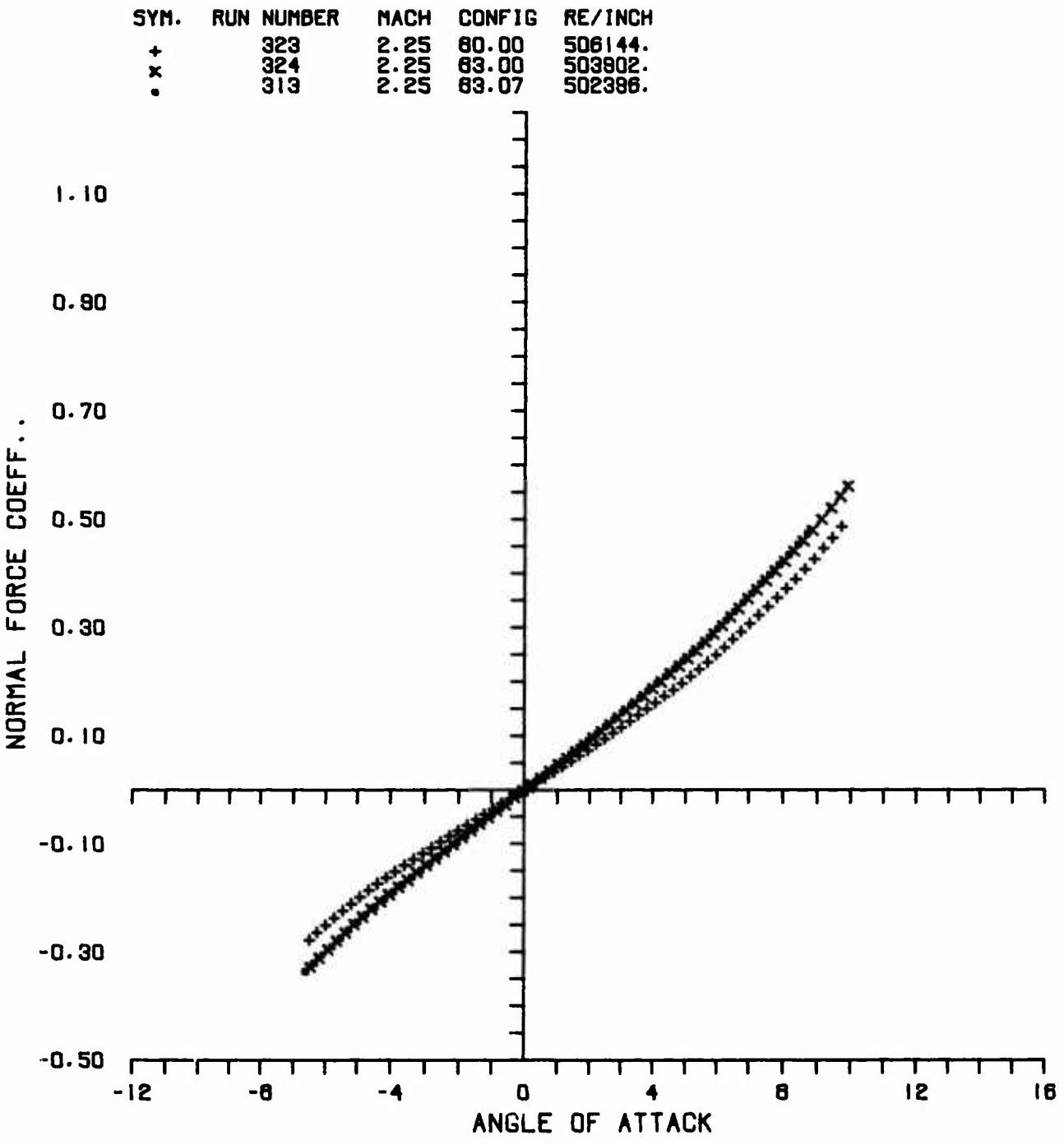

c. Mach Number 2.25

Figure A5. Continued

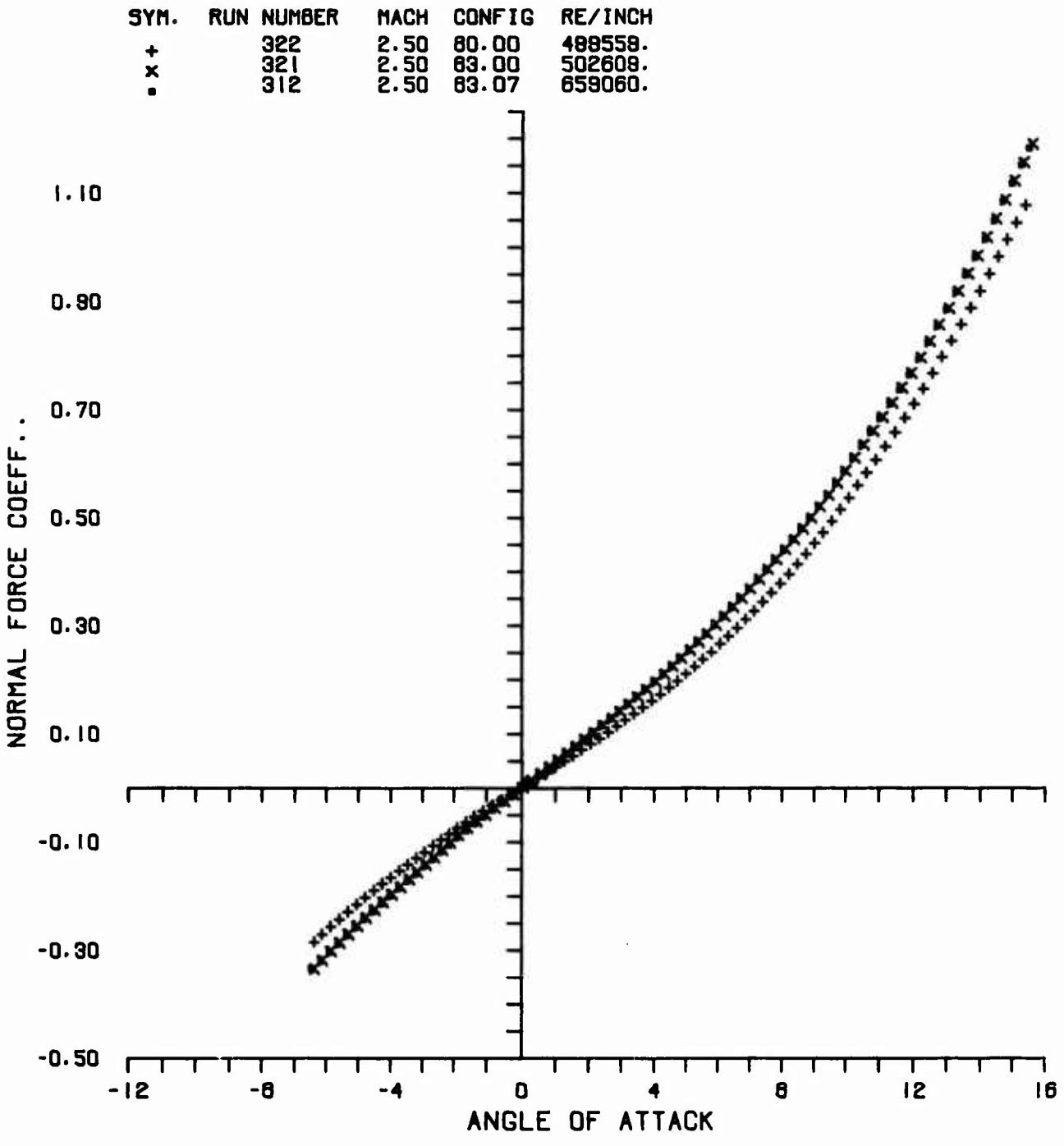

d. Mach Number 2.50

Figure A5. Concluded

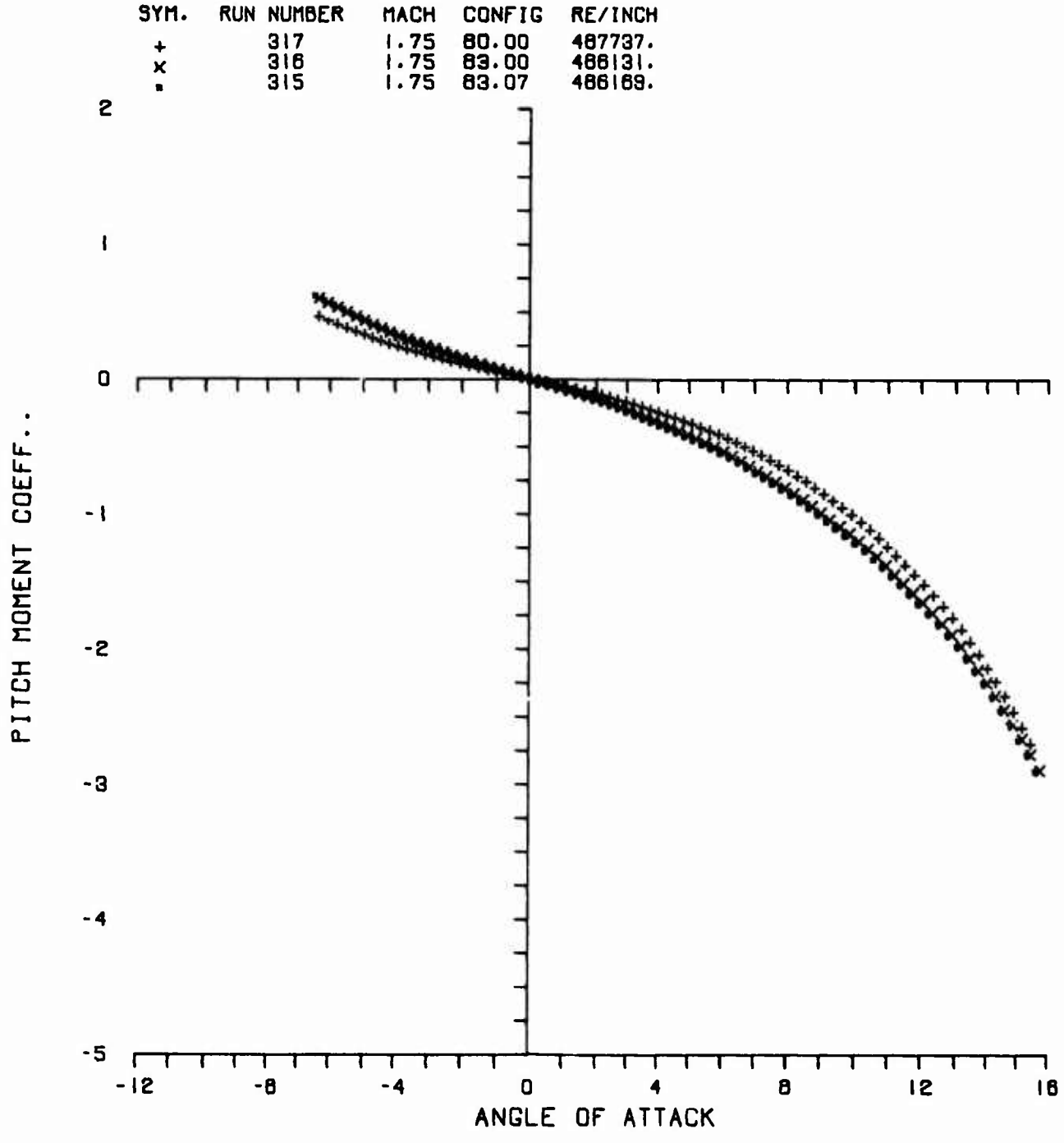

a. Mach Number 1.75

Figure A6. Pitching-Moment Coefficient versus Angle of Attack

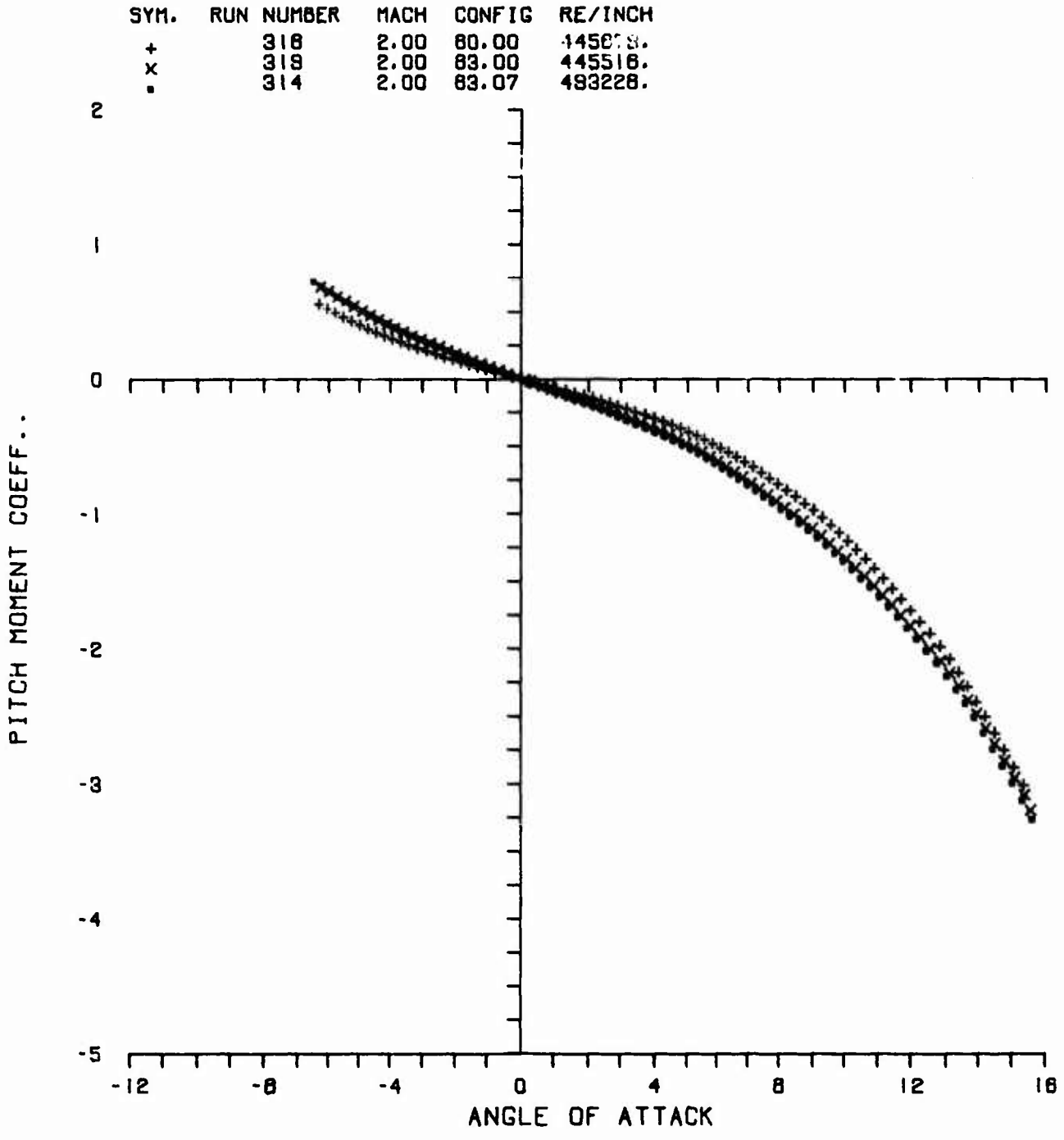

b. Mach Number 2.00

Figure A6. Continued

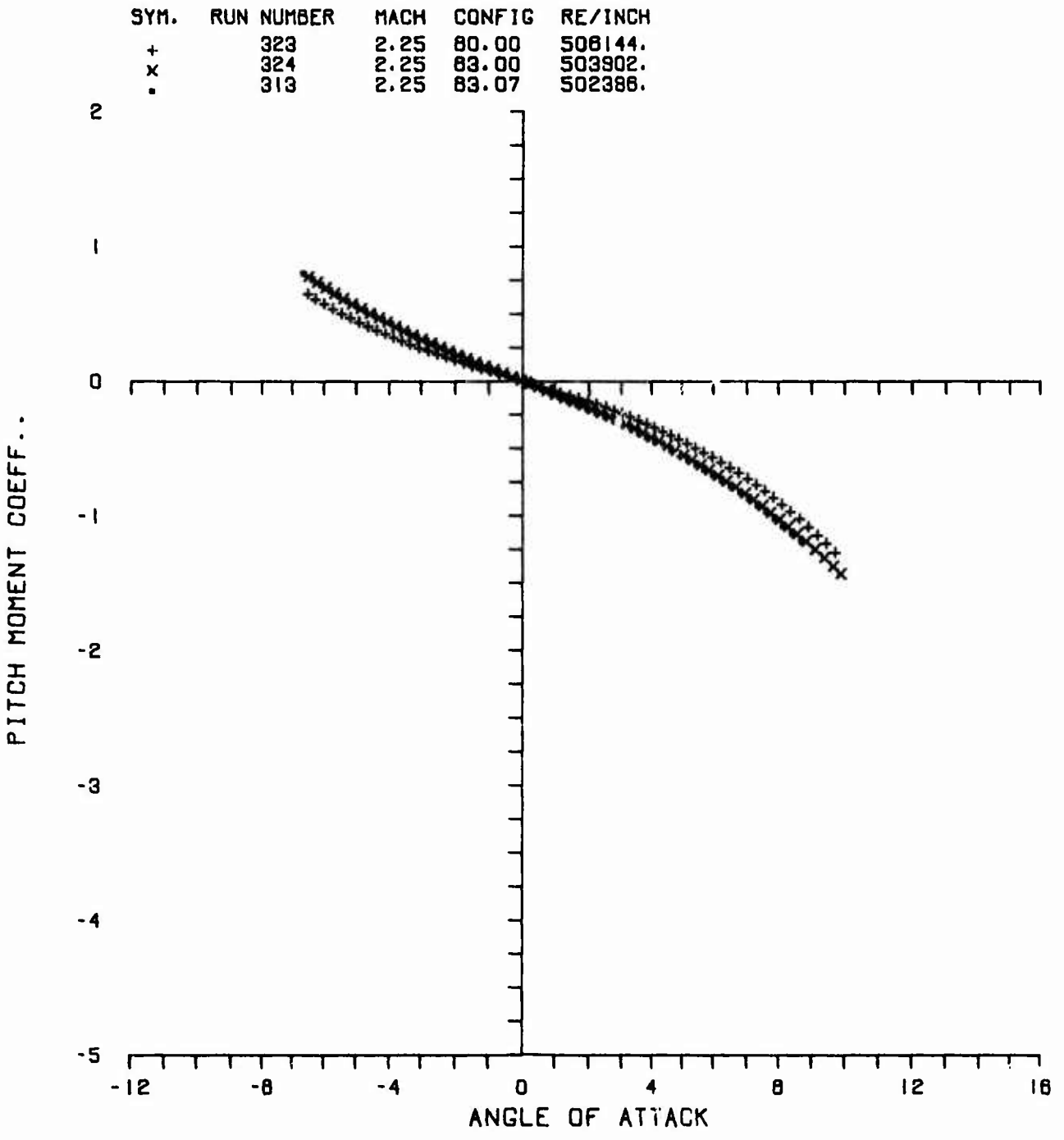

c. Mach Number 2.25

Figure A6. Continued

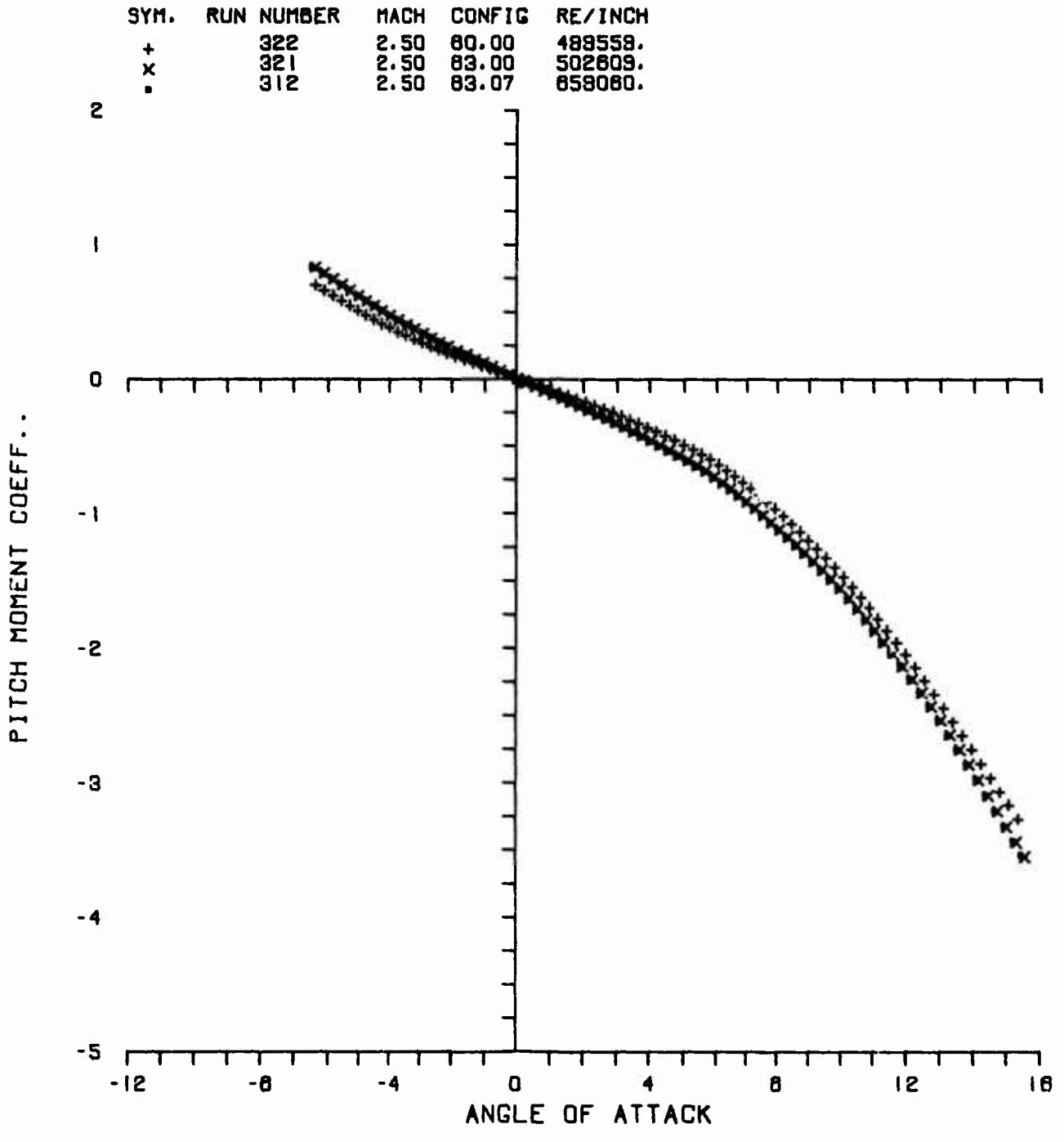

d. Mach Number 2.50

Figure A6. Concluded

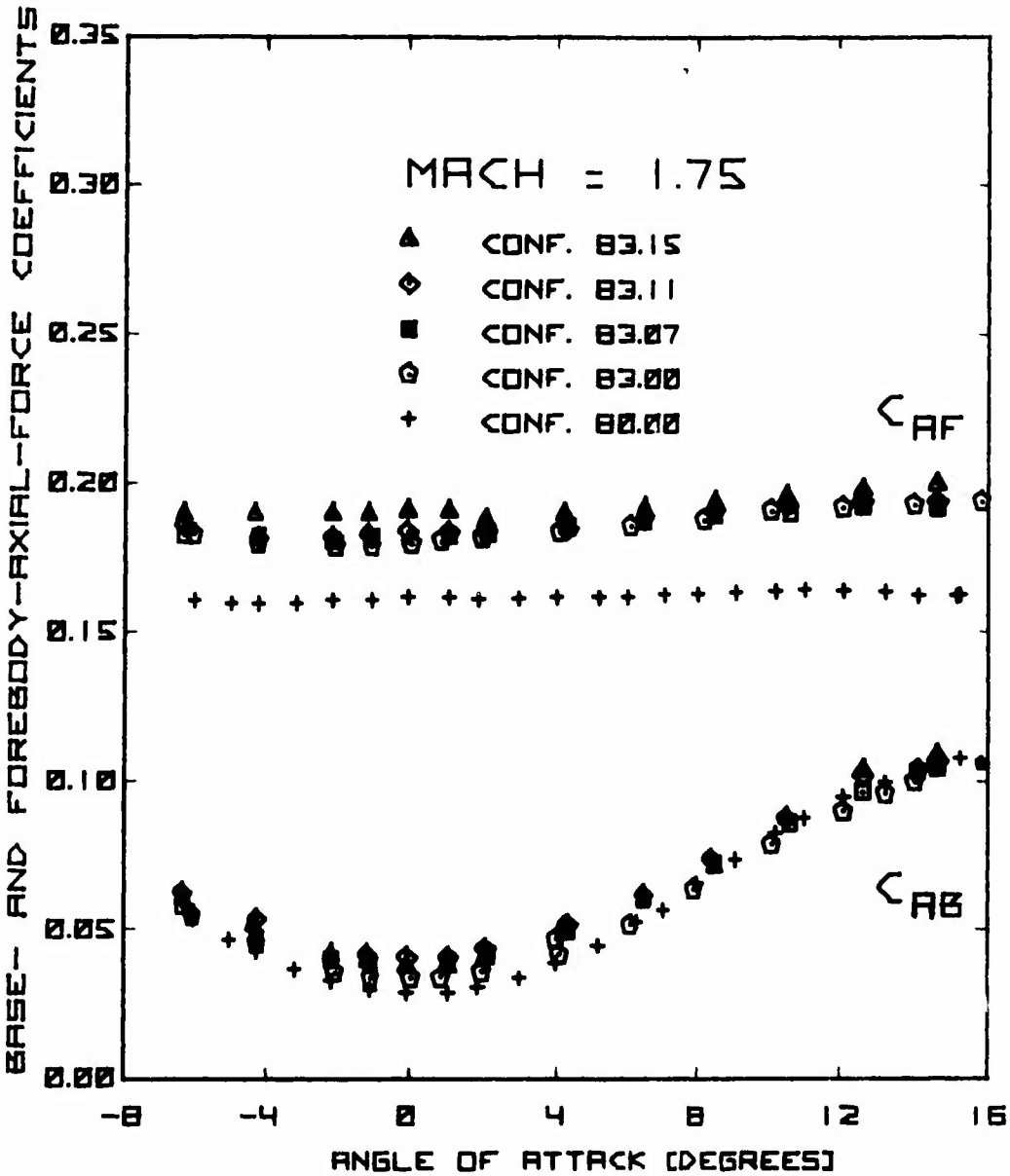

a. Mach Number 1.75

Figure A7. Base-Axial-Force and Forebody-Axial-Force Coefficients versus Angle of Attack

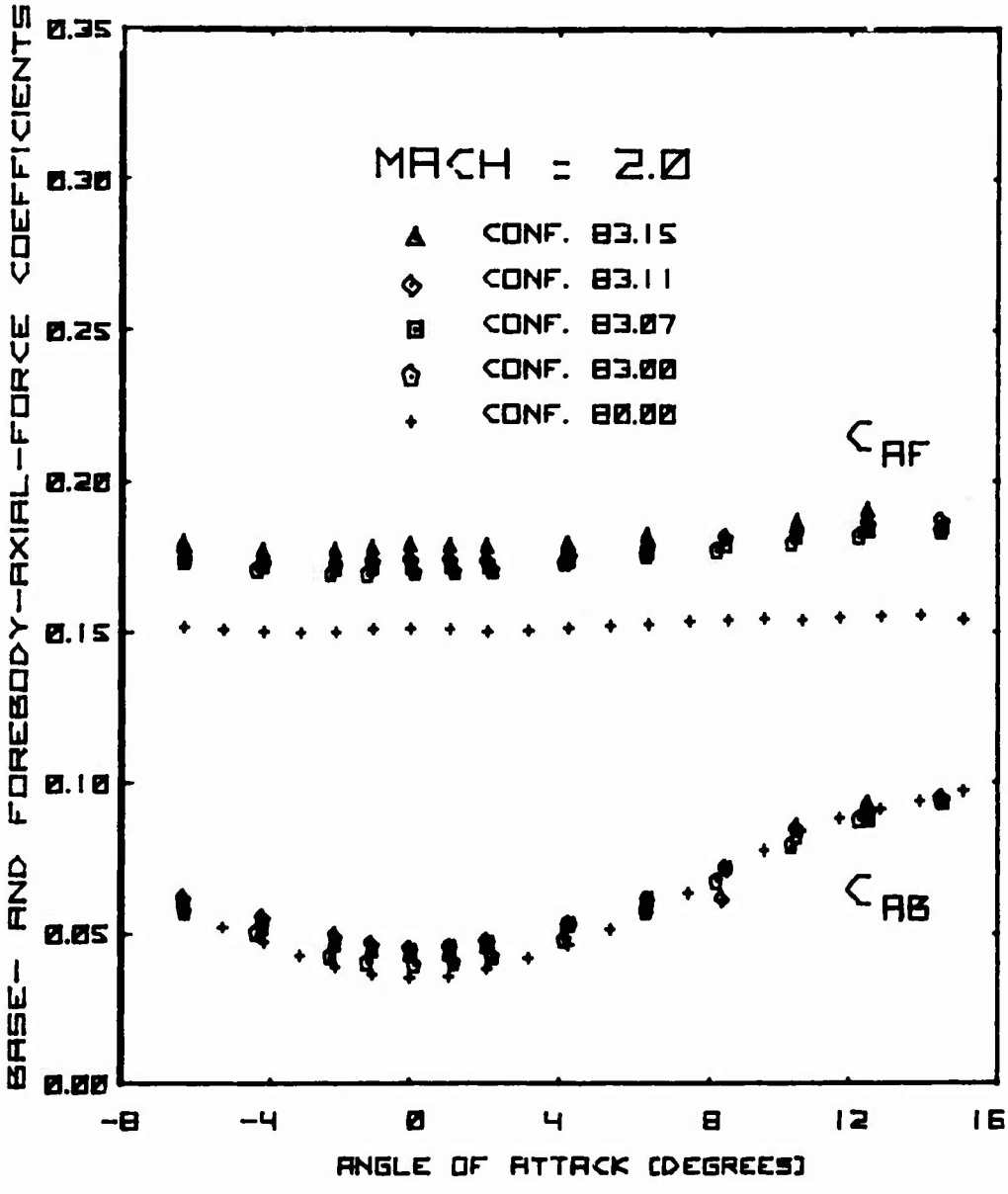

b. Mach Number 2.00

Figure A7. Continued

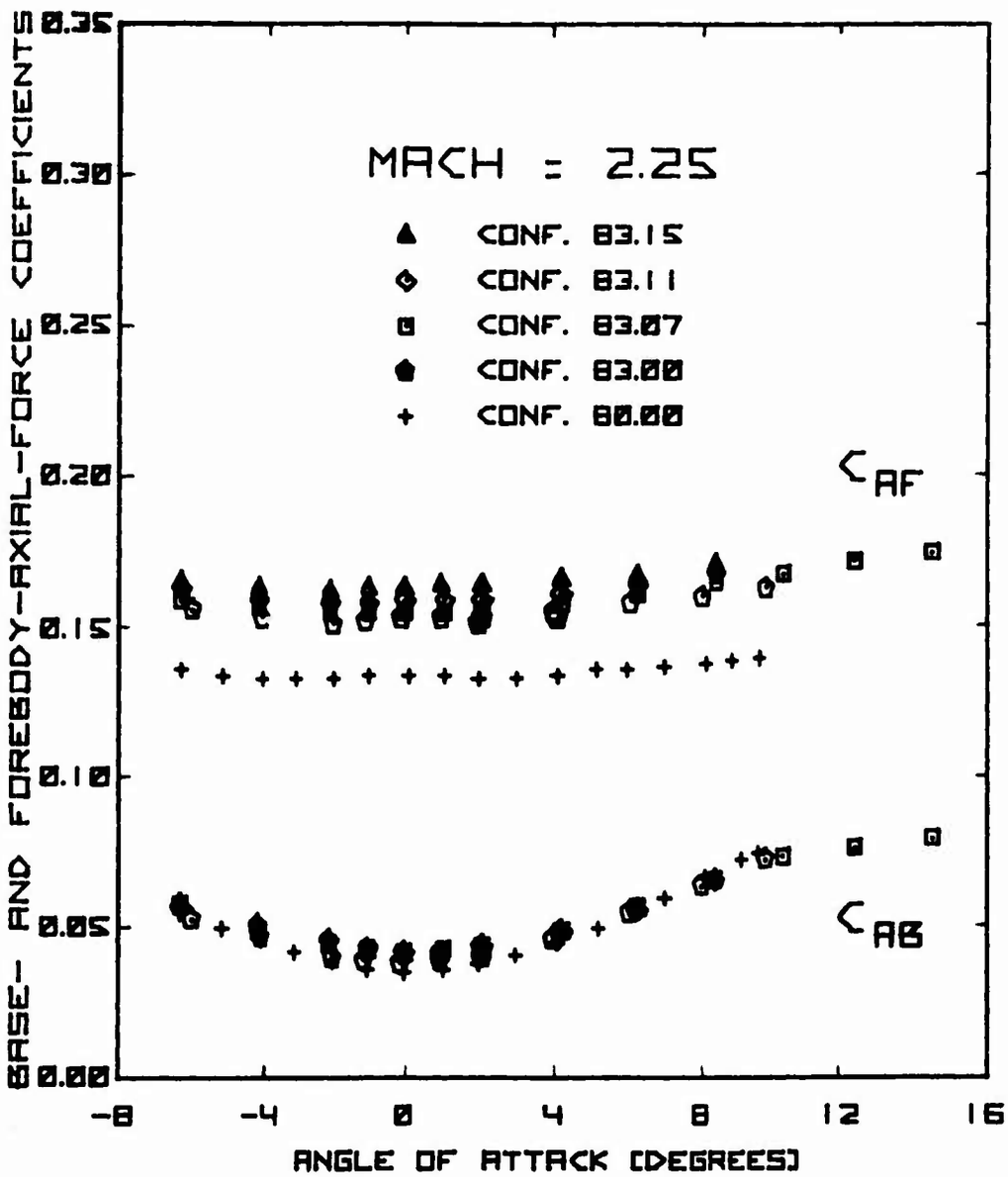

c. Mach Number 2.25

Figure A7. Continued

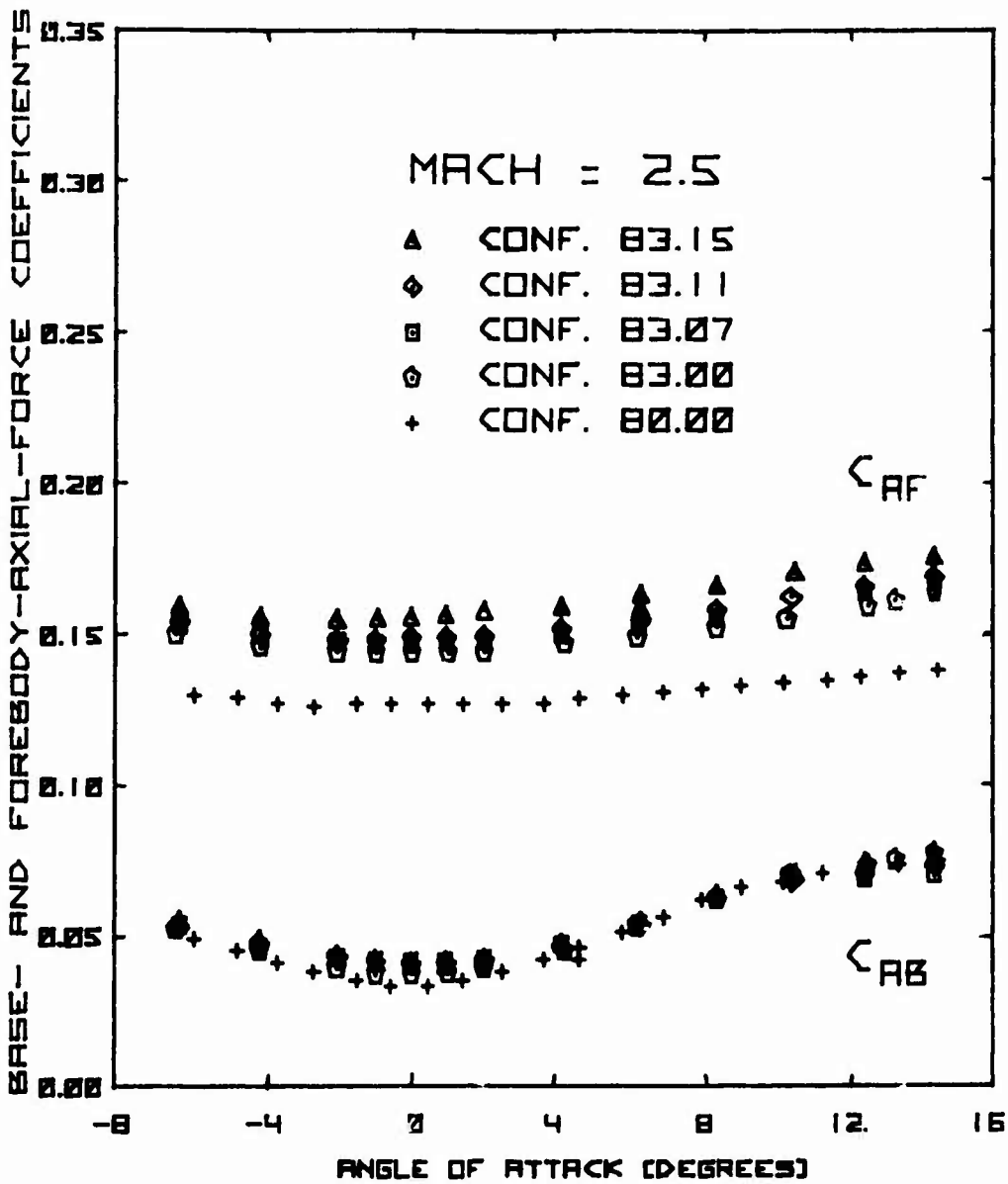

d. Mach Number 2.50

Figure A7. Concluded